KINETIC AND HYDRAULIC STUDIES IN HIGH-RATE BIOLOGICAL FILTERS

JOHN KRSKA

Ph.D. Thesis

July 1982

The University of Aston in Birmingham

Gosta Green

BIRMINGHAM

Kinetic and Hydraulic Studies in High-rate Biological Filters.
John Krska
Submitted for the Degree of Doctor of Philosophy
1982

Summary

Most published work on either low- or high-rate biological filters covers one of three topics: kinetics, microbiology/ecology or hydraulics. These areas have been re-examined together for high-rate filters in order to further integrate them and enable appropriate utilization of low-rate filter experience.

A kinetic model is described for biological oxidation and mass transfer for both single and multiple limiting substrates, and is substantiated for a single substrate by confirmation of the kinetic parameters by two independent methods.

The microbial film composition was shown to be affected by operating conditions and effluent composition, particularly the absolute concentrations of carbon and nitrogen, rather than the carbon/nitrogen ratio. Film composition was found to affect the kinetic model parameters, and the enhanced diffusion coefficients encountered were attributed to bacterial extracellular slime as opposed to "hyphal streaming" in fungi.

The behaviour of a filter is also affected by microbial film composition; in particular, "ponding" is only likely to occur when bacterial slime and fungi are present together, whilst a film with a true dominance of fungi is unlikely to cause "ponding".

A tracer technique and mathematical model were developed for determining the "specific wetted surface area" and degree of liquid mixing as functions of liquid loading. These hydraulic studies were confirmed and the kinetic model was further substantiated using performance data from a laboratory scale filter with a random packing.

The effect of the kinetics and microbial film composition on the long-term performance of a filter are discussed. Three types of filter behaviour are described, namely shedding and long and short sloughing cycles. Shedding results in a pseudo steady state, frequently producing a turbid effluent. The long sloughing cycle is regular, in phase and gives a rhythmic pattern to filter performance, whereas a short sloughing cycle is out of phase and produces erratic performance.

Key words

Tracer analysis, Biological filters, Microbial films, Reaction kinetics.

ACKNOWLEDGEMENTS

I would like to thank Professor G.A.Jeffereys for allowing me to undertake this work in the Chemical Engineering department of Aston University. I am grateful to the Science Research Council for the provision of financial support.

My thanks are also due to various members of technical and academic staff in the departments of Chemical Engineering and Biological Sciences for their invaluable assistance and advice. I am particularly grateful to Dr. E.L. Smith for his guidance and supervision.

Lastly, I would like to thank my wife for her patient help and understanding during the preparation of this thesis and for typing the final draft.

CONTENTS

CONTENTS

CONTENTS

CONTENTS

CONTENTS

LIST OF FIGURES

LIST OF TABLES

CHAPTER 1

INTRODUCTION

The function of a biological filter is to reduce the levels of dissolved/suspended organic matter in an aqueous waste. Some inorganic compounds may be removed in addition to the inorganic compounds that may be essential to the functioning of the filter. The biological filter is in fact a three-phase biological film reactor, the word "filter" originating from the early interpretation of the mechanisms by which suspended solids are removed.

A biological filter consists of an inert support medium (packing) that is retained in an open vessel (bed). A mixture of micro-organisms including bacteria, fungi and protozoa grow on the surface of the packing as a film. The micro-organisms feed on the dissolved/suspended matter in the liquid as it "trickles" (percolates) over the microbial film and through the bed: the liquid flow-pattern accounts for the common alternative names for the reactor - trickling filter and percolating filter. The micro-organisms are generally aerobic and the essential oxygen is supplied by air which passes through the bed by natural convection. The direction of the air flow depends on the local air and liquid temperatures.

Biological filters are particularly useful in treating large volumes of relatively dilute effluents which would be expensive to treat chemically; for example, most domestic sewage works incorporate biological filters. Since the micro-organisms which remove the pollutants are attached to a fixed surface, biological filters can give high turn-down ratios compared to other continuous biological reactors. They can also handle relatively high flow-rates without the danger associated with the use of suspended culture reactors of flushing out the micro-organisms. Because the contact between the liquid phase and the micro-organisms is not wholly

intimate, biological filters can withstand shock loads of biocides such as phenols and hypochlorites: such a shock load in a suspended culture system (e.g. activated sludge process) could destroy all the micro-organisms and so stop the process. These features make biological filters ideally suited to treating irregular flows of waste water which could possibly contain biocides.

Biological filters can be classified into two types: "high-rate" and "low-rate" filters. High-rate biological filters are capable of handling much higher liquid loadings than low-rate filters and generally treat more concentrated effluents. In high-rate filters use is made of specially formed pieces of plastic, which can take the form of vertical sheets or relatively small randomly dumped modules such as Pall rings. Although these special plastic packings are more expensive than the stone packings traditionally used in low-rate filters, their lower bulk density reduces the costs of building large and/or tall filter beds. It is the larger voidage and larger void spaces in plastic packings which make it possible to use high liquid loadings and to handle concentrated effluents. These geometrical and operating features also result in the build-up of more microbial film per unit volume of the filter than is possible with stone packings. Hence, a high-rate filter can be much smaller than a low-rate filter of comparable duty and, with the added potential of taller constuction, a high-rate filter will occupy less ground area.

At sewage works land is generally more available than at industrial sites, and low-rate filters are generally cheaper to run due to the lower pumping costs arising from the lower height. Hence, there is a continued interest in

the well established low-rate filters. Since high-rate filters can handle high liquid flow-rates and higher pollutant concentrations, they are often used for primary treatment to increase the handling capacity of existing sewage works where land may be restricted. They are also used in manufacturing industries to pre-treat effluents prior to their discharge into the sewage system.

To ensure good liquid distribution at the liquid loadings used with low-rate filters, an intermittent liquid dosing cycle is used. This is conveniently achieved using rotating arm distributors. The size of the rotating arms places both a practical and economic limit on the diameter of low-rate filter beds. Good liquid distribution is easier to achieve at the higher liquid loadings used in high-rate filters. Hence, as full advantage of the light-weight packings is made, new records for size are continually being made for rectangular high-rate filter beds using fixed spray heads or reciprocating arm distributors.

Although high- and low-rate filters are seemingly very similar, the different pollutant concentrations and liquid flow-rates used with each type give rise to differences in ecological behaviour. High-rate filters tend to support simpler biological populations than low-rate filters; hence, in studying high-rate filter performence, appropriate mathematical models are easier to develop.

Much of the research on low-rate filters has been concerned with the more complex ecological behaviour arising from the treatment of sewage effluents. This work has necessarily been qualitative and has been carried out by biologists: as a consequence of this emphasis, analyses of the performance of low-rate filters have been mainly empirical.

Often this same approach has been extended to the study of high-rate filters and, in the author's opinion, this has led to an incomplete understanding of filter performance. On the other hand, chemical engineers have tended to ignore the ecological factors that influence high-rate filter performance and have been inclined to place undue emphasis on kinetic modelling: this has resulted in increasingly perplexing mathematical models which can not be related to the ecological factors. Finally, many of the hydraulic studies which have been concerned with the effect of liquid loading and turn-down have been carried out by civil engineers: the results from such research have been mainly empirical and, whilst being compatible with other empirical studies, they can not be readily related to kinetic models.

The aim of the author's research has been to re-examine these three subject areas - kinetics, ecology and hydraulics - and to attempt to further integrate them. In doing this the overall understanding of high-rate biological filters should be improved, and improvements in design and operating procedures should be possible.

A realistic but simple kinetic model which uses a minimum number of parameters is presented in Chapter 2. The model is developed for single- and multi-substrate limiting kinetics. The kinetic model is verified experimentally and the model parameters are quantified in the case of a single limiting substrate in Chapter 6. Common aspects and differences in low- and high-rate filter ecological and physical behaviour are discussed in Chapter 3, so that the potential operating problems which may arise in high-rate filters can be identified and mitigated using low-rate filter experience where appropriate. The points raised in Chapter 3 also have bearing on the experimental methods used in quantifying the kinetic

parameters, as described in Chapter 4, and the terminology used in the remainder of the thesis. Chapter 5 describes and discusses the changes in ecology and physical behaviour that were observed when obtaining the kinetic data. These observations give a further insight into the points raised in Chapter 3 and have bearing on the methods of data analysis used in Chapter 6. In addition the changes observed are used to demonstrate the effects of ecological factors on the kinetic parameters in Chapter 6. Finally, a method of quantifying the effect of changes in liquid loadings on the overall filter performance is described in Chapter 7; the method uses a hydraulic model which was developed independently of the kinetic model and does not use kinetic data. The parameters of the hydraulic model are quantified in Chapter 8 and are presented in a form which can be readily incorporated with the kinetic parameters into an overall mass balance over a high-rate biological filter using a random packing.

Although the author's research has been concerned with high-rate biological filters, some of the work may be applicable to studies of other process equipment. The kinetic studies and, to a lesser extent, the ecological studies may be relevant to work with other biological reactor systems in which films or flocs of micro-organisms are formed. The hydraulic studies may also find application in the analyses of the performance of other three-phase absorption/reaction systems e.g. trickle bed catalytic reactors.

CHAPTER 2

KINETIC MODELLING

2.1. Introduction.

In the literature, there are many different mathematical models and approaches used to account for the performance of biological filters. The models vary in complexity from a simple first-order reaction with plug flow (1,2) to substrate diffusion coupled with Monod(3) - type kinetics (4,5). Comprehensive reviews of many of the published models have been presented by Roberts (6) and Atkinson and Howell (7); some of these will be discussed later.

Many of the models include hydraulic parameters such as "wetted surface area" e.g. (8,9,10), which have been evaluated using substrate removal data. In such cases, it is difficult to decide whether or not the calculated hydraulic parameters have any real physical significance: given a sufficient number of parameters, it is not difficult to fit the available data to a number of models. It is for this reason that this Chapter will only cover the bulk reaction kinetics arising from local mass-transfer limitations coupled with intrinsic reaction kinetics. The hydraulic parameters associated with bulk liquid mixing and wetted surface area are considered in Chapters 7 & 8.

2.2. Diffusion/Reaction Models.

Heterogeneous models based on the diffusion/reaction approach have become widely accepted (6,7) and are supported by visual observations. These heterogeneous models may incorporate various kinetic expressions and mass-transfer limitations but are all developed from the same concepts, shown diagrammatically in Figure 2.1.

Figure 2.1 Diagrammatic Representation of the Heterogeneous Kinetic Models.

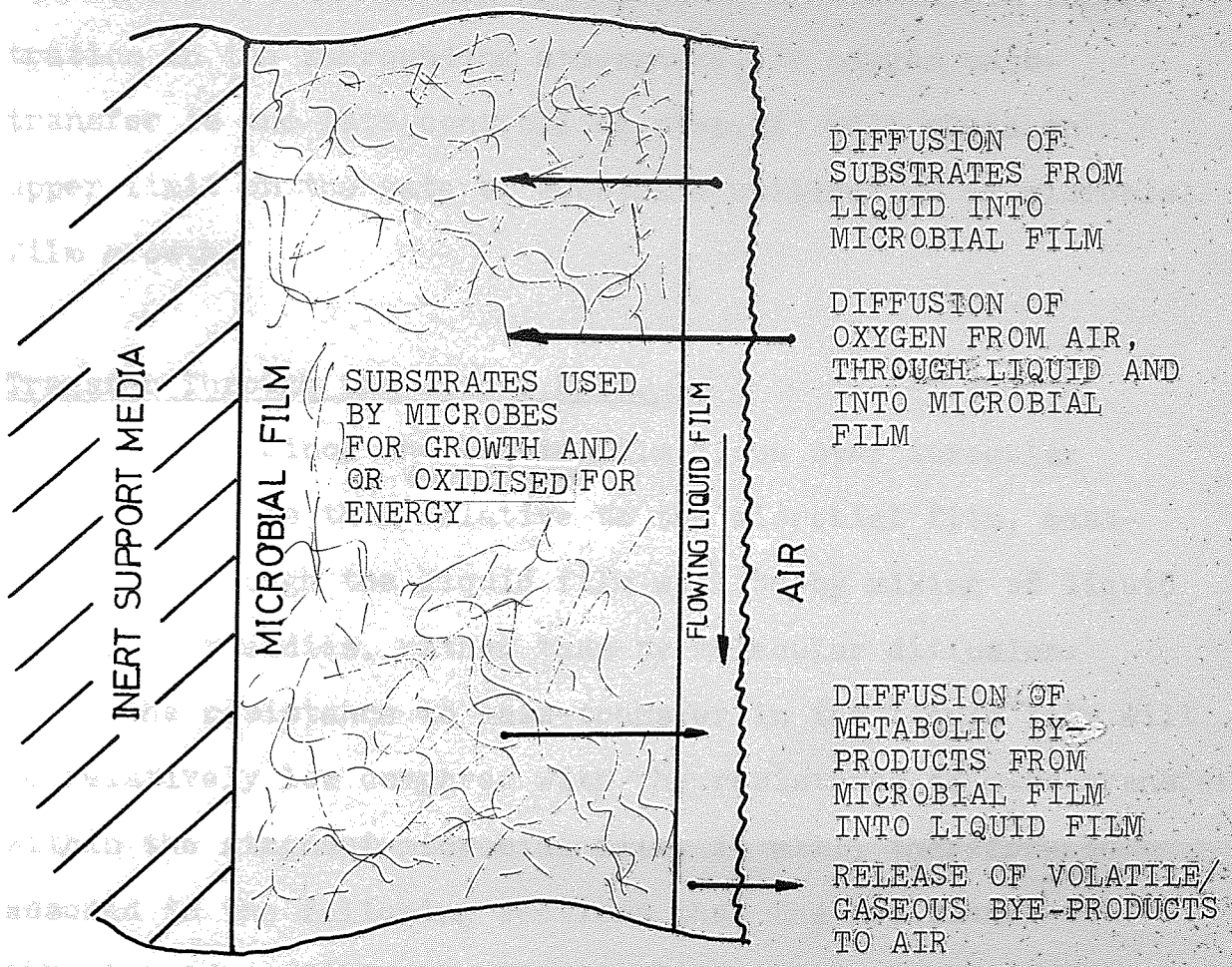

The liquid effluent flows over the microbial film which grows on the surface of the inert support medium. Oxygen from the air diffuses into the liquid film and then into the microbial film. The dissolved substrates in the liquid diffuse into the microbial film where they are metabolised for growth or oxidised. The metabolic by-products diffuse out of the microbial film into the liquid; volatile and gaseous compounds, such as CO_2, may then be released to the air.

2.3. Mass-Transfer, Oxygen Transfer,

It has been demonstrated by several workers (6,11) that oxygen transfer is not a rate-limiting step.

However, at relatively high substrate concentrations , not covered previously, oxygen may become rate-limiting. In this case the performance will be dependent on the oxygen concentration in the surrounding atmosphere. If oxygen mass-transfer is the rate-controlling step, it will place an upper limit on the rate of substrate utilisation or microbial film growth.

Transfer Through the Liquid Film.

Since the liquid film flows over irregular surfaces and is thin relative to the microbial film, mass-transfer through the liquid film will be by mixing of liquid elements or eddies, rather than by molecular diffusion. Hence the resistance to mass-transfer in the liquid film will be relatively low compared with the resistance to mass-transfer within the stagnant microbial film. It will, therefore, be assumed in the following sections that the resistance to mass-transfer within the flowing liquid film is negligibly small.

Transfer across the Liquid/Microbial Film Interface.

Since the microbial film is largely made up of water physically held to the external surfaces of the individual microbes (12), the interface between the flowing liquid and the microbial film will be assumed to offer no resistance to mass-transfer.

Metabolic By-Product Diffusion.

The metabolic by-products produced, if any, are likely to have a lower molecular weight than the substrates and hence the former will be able to diffuse out of the

microbial film relatively quickly. It will be assumed that the diffusion of such by-products will not be a rate-limiting step.

To summarise, the diffusion of substrate(s) or oxygen within the microbial film will be assumed to be the slowest step in the overall mass-transfer process.

2.4. The Kinetics of Biological Oxidation.

2.4.1. A Qualitative Introduction.

The simplest form of expression arises from intrinsic first-order biochemical oxidation kinetics: the solution of a diffusion/first-order reaction model takes the form of an overall first-order equation (13), hereafter referred to as bulk first-order kinetics. Many early workers found that bulk first-order kinetics did not apply and used so-called "retardant models" (6,8). The retardant models incorporate various parameters which empirically account for the change in treatability (8), a function of flow-rate. This change in treatability is due to the fact that the less easily assimilated substrates of a multisubstrate effluent are utilised relatively slowly and after the more easily assimilated substrates have been almost depleted (8). In evaluating a first-order rate constant, a reasonable "fit", within experimental accuracy, may often be obtained from data obtained from a once-through pilot-plant system. However, when a recycle is employed, the value of the rate constant is often different, implying that the kinetics are not really first-order. This sort of experience may account for the use of retardant models to account for the effect of recycle (for example, see Eckenfelder (8)).

In the more sophisticated models proposed by Atkinson (4), Monod-type kinetics are incorporated into a diffusion/reaction model after assuming that a single substrate is rate-controlling. This type of approach leads to a complex numerical solution, which can be simplified and expressed as a number of functional relationships to cover different ranges of the independent parameters, in particular the microbial film thickness and the substrate concentration. When applied to a single substrate system, there can be little doubt that this approach is widely applicable.

Bailey and Ollis (15) have described kinetic models which account for situations not adequately described by the Monod (3) equation. In biological filters, both substrate and product concentrations are low relative to those encountered in other biological reactor systems: consequently, inhibition due to either high substrate or high product concentration is unlikely to arise. However, substrate inhibition may occur with compounds such as phenols, nitrates and isocyanates (16). One method of avoiding such undesirable inhibition is to recycle treated water to dilute incoming effluent: in this way it is possible to use the simpler forms of equation.

In biological filters, the maintainence energy requirement may often be significant: this is dealt with later when considering the yield of microbes from a known mass of substrate (see section 2.6).

Whilst a complex retardant model may numerically describe the total substrate removal for a particular system, its utility in predicting the effect of changes such as flow rate and recycle rate may be limited. On the other hand, a multisubstrate model will inherently require many parameters

and at least as many as a retardant model. However, in the author's opinion, when sufficiently simplified, such a model is likely to be of more use in predictive situations, since it should numerically describe both the total substrate removal and the removal of any chosen compound. Ideally, the utilisation of each component in a multi-substrate system would be described by a Monod-type equation: also, consideration would have to be given to maintainence energy requirements. This approach would, of course, result in a very complex model; and, as is often the case, the modeller must use considerable judgement in deciding what is an appropriate level of complexity.

Whilst it has been appreciated that sequential reactions take place, not all the different types of microbes present in the film will be in competition for the same compounds. There will be simultaneous reactions which will minimise the effect of preferential utilisation. A possible method of modelling multi-substrate utilisation is to group the substrates into two or more main types, according to the speed with which each substrate is used: say, "fast", "intermediate" and "slow". It can then be assumed that:
(i) the "fast" substrates are utilised before and more rapidly than the "intermediate" substrates and so on, and:
(ii) each group of substrates is consumed according to simplified Monod-type kinetics in a diffusion/reaction model.
The larger the number of component groups, the more parameters will be introduced, and hence the better will be the fit between the numerical solution and the experimental data.

2.4.2. Simplified Monod-type Kinetics.

The Monod-type rate equation is

$$(-r_v) = \frac{k_o C}{k^* + C} \qquad 2.1$$

where C ——— concentration of rate-limiting substrate (M/L^3).

k_o ——— constant ($M/L^3/\theta$).

k^* ——— constant (M/L^3).

$(-r_v)$ ——— intrinsic rate of removal of limiting substrate, expressed per unit volume of microbial film ($M/L^3/\theta$).

This may be simplified by considering the two extreme cases - relatively high and low values of C.

High Values of C.

Given $C >> k^*$, $(C > 10k^*)$

$$(-r_v) \simeq k_o \qquad 2.2$$

This gives rise to an intrinsic zero-order rate expression.

Low Values of C.

Given $k^* >> C$, $(k^* > 5C)$

$$(-r_v) \simeq \frac{k_o C}{k^*} \qquad 2.3$$

This gives rise to an intrinsic first-order rate expression.

When these two extreme cases are incorporated into a diffusion/reaction model, there are three possible bulk rate equations. The rigorous proofs are given in Levenspiel (13) and Harremoes (17): the first two cases are also presented in Appendix 1 .

Case 1.

When C is relatively high and the microbial

film is relatively thin, the resulting bulk rate of substrate removal, $(-r_a)$, can be expressed in terms of "unit wetted surface area":

$$(-r_a) = k_o F \qquad \text{2.4}$$

where F ——— microbial film thickness, (L).

$(-r_a)$ ——— bulk rate of removal of limiting substrate, $(M/L^2/\theta)$.

The bulk rate of removal of substrate is thus zero-order with respect to concentration, C, and first-order with respect to microbial film thickness.

Case 2.

When C is relatively high and the microbial film is relatively thick, the resulting bulk rate of substrate removal is:

$$(-r_a) = \sqrt{2 D k_o C} \qquad \text{2.5}$$

where D ——— apparent diffusivity of substrate through the microbial film, (L^2/θ).

C ——— substrate concentration in the bulk liquid phase, (M/L^3).

The bulk rate of substrate removal is thus half-order with respect to the concentration, C.

Case 3.

When C is relatively low

$$(-r_a) = \frac{k_o C}{k^*} \cdot \tanh\left(F\sqrt{\frac{k_o}{k^* D}}\right) \Big/ \sqrt{\frac{k_o}{k^* D}} \qquad \text{2.6}$$

$$\simeq \sqrt{\frac{k_o D}{k^*}} \cdot C \quad @ \quad F\sqrt{\frac{k_o}{k^* D}} > 5$$

&

$$\simeq \frac{k_o}{k^*} F C \quad @ \quad F\sqrt{\frac{k_o}{k^* D}} < 0.5$$

The point at which equations 2.4 and 2.5 are

equal gives rise to the critical film thickness, F_{crit}; setting these equations equal and rearranging:

$$F_{crit} = \sqrt{\frac{2DC}{k_o}} \qquad 2.7$$

F_{crit} also describes the depth of penetration of substrate while the half-order regime applies.

These three rate equations have been used by Harremoes (17) to analyse data from experiments with de-nitrification filters: he has also shown that they provide a reasonable fit to data generated using the more rigorous diffusion/reaction model.

As already suggested (see page 11), the effect of preferential utilisation of substrates may be reduced in high-rate biological filters. It will be assumed that this is the case whenever the first-order regime is not encountered.

2.4.3. Simultaneous Reactions.

Numerically, two simultaneous zero-order reactions may be combined to form a single zero-order rate expression until one of the components is exhausted, as is shown in Figure 2.2.

Figure 2.2 Graphical Representation of Simultaneous Zero-Order Reactions.

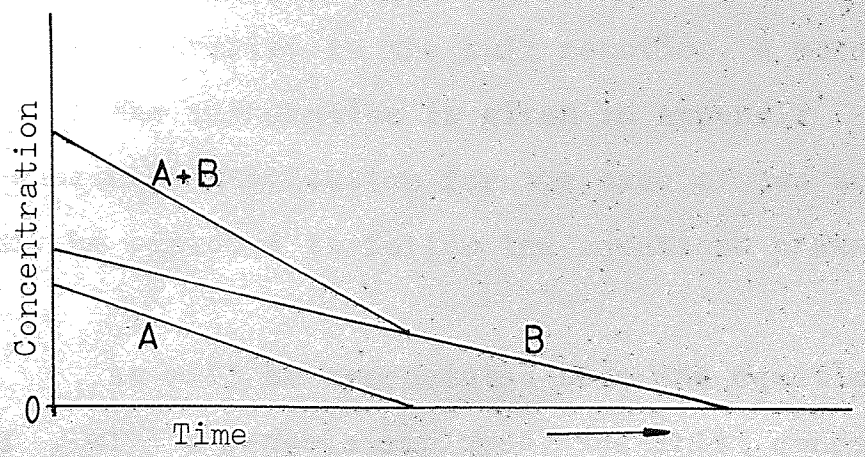

In a real system, there are likely to be many more simultaneous reactions taking place and so the effect of a single component becoming exhausted will be greatly reduced. The above type of summation can be used whilst bulk zero-order kinetics (see equation 2.4) apply. However, with bulk half-order kinetics (see equation 2.5) the diffusivity of each component will need to be considered. Chemically similar compounds are likely to have similar diffusivities, e.g. sucrose and glucose, and so preferential utilisation is more likely to occur between chemically dissimilar compounds. It would seem reasonable, therefore, to use an average diffusivity value for each group of substrates.

2.4.4. Sequential Reactions.

Harremoes and Riemer (19) have made use of sequential substrate utilisation in the study of de-nitrification filters. They have shown that sequential utilisation both down the filter and into the microbial film must be anticipated; this is shown diagrammatically in Figure 2.3 As the liquid flows down the filter, the thickness of microbial film in which the more easily assimilated substrates (group 'A') is used will decrease, at the same time, allowing more rapid utilisation of the less easily assimilated substrates (group 'B'). With sequential intrinsic utilisation there may be considerable overlap in the bulk reaction. A more rigorous treatment of the mathematics is given in Appendix 1 . The rate of substrate utilisation for the case of two substrate groups may be expected to follow the equations presented in Table 2.1.

As will be appreciated from the equations in Table 2.1 , with a recycle employed, the inlet concentration

Figure(2.3) Concentration Profiles Within the Microbial Film for Squential Substrate Utilization

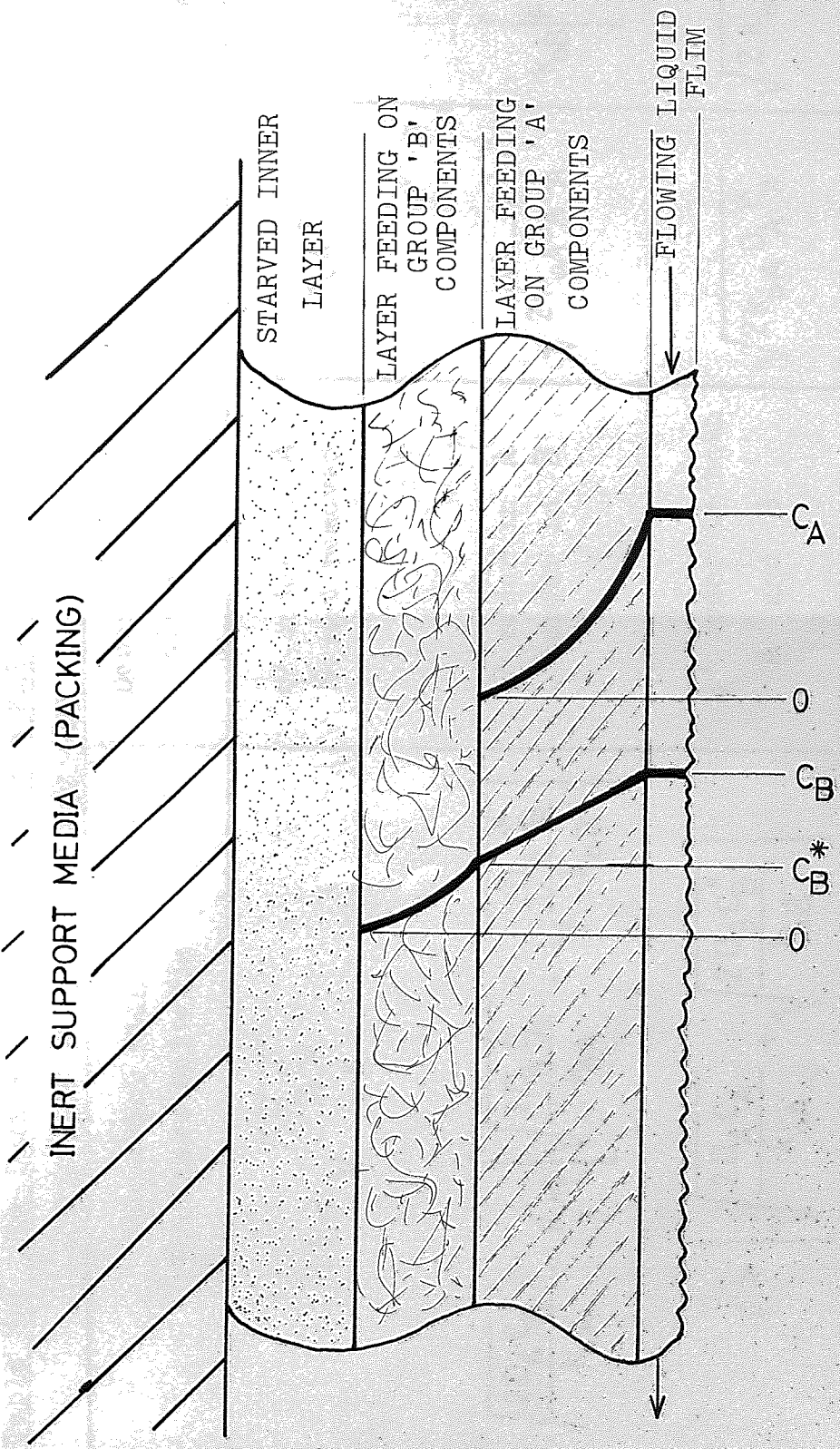

Table 2.1 The Bulk Rate Equations for a Multicomponent System Comprising Two Substrate Groups

Microbial Film Thickness Criteria	Description of Kinetics	$(-r_a)_A$ rate of removal of substrate(s) A	$(-r_a)_B$ rate of removal of substrate(s) B
$F < \sqrt{\frac{2 D_A C_A}{k_{oA}}}$	0' order in A B not removed	$k_{oA}.F$	0
$\sqrt{\frac{2 D_A C_A}{k_{oA}}} < F < \left[\sqrt{\frac{2 D_A C_A}{k_{oA}}} + \sqrt{\frac{2 D_B C_B^*}{k_{oB}}}\right]$	$\frac{1}{2}$' order in A 0' order in B	$\sqrt{2 k_{oA} D_A C_A}$	$k_{oB}\left[F - \sqrt{\frac{2 D_A C_A}{k_{oA}}}\right]$
$F > \left[\sqrt{\frac{2 D_A C_A}{k_{oA}}} + \sqrt{\frac{2 D_B C_B^*}{k_{oB}}}\right]$	$\frac{1}{2}$' order in both A and B	$\sqrt{2 k_{oA} D_A C_A}$	$\sqrt{2 k_{oB} D_B C_B^*}$

$$C_B^* = C_B + 2 C_A \sigma - \sqrt{4 C_A C_B \sigma + 4 C_A^2 \sigma^2} \qquad \sigma = \frac{k_{oB} D_A}{D_B k_{oA}}$$

of the group 'A' substrates will decrease and hence the group 'B' substrates may be utilised more readily. However, since

$$k_{oA} \cdot D_A > k_{oB} \cdot D_B$$

a reduction in the rate of removal of the combined substrates will be apparent.

Because of the complex interactions between kinetics, mass-transfer, hydraulics and microbiology, it is first necessary, in the author's view, to investigate the application of zero- and half-order kinetics to a single substrate. Only then can the multi-substrate kinetic model be studied with confidence.

2.5. Temperature Effects.

The effect of temperature may be incorporated into the kinetic model. Many published works quote the biological rate constant or constants as functions of temperature, usually in the form (6):

$$K_T = K_B(k_T)^{(T-T_B)} \qquad 2.8$$

where K_B ——— rate constant at base temperature T_B.

K_T ——— rate constant at temperature T.

k_T ——— gain constant

T ——— temperature considered

T_B ——— base temperature

It is important to note that, in many cases, it is the bulk rate constants and not the intrinsic rate constants that are expressed in this way. Roberts (6) raises the point that the effect of temperature is much less than that expected for a biological rate process. However, if the expected effect is applied to the intrinsic rate constant of a diffusion/reaction model, it is seen that the bulk rate of reaction is affected

to a much lesser extent.

The diffusivity, D, is thought to be proportional to the absolute temperature (20).

$$D \propto T_{absolute} \qquad 2.9$$

At room temperatures, a 10°C rise changes the diffusivity by only 3 to 4%. Therefore, within the range of temperatures normally encountered during the operation of biological filters, diffusivity may be assumed to be independent of temperature. A worked example of Roberts' (6) temperature correction is shown in Appendix 5.

2.6. Yield Coefficients.

2.6.1. Introduction.

The term 'yield' refers to the quantity of microbes and/or metabolic products produced per unit of substrate consumed. In the case of biological filters, it is the quantity of microbial film produced per unit of substrate consumed that is of primary importance. It is desirable, if possible, to minimise the production of microbial film, since disposal of this presents an additional problem.

There are several ways available of defining the yield; three examples are given below. The ratios chosen are a matter of convenience and not convention.

2.6.2. Definitions of the Yield Coefficient.

Definition 1.

$$\text{Yield } (Y_{dm}) = \frac{\text{Dry mass of microbes produced}}{\text{Mass of substrate consumed}} \qquad 2.10$$

Definition 2.

$$\text{Yield} = \frac{\text{Mass of filtered microbes produced}}{\text{Moles of substrate consumed}} \qquad 2.11$$

Definition 3.

$$\text{Yield } (Y_{vm}) = \frac{\text{Volume of microbes produced}}{\text{Mass of substrate consumed}} \quad \text{---} \quad 2.12$$

In this study, definitions 1 and 3 are used. The dry mass yield, Y_{dm}, is related to the volumetric yield, Y_{vm}, by equation 2.13 below:

$$Y_{dm} = W_d \cdot Y_{vm} \cdot \rho_w \quad \text{---} \quad 2.13$$

where ρ_w ——— wet density of microbial film (M/L^3).

W_d = weight of microbial mass dried to constant weight at 105°C / original wet weight

By definition

$$Y_{vm} = \frac{\text{Rate of film growth}}{\text{Rate of substrate removal}} \equiv \frac{\Delta V}{\Delta S} \quad \text{---} \quad 2.14$$

where & ΔS = mass of substrate used

ΔV = volume of microbial film produced

2.6.3. Maintenance Energy Requirements.

Substrates, such as glucose, are used to provide some of the chemical constituents for growth, the energy for growth and the energy for maintenance (15). The maintenance energy can be regarded as a fixed quantity of energy required by microbial cells merely to remain viable (alive and able to grow). Any substrate utilised in excess of this requirement is used for growth. Aiba et al. (21) use equation 2.15 to describe substrate utilisation in chemostats.

$$\text{Rate of substrate utilisation} = \frac{\text{Rate of cell production}}{Y_g} + m_s X \quad 2.15$$

where m_s ——— specific rate of substrate utilisation for maintenance

X ——— concentration of cells

Y_g ——— yield coefficient of substrate used for growth only

Bailey and Ollis (15) adopt an alternative approach: they regard the overall yield as constant and incorporate a death rate into the overall expression, as shown below:

$$\text{Rate of substrate utilisation} = \frac{1}{Y_o}\left(\text{Net rate of cell production}\right) \quad \text{—— 2.16}$$

$$= \frac{1}{Y_o}\left(\text{Actual rate of cell production} + \text{death rate of cells}\right)$$

where Y_o = overall yield

In the case of a film reactor, the substrate used for maintainence is likely to be proportional to the quantity of active microbial film; this is expressed in terms of unit "wetted surface area" by equation 2.17 :

$$\text{Maintenance requirement} = m_f . F_a \quad \text{———————} \quad 2.17$$

where F_a = active microbial film thickness (L).

and m_f = maintenance coefficient ($M/L^3/\theta$).

The active microbial film thickness is the actual thickness when bulk zero-order kinetics apply and F_{crit} when bulk half-order kinetics apply (see equation 2.7).

Now, the total substrate rate of utilisation is described by

$$\left(-r_a\right) = k_o . F \quad \text{———————} \quad 2.4$$

when $F < F_{crit}$. Under these conditions, equation 2.15 can the be modified for film cultures as follows:

$$k_o . F = \left(\left(+r_g\right)/Y_g\right) + m_f . F \quad \text{———————} \quad 2.18$$

This, on rearrangement, leads to

$$(+r_g) = (k_o - m_f) F Y_g \qquad 2.19$$

When $F > F_{crit}$,

$$(+r_g) = (k_o - m_f) Y_g \sqrt{\frac{2DC}{k_o}} \qquad 2.20$$

To obtain an expression for the overall yield coefficient, Y_{vm}, either equation 2.19 is divided by 2.4 or equation 2.20 by 2.5.

$$Y_{vm} = \frac{(+r_g)}{(-r_a)} = \frac{(k_o - m_f) Y_g}{k_o} \qquad 2.21$$

The overall yield, Y_{vm}, is therefore a constant.

In a multisubstrate system, each group of substrates may be expected to have different yield coefficients.

2.7 References.

1) Velz, C.J. A basic law for the performance of biological filters. Sewage Works Journal 20, p607 - 617 (1948).

2) Bruce, A.W. & Merkens, J.C. Recent studies in high-rate biological filtration. Water Pollution Control 69 (12), p113 (1970).

3) Monod, J. Ann. Review Microbiology 3, p371 (1949).

4) Atkinson, B & Daoud, I.S. Diffusion effects within microbial films. Trans. Inst. Chem. Engrs. 48, p245 - 254 (1970).

5) Williams, K.J. & McCarty, P.L. A model of substrate utilization by bacterial films. J. Wat. Poll. Cont. Fed. 48 (1), p9 - 24 (1976) & 48 (2) p281 - 196 (1976)

6) Roberts, J. Towards a better understanding of high-rate biological film flow reactor theory. Water Research 7, p1568 - 1588 (1973).

7) Atkinson, B & Howell, J.A. J. Env. Eng. Div. A.S.C.E. 101, p585 (1975).

8) Eckenfelder, W.W. Industrial water pollution control. p188 - 198. McGraw - Hill, New York. (1966).

9) Schulze, K.L. Load and efficiency of trickling filters. J. Wat. Poll. Cont. Fed. 32, p245 - 261 (1960).

10) Atkinson, B. & Ali. Wetted area, slime thickness and liquid phase mass transfer in packed bed biological reactors. Trans. Inst. Chem. Engrs. 54, p 239 - 252 (1976).

11) Atkinson, B. & Williams, D.A. Trans. Inst. Chem. Engrs. 49, p 219 (1971).

12) Rose, A.H. Chemical Microbiology. Butterworth, London. (1965).

13) Levenspiel, O. Chemical Reaction Engineering. Wiley & Sons, New York. 2nd edition. (1966).

14) Quirk, Lawler & Matusky Engrs. Whey effluent packed tower trickling filtration. Report for the Office of Research and Monitoring Environmental Protection Agency. Project no. 12130DUJ (1971).

15) Bailey, J. & Ollis, D. Biochemical Engineering Fundamentals. McGraw - Hill, U.K. (1977).

16) Andrews, J.F. A mathematical model for the continuous culture of micro-organisms utilizing inhibitory substrates. Biotechnol. Bioeng. 10, p 707 (1968).

17) Harremoes, P. The significance of pore diffusion of filter denitrification. J. Wat. Poll. Cont. Fed. 48, p 377 - 388 (1976).

18) Atkinson, B. & Davies, I.J. The overall rate of substrate uptake (reaction) by microbial films. Part 1: A biological rate equation. Trans. Inst. Chem. Engrs. 52, p 248 - 259 (1974).

19) Harremoes, P. & Riemer, M. Multicomponent diffusion in denitrifying biofilms. I.A.W.P.R. Conference, Stockholm, (1978).

20) C.R.C. Handbook of Physics and Chemistry. 60th edition 1979 - 1980. Chemical Rubber Company, Florida, U.S.A.

21) Aiba, S., Humphrey, A.E. & Millis, N.F. Biochemical Engineering 2nd edition. Academic Press, (1973).

CHAPTER 3

MICROBIOLOGY AND FILTER BEHAVIOUR

3.1. Introduction.

The theory of biological oxidation kinetics in high-rate filters follows almost classical chemical reaction engineering lines. However, an important feature of biological filters is that the microbial film is in a complex transient state of growth and decay. Should the microbial film grow excessively, the void spaces within the packing become partialy blocked, causing liquid maldistribution and an effective loss of the "wetted surface area" available for mass transfer. In extreme cases the blockage may become total, such that "ponds" of liquid form on top of the filter; hence the term "ponding".

High-rate filters tend to give rise to thicker microbial films; this is made possible by using packings of large voidage compared with that of the support media used in low-rate filters. However, control of the microbial film thickness may still be important even with these special packings. Often, the microbial film thickness is kept at a satisfactory level by the physical/biological processes alone, so that the filters do not require any attention. In other instances, care must be exercised in the design and/or operation of the filters to prevent "ponding". Clearly, time and resources may be saved if situations in which ponding may occur are identified at the design stage.

Various methods of preventing ponding in high-rate filters exist. However, process engineers have, without sufficient analysis, used methods based on the operation of low-rate filters, and, in many cases, these have made the problem worse (1). A clear, concise understanding of the mechanisms by which low-rate filters are operated to avoid ponding is therefore considered necessary and relevant at this stage in the thesis. The subjects raised also have

bearing on subsequent terminology, experimental technique and the methods used in data analysis.

3.2. Microbial Film Characteristics.

The microbial film consists of a mixture of micro-organisms - mainly different types of bacteria and filamentous fungi. Under various conditions either bacteria or fungi may be dominant. A thickening of the microbial film is often associated with a high concentration of fungi, particularly in colder months (1). Other groups of microbes may also be present, such as protozoa and algae.

The bacteria in high-rate filters are generally aerobic saprophytes, feeding on organic compounds for both energy and growth materials. The autotrophic nitrifying bacteria, which are often present in low-rate filters and convert ammonia to nitrite and nitrite to nitrate for energy, are generally not found in high-rate filters, their growth rate being too low for them to become established in significant numbers (2). Many of the commonly found bacteria produce an extra-cellular slime of polysaccharide or polypeptide by which they cohere together and adhere to the surface of the inert support medium (3).

The fungi are also saprophytes and grow within the bacterial "slime". Under normal conditions of liquid shear the fungi present are not capable of attaching themselves to an inert surface; they require an existing covering of bacterial slime (4). However, in conditions of high hydraulic shear, fungi capable of direct attachment may be present (4).

High carbon/nitrogen ratios associated with industrial effluents are reported to generally encourage fungal growth, while low carbon/nitrogen ratios associated

with domestic sewage effluents encourage bacterial growth (5).

Fungi isolated from low-rate filters have been shown to grow more rapidly at reduced temperatures than bacteria (5). Certain isolated fungi have been found to grow most rapidly at 15°C and as rapidly at 5°C as at 20°C. Bacteria generally favour temperatures between 25°to 30°C. This difference in temperature sensitivity may explain the greater occurence of fungi in colder weather.

In addition to the increased film thickness which can arise at lower temperatures due to increased substrate penetration (see Section 2.5), the following points, which may, in part, account for the occurrence of thicker films when fungi predominate, should be noted.

(i) The transport of nutrients and oxygen through a fungal film has been reported to be "ten times higher than by molecular diffusion in water and many times higher than through a bacterial film" (6). This phenomenon has been called "hyphal streaming" and justifies the use of high "apparent diffusivities" in the rate equations.

(ii) In low-rate filters the yield of microbial film, as described by equations 2.10 or 2.12 , is reported to be higher for fungi than bacteria (7).

3.3. Sloughing.

Sloughing is the natural, spontaneous loss of large portions of microbial film. The loss of film may be almost total, leaving only a small, patchy covering of microbes on the filter packing; these patches then regrow to form a new film. Sloughing in the U.K. has been reported to follow two superimposed cycles, a short cycle of period two to four weeks and an annual cycle which follows the seasons (18).

The microbial film builds up and sloughs regularly in the summer months and builds up slowly and continuously during the winter to slough in the spring.

The sloughing cycle can be interpreted using the diffusion/reaction approach to the kinetics. While the microbial film is relatively thin, less than F_{crit} according to equation 2.7 , the whole film is feeding on the effluent and growing. When a diffusion limitation is reached, i.e. when F_{crit} is exceeded, the inner layers of the microbial film may become starved of nutrients (see Figure 2.3). At this point the bacteria and fungi may start to feed on the extra - cellular slime, thus reducing the cohesion and adhesion of the microbial film (9). Further degradation can occur leading to autolysis (cell break-up) of bacteria (10) and the formation of gas pockets under the film (11). This suggests that, in some cases at least, the break down of adhesion is not sufficient to cause the microbial film to fall free. It is possible that the healthy, outer layers of the microbial film are strong enough to form an "envelope" around the weakened region, the microbial film being reinforced by the fibrous network of fungal hyphae. Tomlinson (4) has assessed the strength of fungal hyphae and shown how they can be slowly degraded by starving bacteria over a period of approximately ten days: when bacteria were absent, he did not observe such degradation.

3.4. Grazer Activity.

In low-rate filters fly larvae, small worms, nematodes and other higher organisms feed on the microbial film. In the summer, this removal process may adequately control film thickness (10). Indeed, the grazer activity may

so balance the growth rate that the microbial film never becomes thick enough to start sloughing, as can be seen in data from Hawkes and Shepherd (12). In winter months, grazer activity is reduced (10), and other forms of control may be required. Grazers of this kind are generally not found in high-rate filters, as it is often too wet or the substrate concentration is too high for them to survive; this is certainly the case with fly larvae(1) and rotifers (13) respectively. A further reason for the absence of grazers might be that the incubation period of the grazers' eggs exceeds the sloughing cycle.

The occurence of turbidity in the final effluent of high-rate filters has been attributed to protozoa activity: it is suggested that the protozoa break up the microbial film into small pieces whilst feeding on it and that the particles so formed are washed away and do not sediment out (14). However, it should be noted that protozoa are also observed in low-rate filters which do not give rise to turbidity (5). Consequently, the cause and effect relationship between protozoa and the turbidity of high-rate filter effluent does, in the author's opinion, require further investigation.

3.5. Shedding.

"Shedding" of microbial film, in contrast to sloughing, is the continuous physical loss of microbial film. The loss is balanced by new growth, so that the local average film thickness is kept constant. Shedding has been associated with turbidity and thin microbial films but without reference to the presence of protozoa (15). It is possible that there will be circumstances in which no clear

distinction between shedding and sloughing can be made.

3.6. Dosing Cycle.

When rotating arm (or reciprocating arm) distributors are used, as opposed to fixed spray heads, the frequency of liquid dosing may be varied. Hawkes (1), in a successful attempt to reduce fly nuisance from a low-rate filter, noted that slowing down the rotating arm distributor, while maintaining the same flow rate, reduced the microbial film thickness near the top of the filter, where it is most important. This reduction in microbial film thickness was thought by him to be due to the reduction in available substrates and not to the increased liquid shear. An investigation by the same author into the use of different nozzles to jet the liquid onto the top of a filter (16), while maintaining the same flow-rate and frequency of dosing as in a control filter bed, increased the microbial film thickness at the surface. The increased microbial film thickness was possibly due to the evolution of a tougher microbial film in response to the higher hydraulic shear; such a possibility has already been outlined on page 27 . Williams (5), however, suggests that the changes in hydraulic shear, within low-rate filter operating limits, have no real effect on microbial film thickness. This view is also supported by Hawkes (16) who attributed increased microbial film thickness to a reduction in grazer activity because of excessive wetting.

A limit to the reduction in frequency of dosing will be reached when the decrease in filter performance due to the maldistribution of liquid outweighs the benefits of controlling the microbial film thickness. The optimum period of dosing in low-rate filters is dependent on the source of

the effluent, temperature and rate of liquid application. No data about the effect of dosing frequency on the performance of high-rate filters have been found.

Hawkes (1) has investigated local liquid flow-rates as a function of time at various depths in a low-rate filter. He reported that the intermittent flow was stabilised at depths of 2 - 3 feet. The stability was possibly achieved by lateral mixing (17) and/or the hold-up of liquid by the microbial film. These results suggest that in high-rate filters, which are usually much deeper than low-rate filters, the effect of low frequency dosing will be of little significance over a sufficient portion of the bed-height.

3.7. Alternate Double Filtration (A.D.F.).

A.D.F. involves two filter beds which are used alternately as primary and secondary filters in series. The bulk of the organic load is removed in the primary filter where the microbial film grows; meanwhile, the secondary filter loses its microbial film through starvation. After a suitable period of time, the roles of the two beds are reversed. This system may prove costly because capital is required for two filter beds when effectively only one is operating full-time.

It is reported that A.D.F. is often ineffective under conditions which encourage the growth of fungal films (1). This is due to the fact that the time required for the secondary filter to lose film is often much greater than the time taken for the primary filter to reach the most suitable change-over state. Once the latter condition is passed, the secondary filter takes more of the organic load and the film starts to grow again, with obvious consequences.

3.8. Recycle.

Recycle is commonly used in high-rate filters to reduce the inlet concentration to the required working level; it is reported to be an effective method of preventing ponding. The reduced film thickness can be explained in terms of a reduced F_{crit} value (see Equation 2.7), and this means that the microbial film will slough earlier. This explanation is likely to hold in the case of bacterial films, which soon lose adhesion and slough once F_{crit} is exceeded. However, in the case of fungal films, which require a considerable period of time to degrade and break free, acceptance of this obvious mechanism may seem naive. However, no reports of the ineffectiveness of recycle in controlling fungal films have been seen.

3.9. Choice of Packing.

There is a large selection of commercial packings available for use in high-rate filters. Several independent workers (1) have compared the performance of different packings, and all support the general view that no one packing, given good liquid distribution, is better than any other e.g. (18). However, the need for good liquid distribution is more important when using vertical tube packings than when using modular sheet packings; it is least important in the case of random packings.

The choice of packing may determine the level of film thickness control required. A very open, random packing, such as Biopac 90, will, in return for a reduction in specific surface area, allow thicker films to grow before ponding takes place. Packings which use fine corregations to provide a high specific surface area may be expected to suffer from a

considerable loss in effective surface area once a microbial film has "filled in" and levelled off the corregations. The author would only recommend the use of this latter type of packing for conditions which result in the formation of very thin microbial films.

3.10 References.

1) Hawkes, H.A. Seminar for the National Water Council, at the University of Aston in Birmingham, April, 1977.

2) Jones, G.L. Personal communication, Open day, Water Research Centre, Stevenage, 1978.

3) Aiba, S.,Humphrey,A.E. & Millis, N.F. Biochemical Engineering 2nd edition. Academic Press (1973).

4) Tomlinson, T.G. Some aspects of microbiology in the treatment of sewage. J. Soc. Chem. Ind., London. 61, p53 - 58 (1942).

5) Williams, I.L. A study of factors affecting the incidence and growth of fungi in sewage bacteria beds. M. Sc. Thesis, University of Aston in Birmingham (1971).

6) Tomlinson, T.G. & Snaddon, D.H.M. Biological oxidation of sewage by films of micro-organisms. Int. J. Air Poll. Cont. 10, p865 - 881 (1966).

7) Hawkes, H.A. The Ecology of Waste Water Treatment. Pergammon Press, Oxford (1963).

8) Atkinson, B. & Howell, J.A. Sloughing of microbial film in trickling filters. Water Research 10, p307 - 315 (1976).

9) Painter,H.A. Seminar for the National Water Council, at the University of Aston in Birmingham, April, 1977.

10) Hawkes, H.A. Film Accumulation and grazing activity in sewage filters at Birmingham. J. Proc. Inst. Sew. Purif. 2 p88 - 110 (1957)

11) Atkinson, B., Swilley, E.L., Busch, A.W. & Williams,D.A. Kinetics, mass transfer and organism growth in a biological film reactor. Trans. Inst. Chem. Engrs. 45, T257 - 264 (1967)

12) Hawkes, H.A. & Shepherd, M.R.N. Laboratory studies on the effects of temperature on the accumulation of solids in biological filters. Wat. Poll. Cont. (1976).

13) Curds, C.R. & Hawkes, H.A. (Editors) Ecological Aspects of Used-Water Treatment. Volume 1: The Organisms and their Ecology.

14) Bruce, A.M. & Macmillan, S.C. Research developments in high-rate biological filtration. J. Inst. Pub. Health. Engrs. p 178 (1970).

15) Calley, A.G., Forster, C.F. & Stafford, D.A. (Editors) Treatment of Industrial Effluents. p 85. Hodder & Stoughton, London, Sydney, Auckland, Toronto. (1977).

16) Hawkes, H.A. Effects of methods of sewage application on the ecology of bacteria beds. Ann. Applied Biology 47 (2), p339 - 349 (1959).

17) Porter, K.E. et al. Trans. Inst. Chem. Engrs. 46, T69, T74, T86 (1968).

18) Bruce, A.W. & Merkens, J.C. Further studies of partial treatment of sewage by high-rate biological filtration. Wat. Poll. Cont. 77, p499 - 527 (1973).

CHAPTER 4

EXPERIMENTAL DEVELOPMENTS

4.1. System Requirements.

In order to evaluate the kinetic parameters of a zero - $\frac{1}{2}$ order model, it must be possible to relate substrate utilisation to microbial film thickness for a known "wetted surface area" of microbial film.

Firstly, previous workers have found that the exponential growth phase (i.e. when film thickness $< F_{crit}$, see equation (2.7)) of sewage organisms is too small to detect (1); hence, the microbial film thickness measurements must be made accurately.

Secondly, to ensure that the "wetted surface area" is known, the hydraulics and microbial film geometry must usually be simplified.

Thirdly, it is apparent from Hawkes' work (2), discussed in section (3.6), that the test system must not subject the microbial film to any undue hydraulic shear. This point was appreciated in retrospect by La Motta (3), who chose to use a high hydraulic shear-rate system with a well mixed liquid phase to eliminate liquid phase mass-transfer limitations and simplify the hydraulic considerations.

Fourthly, the system must be small enough to be maintained for long periods economically, since the sloughing cycle may be as long as four weeks (4).

Finally, the system must be reliable enough when left running unattended either overnight or at weekends.

4.2. System Specifications.

4.2.1. The Inclined Plane.

An inclined plane of perspex, 2.5 meters long x 7cm wide, was used. Rubber grease was applied to the sides of the plane, using masking tape, to prevent wetting

(and subsequent channelling) in the edges between the plane and the vertical walls; this left a 5cm wide channel. The plane was inclined at 20° to the horizontal, which, in the absence of a microbial film, caused rivulet flow visually similar to that over a random packing at a comparable flow-rate. A flow-rate of 15 $cm^3 min^{-1}$ was maintained for all the experiments, as this gave a similar flow-rate per unit surface area as would a 2.5 meter deep high-rate filter (5); the plane length was then comparable to filter depth.

The substrate solution was made to the required concentration in advance and supplied from a 60 litre storage tank, thus eliminating the need for any in-line mixing equipment. The flow of liquid was maintained by pressurizing the storage tank with air from a high pressure cylinder. This had two advantages: firstly, the use of a metering pump, prone to blockages, could be avoided, and, secondly, the storage vessel was isolated from the atmosphere.

The system is shown diagrammatically in figure (4.1.): equipment used for tracer studies is also included.

The inclined plane was screened from light with black paper to prevent the growth of photosynthesisers such as algae. The ambient temperature was maintained at a constant value of 22°C for all the experiments by operating in a "Controlled Atmosphere Room".

4.2.2. Substrate Composition and Concentration.

Glucose was used as a carbon source with an inlet concentration range of 100 to 1000mg/l. This was chosen as it is inexpensive, non-volatile, non-toxic, readily biodegradable, easily analysed and it contains no nitrogen.

Figure(4.1)Schematic Diagram of the Inclined Plane Rig with Tracer Equipment

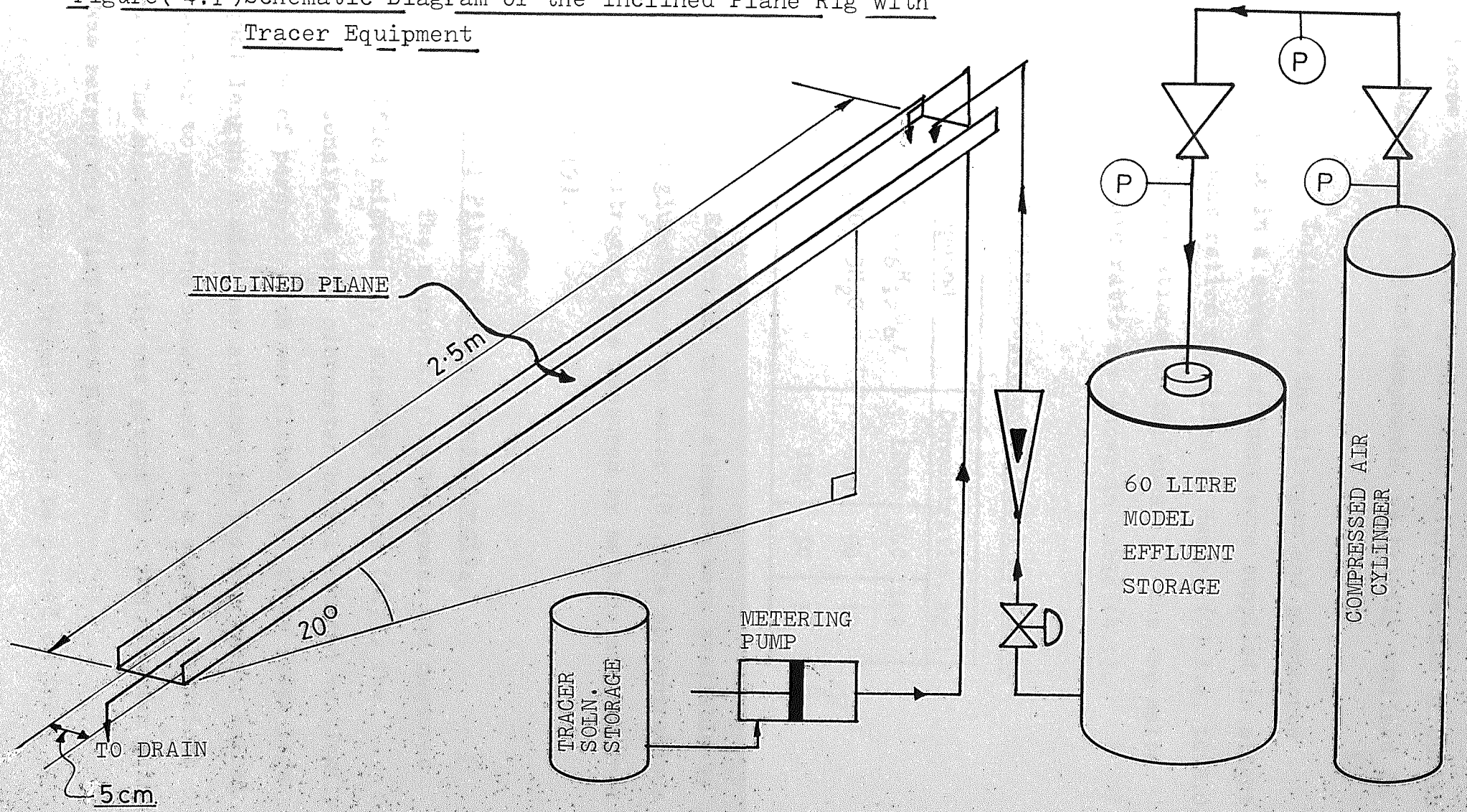

The glucose was analysed by the colorimetric method of Dubias (6) for sugars and related compounds, as briefly outlined in Appendix 6.

Initially, the nitrogen and phosphorus normally present in a sewage effluent were supplied in slight excess of the mass ratios specified by Hawkes (7) i.e. 100B.O.D.:6N:1.5P. The concentrations of the sugar and the two salts used to achieve this ratio are shown in Table (4.1).

Table (4.1) Composition of Model Effluent.

Compound	Concentration mg/l		
Glucose ($C_6H_{12}O_6$)	1000	500	100
$(NH_4)_3PO_4.3H_2O$	100	50	10
NH_4NO_3	100	50	10

Essential trace elements were available by using unrefined glucose and tap water (8). The concentrations of ammonia and nitrogen were measured by methods adapted from Chapman et al.(9).

4.2.3. Microbial Film Thickness Measurements.

The microbial film thickness was measured with a modified micrometer, shown in Figure (4.2). The instrument consisted of a micrometer barrel mounted vertically in a piece of perspex which was fitted with three brass legs of equal length. A wire was attached to the micrometer barrel and another to one of the brass legs via a simple electrical circuit. The micrometer tip was ground to a 1mm diameter point and was zeroed on a flat glass plate.

The instrument could be placed on the

Figure 4.2a The converted micrometer used for taking microbial film thickness measurements

Figure 4.2b Simple circuit diagram for the converted micrometer

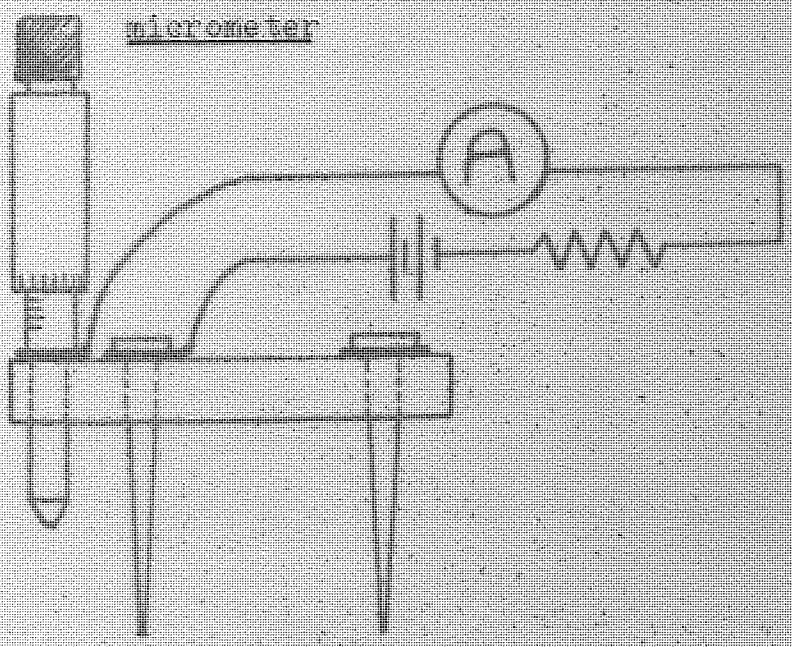

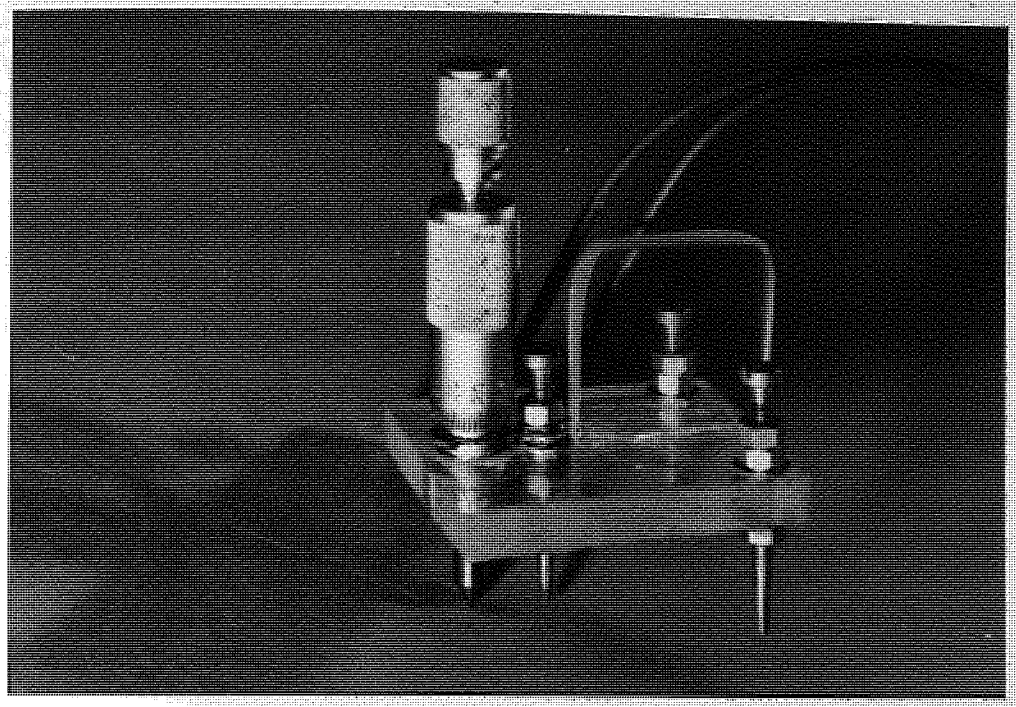

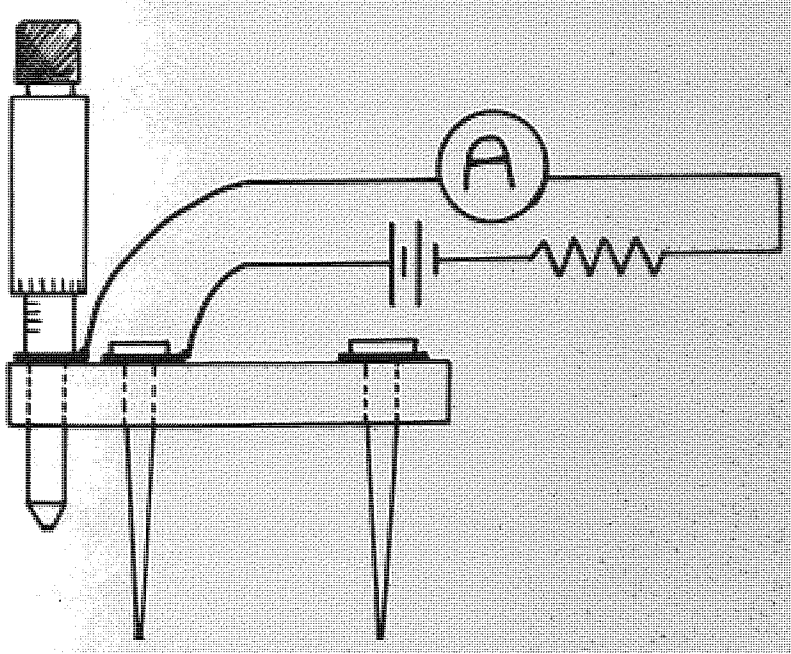
A

inclined plane so that the three legs cut through the microbial film and rested on the perspex surface. On slowly lowering the micrometer tip and making contact with the surface of the microbial film a sharp change in electrical conductivity between the micrometer and the wired leg could be detected. The micrometer tip was dried between each individual measurement. To ensure no bias arose in the placing of the measurements each location was randomly selected in advance, and the underside of the perspex was marked with paint which was visible through the microbial film; these marks are apparent in Figure (7.1).

4.3. Start-up Procedure.

Seeding.

Like most plastics, perspex does not "wet" easily. Because of this, it was difficult to achieve a uniform covering of microbial film at the start of each experiment. This was overcome by allowing a covering of microbes to develop while the plane was lying horizontally and submerged in a "seed culture". Once a covering of microbes had developed, the plane could be inclined and would remain well wetted.

The method described by Atkinson (10) of pouring a seed culture over the plane while inclined and allowing it to dry on was tried, but the subsequent complete wetting was not obtained. Roughening the perspex surface with coarse glass paper was also explored; this did not improve the surface wetting. However, sanding with fine glass paper to a smooth matt finish did improve surface wetting slightly; this was attributed to the surface being freed of grease.

"Seed Culture" Preparation.

The seed culture was originally prepared by

mixing settled sewage with a quantity of the model effluent at a glucose concentration of 500mg/l as in Table (4.1) and then aerating for a period of two weeks: fresh effluent was added daily. This gave a thick mixture of suspended microbes, which, after several attempts to seed the inclined plane, developed a film culture which adhered to the perspex surface.

The first film culture was allowed to develop on the inclined plane for one month. Later, seed cultures were prepared by suspending pieces of microbial film taken from previous experiments.

When changes in substrate concentration were required, the seeding procedure was repeated after the culture had adjusted to the new environment. Microscopic examinations were used to follow such changes, which normally took one to two weeks.

It was found possible to store samples of microbial film for periods of about two to three weeks by placing on agar at $5^{o}C$.

4.4. System Maintenance.

It was found necessary to clean the storage tank, feed lines and drains every second or third day to prevent infection and blockages. This was carried out by hosing or rinsing with fresh water, soaking/flushing with sodium hypochlorite solution and followed by further rinsing.

4.5. Measurement Sampling Problems.

From the early quantitative tracer analysis (see Section (7.4.3)), it was found that liquid mixing on the inclined plane was equivalent to that in the outlet from a series of eight stirred tanks. Partly for this reason, samples

of water for glucose analysis were taken at the inlet and at 8 points equally spaced along the plane; a hypodermic syringe was used to collect such samples from the surface of the microbial film.

The original intention was to relate the changes in glucose concentration to the average microbial film thickness over each of the 8 sections of the inclined plane and then evaluate the kinetic parameters. However, this approach was unsuccessful due to fluctuations in point glucose concentrations which exceeded the limits of acceptable experimental error. This problem arose because of the restrictions placed on sample size ($2cm^3$) and was not due to system geometry. A time-average continuous sampling system would have been ideal but was impractical.

Changes in microbial film thickness over a period of hours provide a useful indication of system behaviour and are not subject to short-term fluctuations in flow conditions. It was therefore decided that such measurements might be used to evaluate "F_{crit}" by locating the limit to exponential growth. However, experience showed that the microbial film developed in an uneven manner, and, because of this, the number of measurements required to provide a meaningful average had to be considered in some detail (see Appendix 6). It was concluded that ten measurements needed to be taken from each of the 8 sections of the inclined plane. The measurements were located using a stratified random sampling technique operating on a grid reference system which is described in Appendix 6. Each location was maintained throughout the series of experiments.

From the start of an experiment, eighty microbial film thickness measurements were taken every four

or five hours until it became apparent, without a detailed analysis, that the concentration-dependent kinetic regime was dominant. This period varied from 2 to 5 days, after which time measurements were taken less frequently, usually twice daily, for 2 to 4 weeks.

4.6. Extremes of the Carbon/Nitrogen Ratio.

Two extreme cases for the carbon/nitrogen were considered when planning the experimental programme. These were:

1) the lowest glucose concentration with the highest salt concentration listed in Table (4.1)
2) the highest glucose concentration with the lowest salt concentrations listed in Table (4.1).

These resulted in the model effluent compositions presented in Table (4.2).

Table (4.2) Model Effluent Compositions with Extreme Carbon/Nitrogen Ratios

Compound	Concentration mg/l	
	High C/N	Low C/N
Glucose	1000	100
$(NH_4)_3PO_4 \cdot 3H_2O$	10	100
NH_4NO_3	10	100

These model effluents were used to investigate the microbial film behaviour and characteristics; no kinetic data were taken during these experiments.

4.7. Preliminary Experiment with a Biopac Rig.

A series of experiments was carried out on Biopac* 50 and Biopac* 90, two commercial random, pall ring packings for high-rate filters. The main aim of these experiments was to investigate the system hydraulics using tracers, as discussed in Chapters 7 and 8. Some kinetic data were also obtained during the running of these experiments, and these have been used to demonstrate how the hydraulic and kinetic parameters relate to filter performance in Appendix 5.

Both types of packing were arranged in a single string, as shown diagrammatically in Figure 4.3. The model effluent used in both cases was 500mg/l glucose with a standard carbon/nitrogen ratio (see Table 4.1). Both sets of experiments were carried out in a pilot-plant laboratory with an ambient temperature of approximately 15°C.

Figure 4.3. Diagrammatic Representation of the Biopac String.

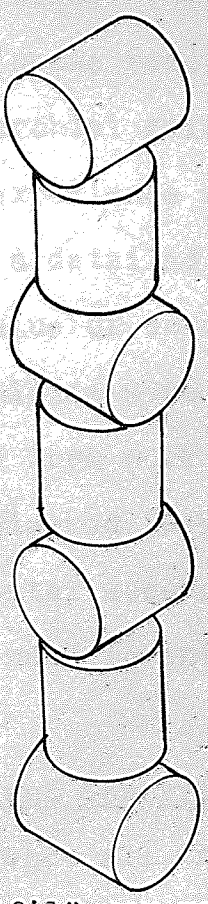

*Previously called "Actifil", now marketed by Norton-Hydronyl.

The Biopac 90 experiments were carried out as part of an undergraduate project by Cheong (11) under the author's direction. The results highlighted some of the difficulties of obtaining useful kinetic data from such a rig. Although the linear growth of the microbial film was readily followed by periodically weighing the Biopac string, the concentration dependence of the transition between exponential and linear growth could not be established.

Figure (4.4) based on Cheong's data shows the development of the microbial film with time on Biopac 90. Cheong (11) was able to estimate the surface area of Biopac 90 that was covered with microbial film by counting the individual surfaces of each piece of Biopac. In this way, it was clearly demonstrated that the substrate removal was a function of microbial film surface area, although it was not possible to quantify the proportion of this surface area that was effectively wetted. Figure (4.5) taken from Cheong's work shows the fraction of glucose removed as a function of Biopac surface covered with microbial film.

This experience with the Biopac rig emphasised the need for a detailed study of hydraulics and further confirmed the value of using the inclined plane for kinetic studies. Similar difficulties were encountered in the analysis of kinetic data obtained from work with Biopac 50, even though the hydraulics were considered (see Appendix 5). It was found that within the experimental accuracy, both $\frac{1}{2}$-order and first-order kinetics could be used to interpret the results.

4.8. Other Measurements and Observations.

Throughout all the experiments on the inclined plane and Biopac rigs, frequent microscopic

Figure 4.4. Weight of Microbial Film Developed on Biopac 90 .vs. Time.

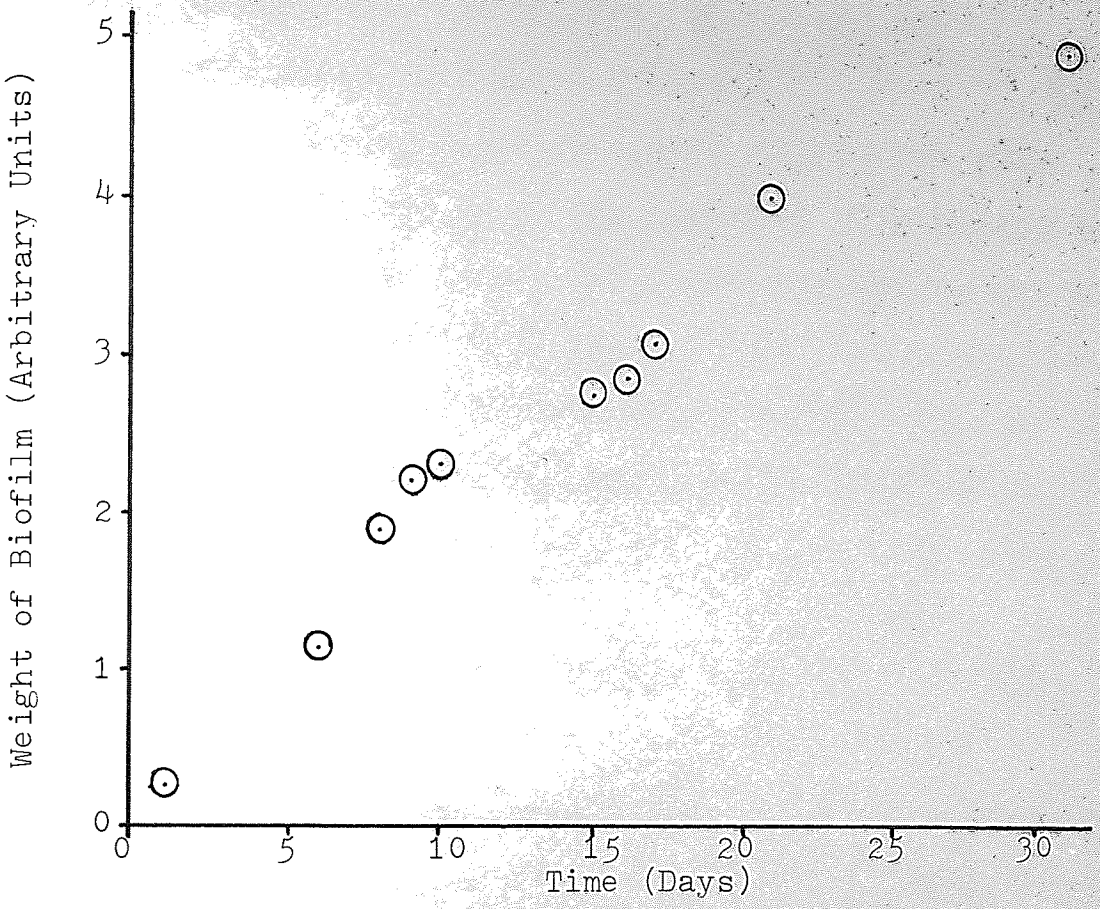

Figure 4.5. Fraction of Glucose Removed .vs. Area of Biopac Surface Covered with Biofilm.

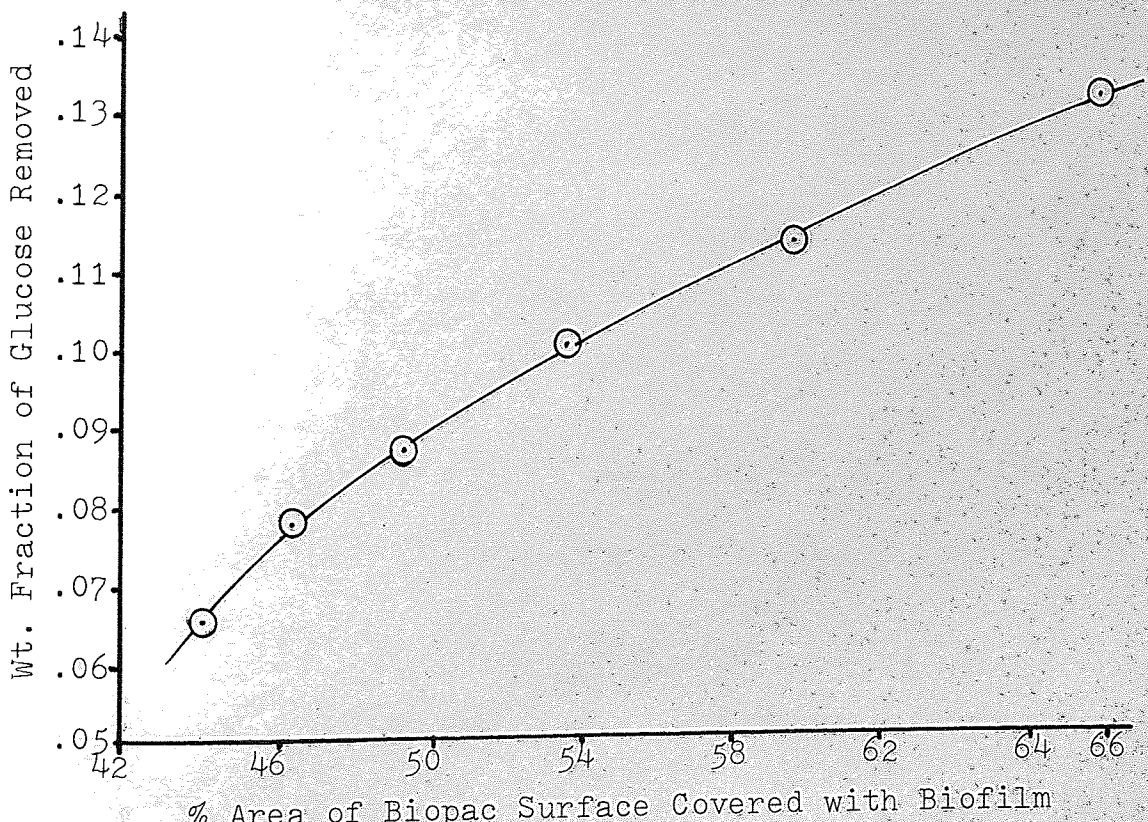

examinations of samples of microbial films were made. Changes in organism predominance and presence were noted and photographs were taken of typical examples.

During each experiment, notes were taken based on visual observations of the microbial film texture and colour, the degree of surface wetting and effluent turbidity.

At the end of each inclined plane experiment the microbial film was collected, weighed and dried to a constant weight at 105°C to evaluate the "Dry Wt%". These qualitative observations, the "Dry Wt%" measurements and a qualitative analysis of the microbial film thickness measurements are presented and discussed in the following chapter.

It was not possible to monitor the dissolved oxygen concentrations within the liquid films on the inclined plane and Biopac rigs: it was also felt that measurements using liquid samples taken at the inlet and outlet would have given no indication of oxygen profiles within the microbial film.

4.9 References.

1) Trinci, A.D.J. A kinetic study of the growth of Aspergillus nidulans and other fungi. J. Gen. Microbiol. 57, p11 - 24. (1969).

2) Hawkes, H.A. Effects of methods of sewage application on the ecology of bacterial beds. Ann. Applied Biology 47 (2), 339 - 349 (1959).

3) La Motta, E.J. Kinetics of growth and substrate uptake in a biological film system. Appl. Env. Microbiol. 31 (2), p286 - 293 (1976).

4) Heukelekian, H. & Crosby, E.S. Slime formation in sewage. Sewage Ind. Wastes 28, p 206 - 210 (1956).

5) Calley, A.G., Forster, C.F. & Stafford, D.A. (Editors) Treatment of Industrial Effluents. Hodder & Stoughton, London, Sydney, Auckland, Toronto. (1977).

6) Dubais et al. Colourimetric method for determination of sugars and related substances. Anal. Chem. 28 (3), (1956).

7) Hawkes H.A. Seminar for the National Water Council, at the University of Aston in Birmingham, April, 1977.

8) Rose, A.H. Chemical Microbiology. Butterworth, London (1965).

9) Chapman, B. Cooke, G.H. & Whitehead, R. Automated Analysis: The determination of ammoniacal nitrous and nitric nitrogen in river waters etc. The Inst. of Water Pollut. Cont. No.2 (1967).

10) Atkinson, B. & Daoud, I.S. Diffusion effects within microbial films. Trans. Inst. Chem. Engrs. 48, T245 - 254 (1970).

11) Cheong. Final year undergraduate project. Dept. Chem. Eng. University of Aston in Birmingham (1979).

CHAPTER 5

OBSERVED BEHAVIOUR OF MICROBIAL FILMS

5.1. Introduction.

During the experimental evaluation of the kinetic parameters on the inclined plane, some marked differences in the microbial film characteristics and behaviour were observed when using the different model effluents. These observations enabled some of the conditions which could give rise to ponding or turbidity to be identified. In addition it was found that the microbial film characteristics influenced the kinetic parameters and the necessary methods used in their evaluation. Consequently these observations are presented here, prior to the numerical evaluation of the kinetic parameters.

5.2. Observations Using an Intermediate Glucose Concentration (500mg/l).

The microbial film was brown in colour, being darker than that formed at the low glucose concentration. It had a firm texture, being tougher than the films formed at the high and low glucose concentrations; relatively large pieces of film could be picked up with forceps. As the film developed, apparently dry patches of mould appeared on the surface; closer inspection revealed that the mould was growing on top of the liquid film surface and producing aerial hyphae and fruiting bodies. In subsequent kinetic experiments the appearance of mould was taken to indicate that the F_{crit} level had been exceeded (see equation (2.7)) and that the film thickness measurements could be made less frequently.

One or two days after the appearance of mould, the film started to darken in colour, eventually becoming dark grey. The darkening of the microbial film often made it difficult to position the film thickness measurements

above the paint marks. As the film darkened gas bubbles began to form under the microbial film, which were visible from the underside of the perspex plane. The gas, when released, had the characteristic foul smell of anaerobic decay. The mould and gas formation are shown diagrammatically in Figure (5.1).

Figure (5.1). Diagrammatic Representation of Mould and Gas Formation from a Microbial Film.

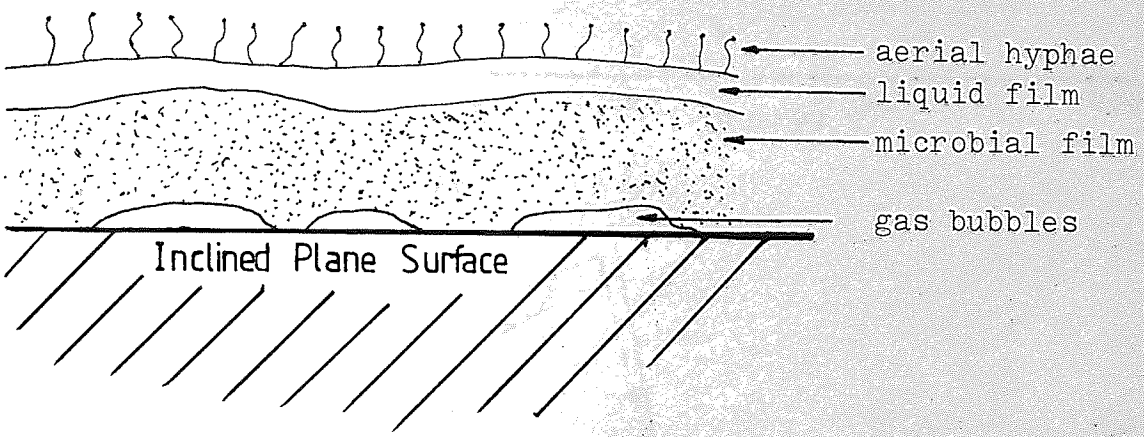

Eventually, large sections of microbial film peeled away, removing most of the film and leaving only a thin covering of microbes. A new microbial film then grew, and the sequence described above was repeated.

The sequence of film growth and loss is shown quantitatively in terms of average film thicknesses over 3 of the 8 sections of the plane and at selected single points in Figure (5.2). It will be seen that the single points follow the same pattern as the average film measurements although large differences between the individual points exist. The film thicknesses reached prior to sloughing tended to be greater nearer the inlet; as Figure (5.2a) shows. The sudden rise in the apparent growth rate at some points prior to sloughing is due to gas formation lifting the film. The sloughing cycle is shown to have a period of approximately

Figures(5.2a,b & c) Film Thickness Measurements .vs. Time at the Intermediate Glucose Concentration, 500mg/l

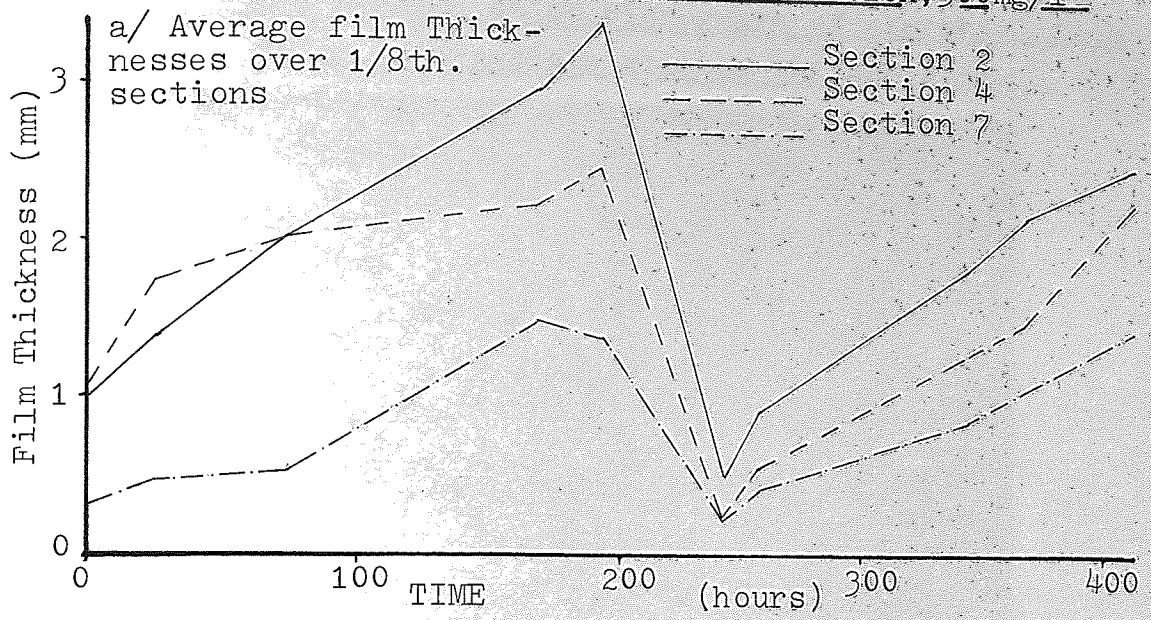

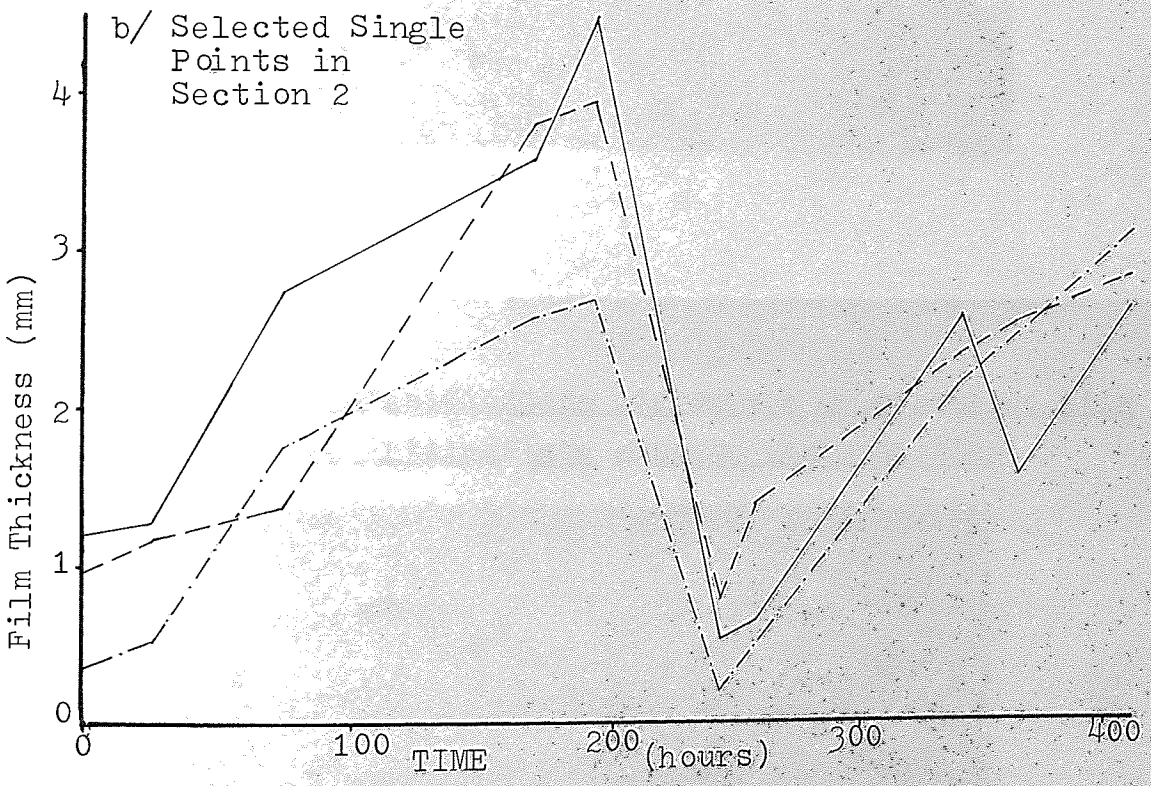

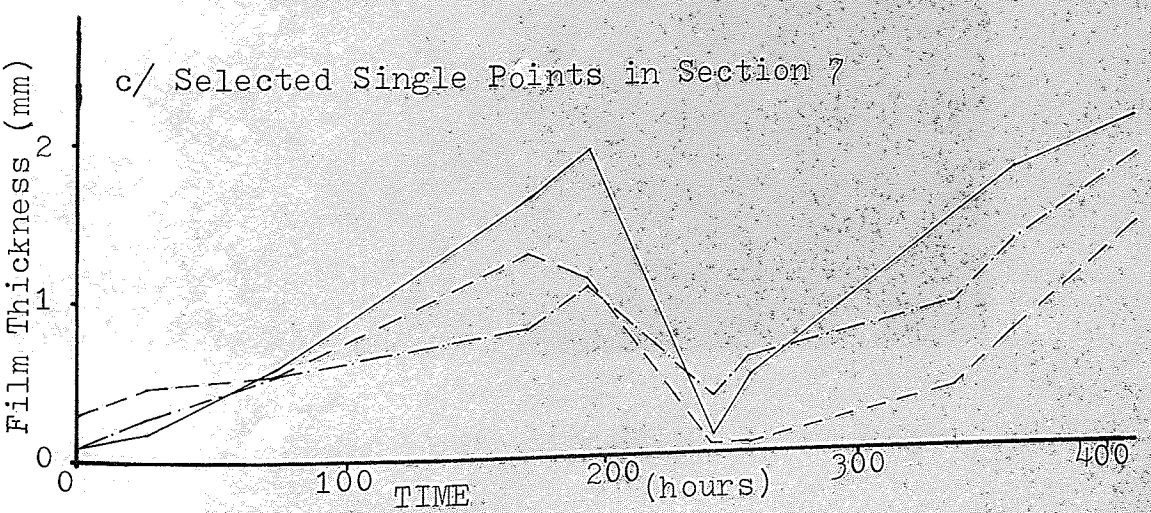

Figure 5.3 Low magnification micrograph of microbial film at an intermediate glucose concentration

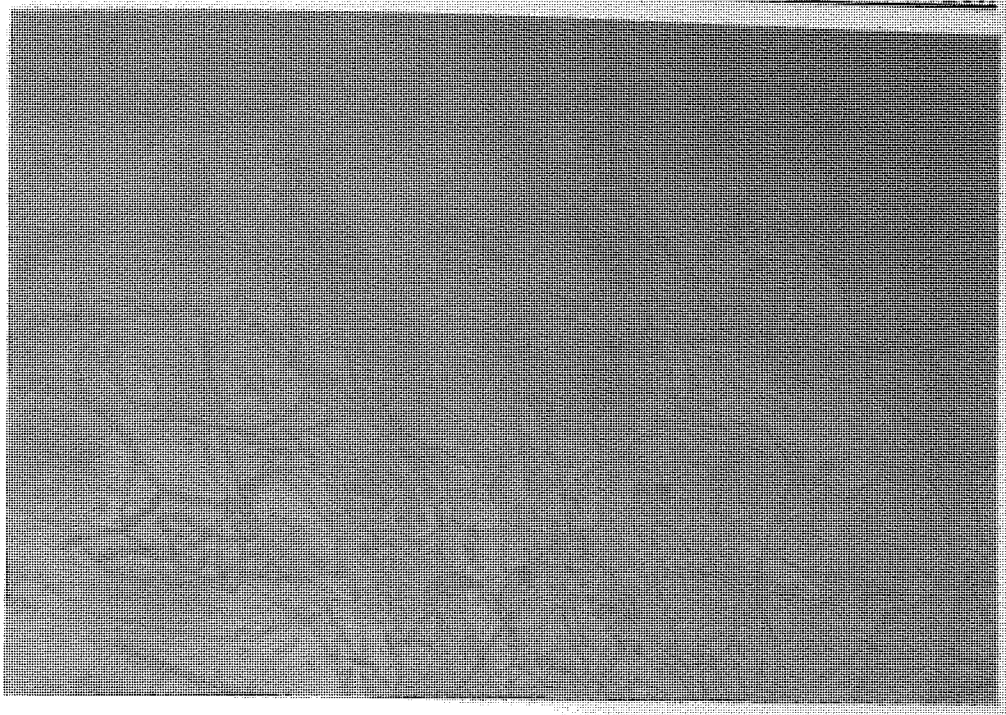

Figure 5.4 High magnification micrograph of microbial film at an intermediate glucose concentration

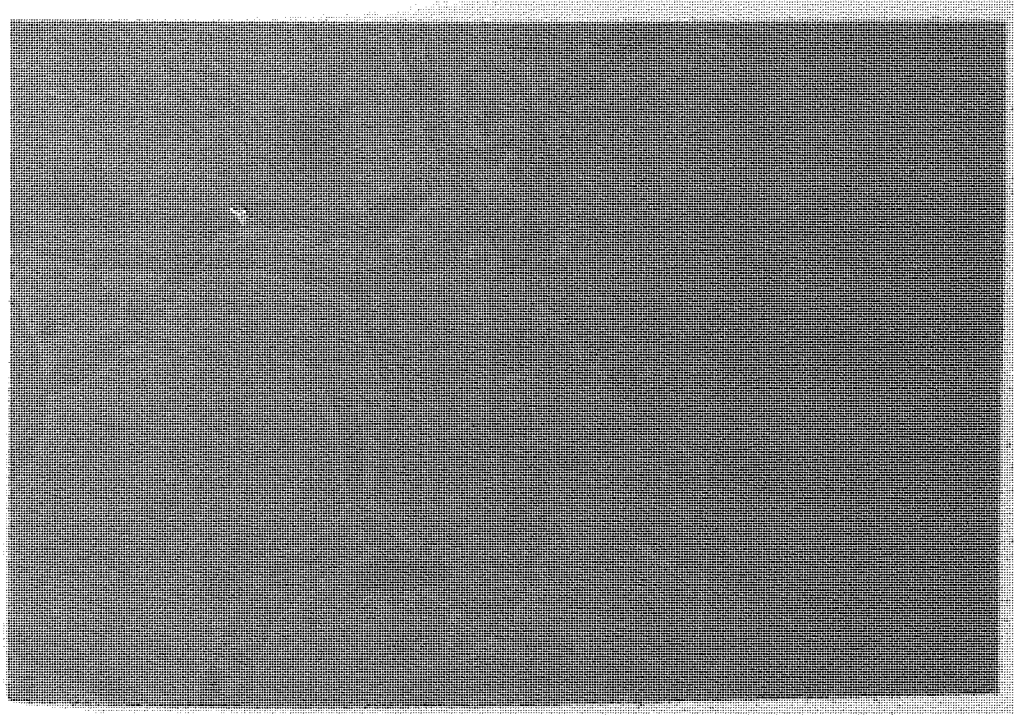

ten or eleven days.

When viewed under a microscope the microbial film was seen to consist of long, twisted and interwoven fungal hyphae with closely held bacteria (mainly bacilli) filling in the remaining spaces, as may be seen in Figures (5.3) and (5.4); the absence of Brownian motion indicated that the bacteria were firmly held in position. It was noted that after sloughing the remaining film consisted mainly of bacteria with a few short hyphae and fungal spores. The microbial film composition then returned to the condition described above within two or three days. No protozoa were seen throughout any of the experiments at this glucose concentration, and the effluent was always clear.

5.3. Observations Using a High Glucose Concentration (1000mg/l).

The microbial film was similar in colour to that formed at the intermediate glucose concentration. However, the film surface appeared to be smoother and more uniform than those formed at the intermediate and low glucose concentrations. As the film developed no changes in its appearance were noted until large pieces of film broke away, leaving a thin covering of microbes and patches of undamaged film. A new film then grew and the sequence was repeated.

Figure (5.5) shows the film growth and loss in terms of average measurements over 2 of the 8 sections of the plane and for selected single points. The single point measurements are seen to follow the pattern of the averaged measurements, although contrary to visual observations the differences between individual measurements were large. Sloughing behaviour is clearly shown, each cycle occupying a period of approximately five days; nevertheless, at some

Figures(5.5a,b & c) Film Thickness Measurements ,vs. Time at the High Glucose Concentration,1000mg/l

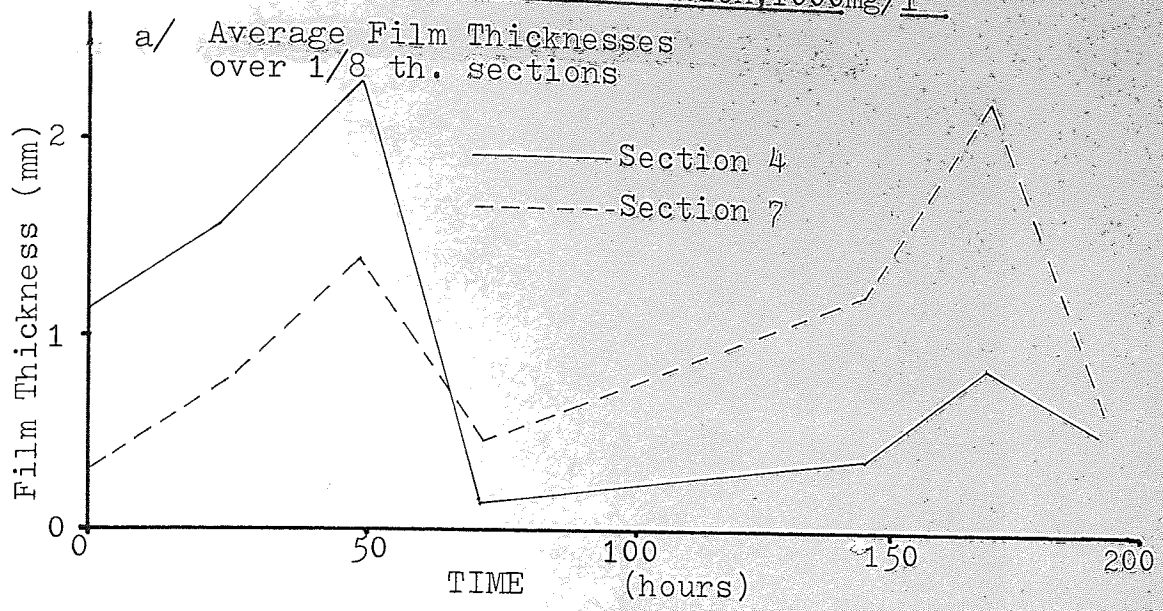

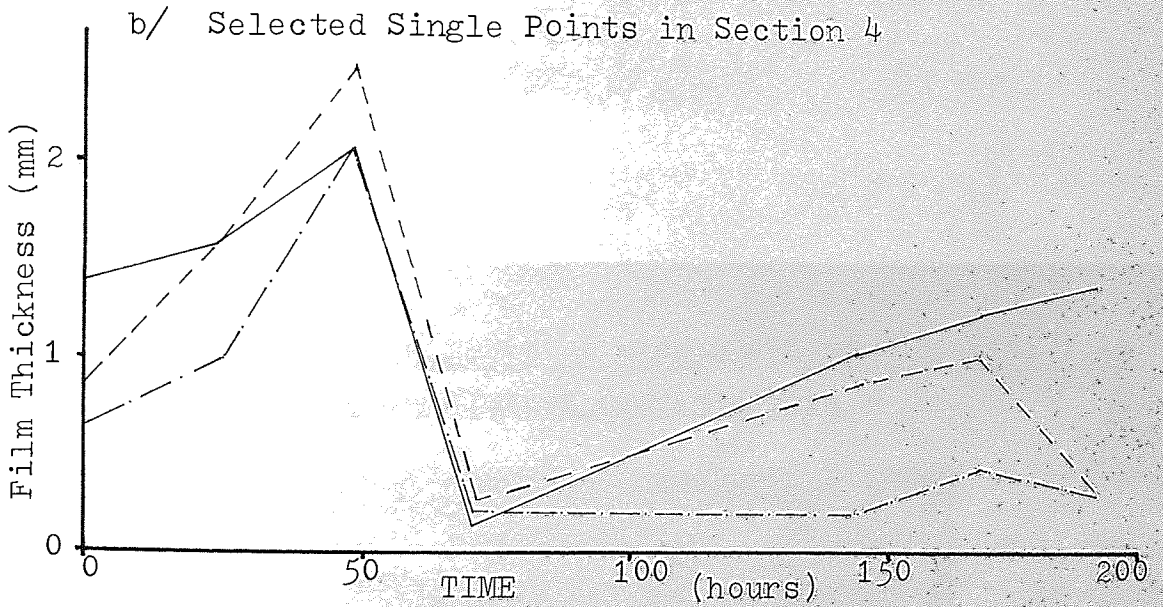

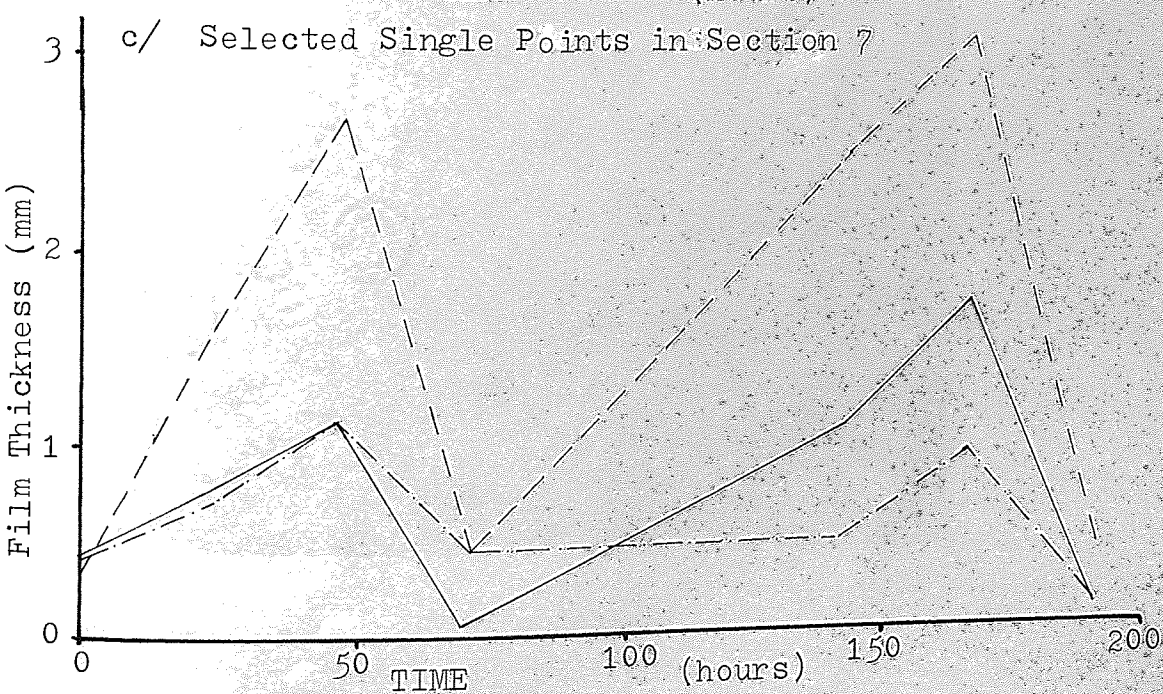

Figure 5.6 Low magnification micrograph of microbial film at a high glucose concentration

Figure 5.7 High magnification micrograph of microbial film at a high glucose concentration

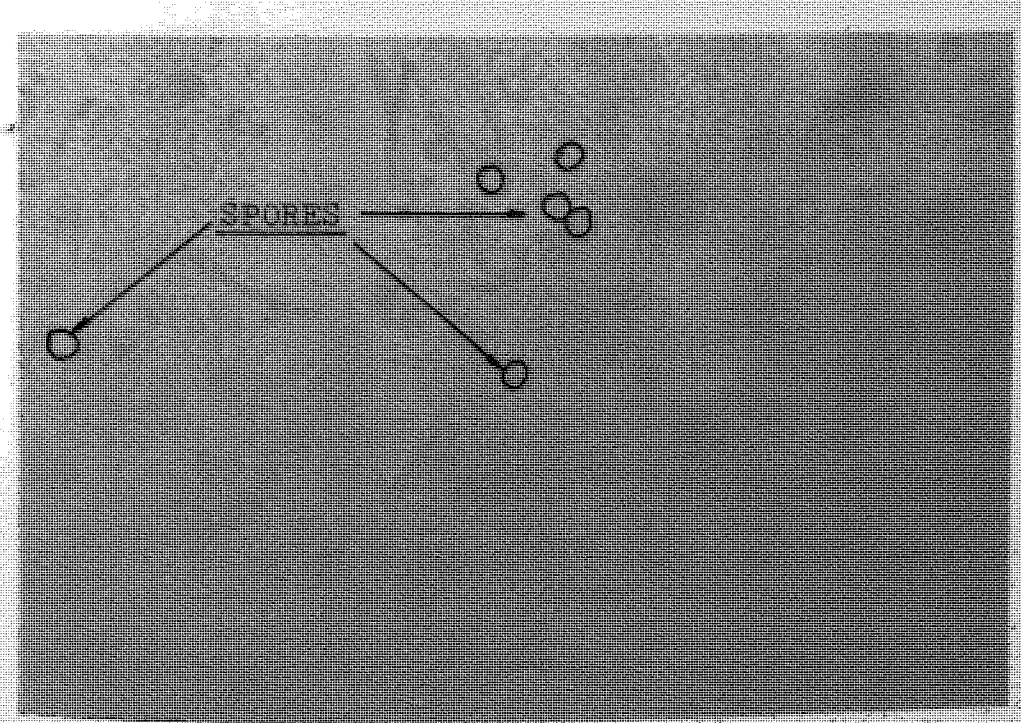

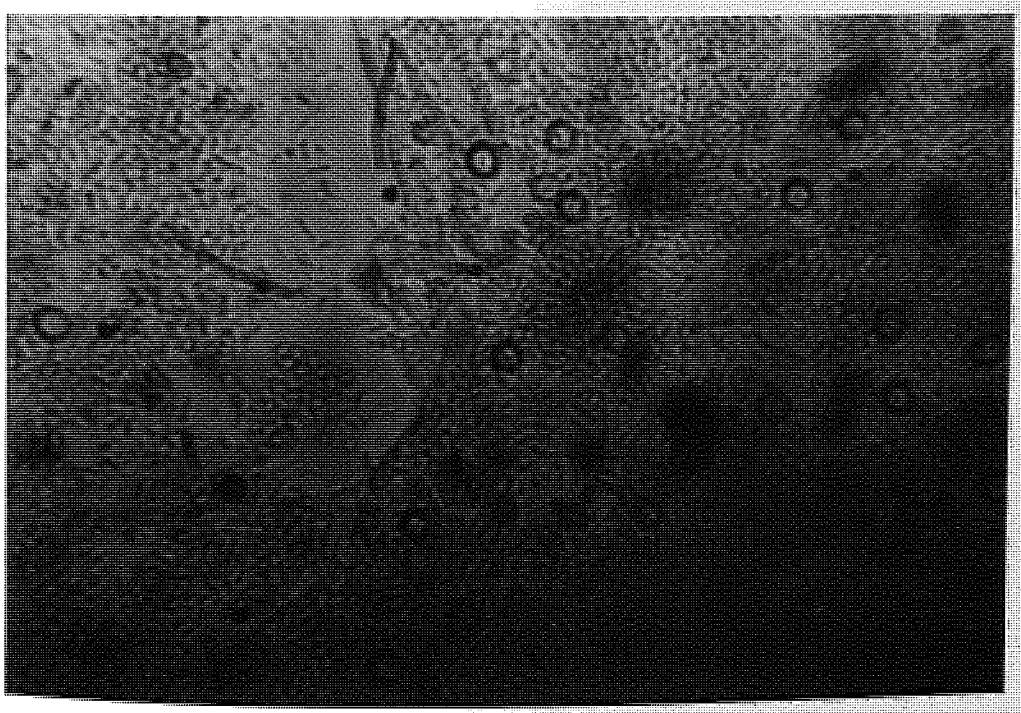

points, there was a tendency for patches of undamaged film to remain, as illustrated by the solid line in Figure (5.5b).

When viewed under the microscope the microbial film was seen to consist almost exclusively of bacteria, mainly bacilli, which were closely held together. Again the absence of Brownian motion indicated the bacteria were firmly held in position. A few, generally short, fungal hyphae and many fungal spores were also present. These features are shown in Figures (5.6) and (5.7). Protozoa were also seen but only on rare occasions; they were observed to feed only in regions where the bacteria were less closely packed. The effluent was usually slightly turbid despite the presence of protozoa.

5.4. Observations Using a Low Glucose Concentration (100mg/l).

The microbial film was pale brown in colour and had a loose, soft texture with an apparently uneven surface. It did not cohere or adhere to the perspex plane well and easily broke up and away from the plane if disturbed. As the film developed, small pieces of film broke away in an unpredictable manner and this became more frequent as film thickness increased; eventually, a point was reached when the film appeared to change little from day to day. Figure (5.8) shows the film behaviour in terms of average measurements over 2 of the 8 sections of the plane and at selected single points. It will be noted that film thickness rose and fell in a quite random fashion at single points, while the averaged figures slowly attained a steady state. This behaviour is consistent with a shedding mechanism, although it should be noted that the averaged film thicknesses were relatively high after about one week.

When viewed under the microscope the microbial

Figures(5.8a,b & c) Film Thickness Measurements .vs. Time at the Low Glucose Concentration,100mg/l

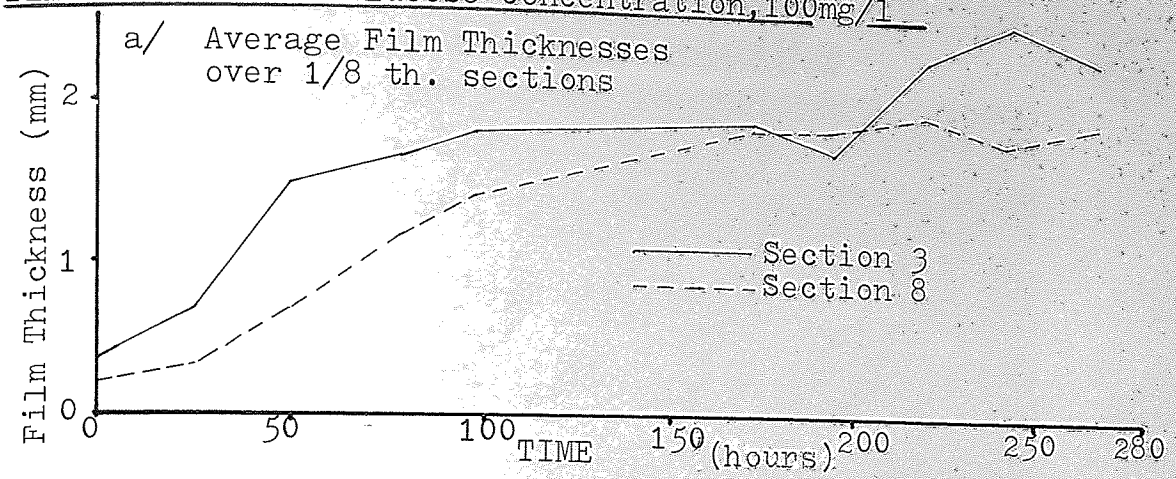

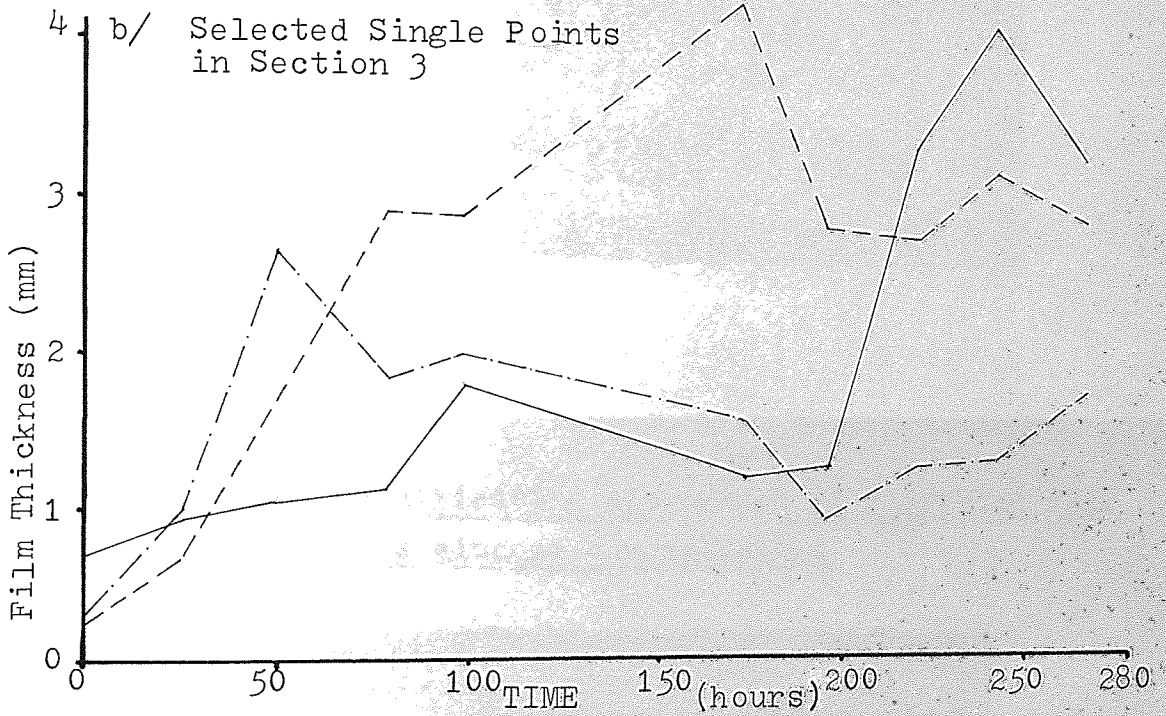

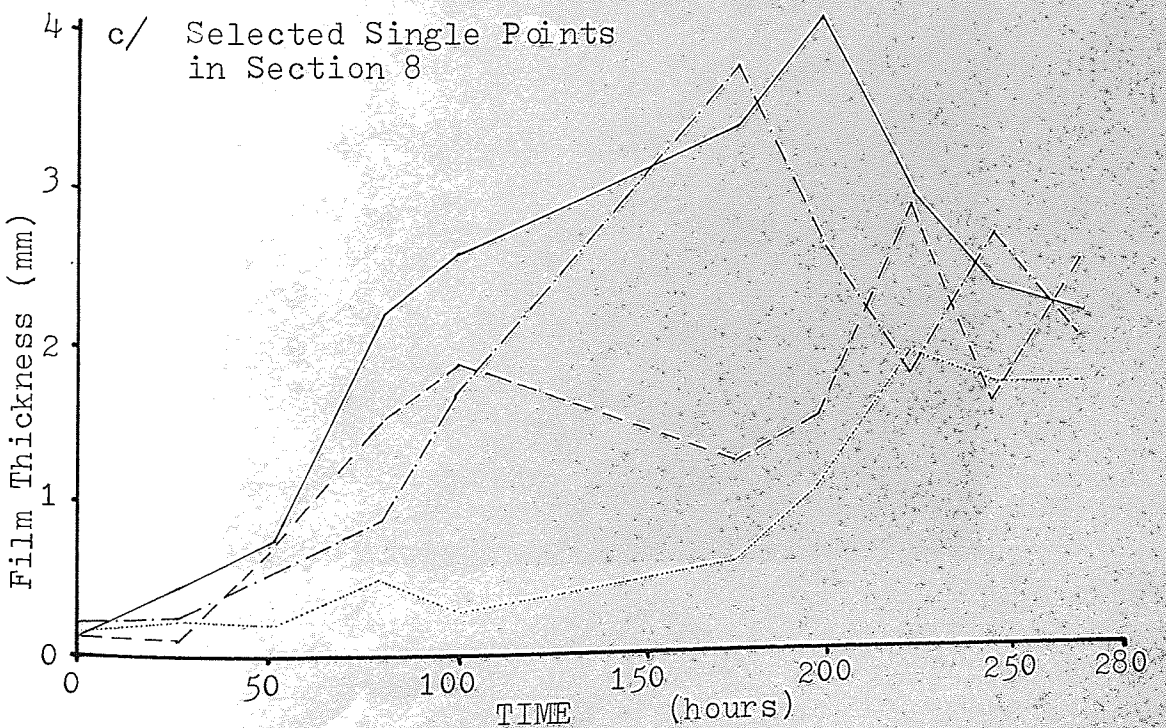

Figure 5.9 Low magnification micrograph of microbial film at a low glucose concentration

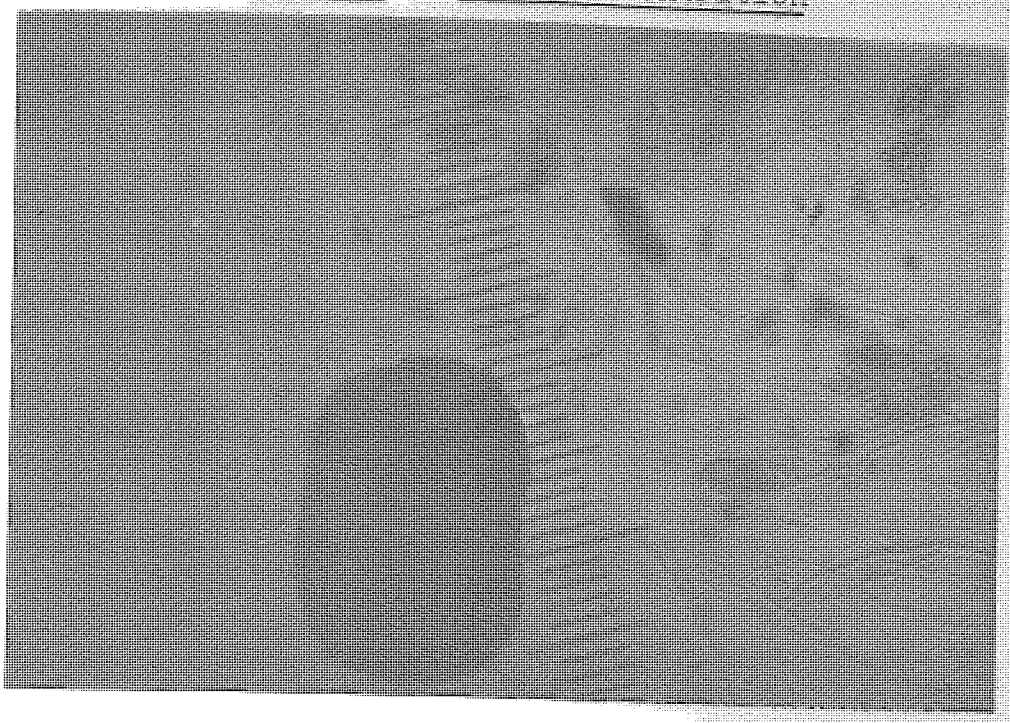

Figure 5.10 Low magnification micrograph of microbial film at a low glucose concentration

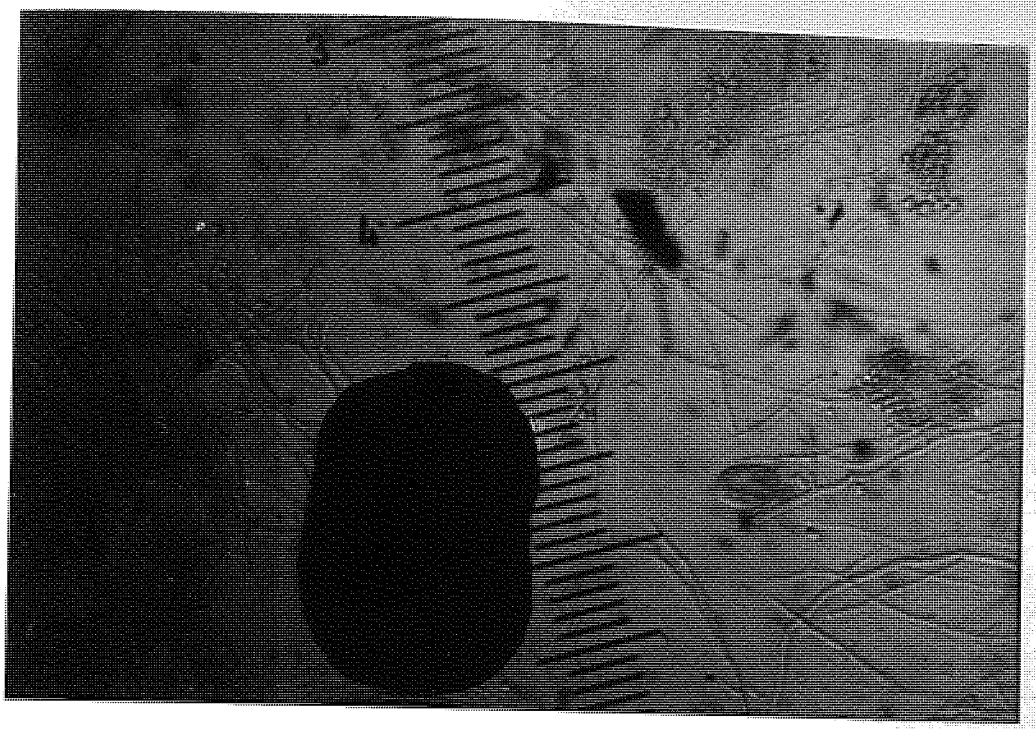

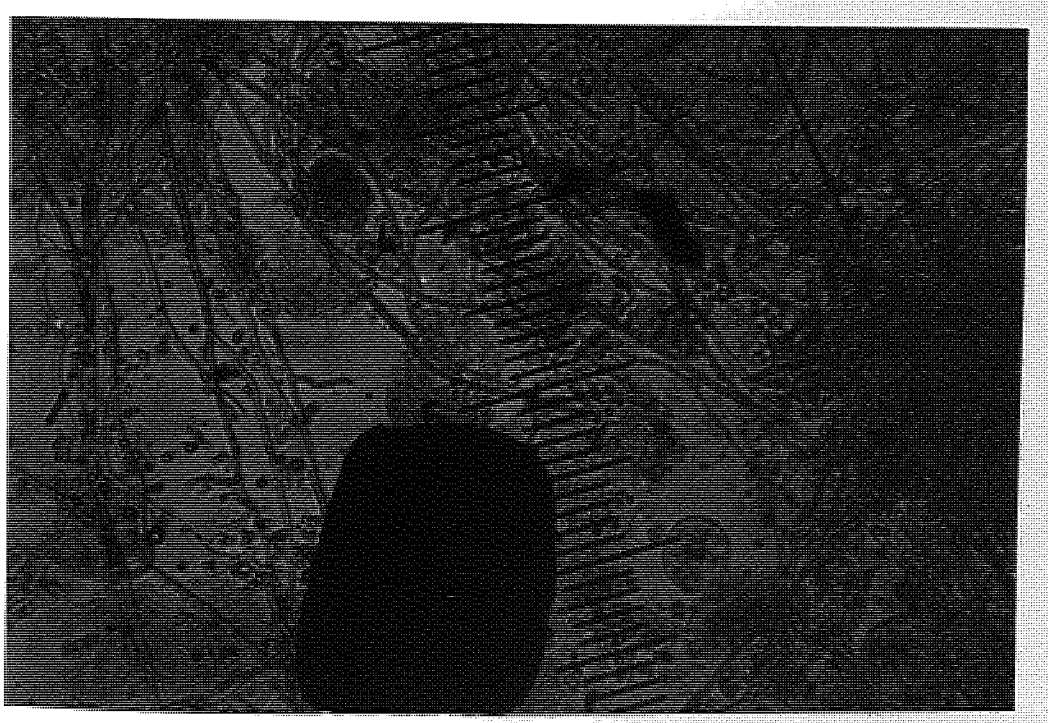

film was seen, in the early stages of development, to consist of bacteria and short fungal hyphae; generally the appearance was similar to that of the film formed with the intermediate concentration shortly after sloughing. As the film developed, its composition changed and it appeared to consist mainly of long twisted hyphae with void spaces between the hyphae; the bacteria were then only seen in small patches. These later features are shown in Figures (5.9) and (5.10). The presence of Brownian motion and freely motile bacteria indicated that the bacteria were not firmly held in position. Protozoa were frequently observed and were seen to feed only on the bacteria. The relative quantities of fungi and bacteria did not, however, appear to depend on the presence of protozoa. It was noted that the movement of protozoa could be completely restricted by fungal hyphae and partially resticted by any dense patches of bacteria: Figures (5.11a and b) show protozoa under these conditions. The effluent was always turbid.

5.5. Observations Using a Low Glucose Concentration (100mg/l) with a Low Carbon/Nitrogen Ratio.

The microbial film was dark brown, being darker than that formed at the intermediate glucose concentration and standard C/N ratio. In texture, it was like a loose, wet powder and had a smooth surface; it did not adhere to the perspex plane and broke away in small pieces if disturbed.

When viewed under the microscope it was seen to consist almost exclusively of bacteria which were closely, but not firmly, held together; Brownian motion was observed. Fungal spores and short hyphae were also observed, as was the case when using the high glucose concentration and standard C/N ratio. No protozoa were seen. The effluent was turbid.

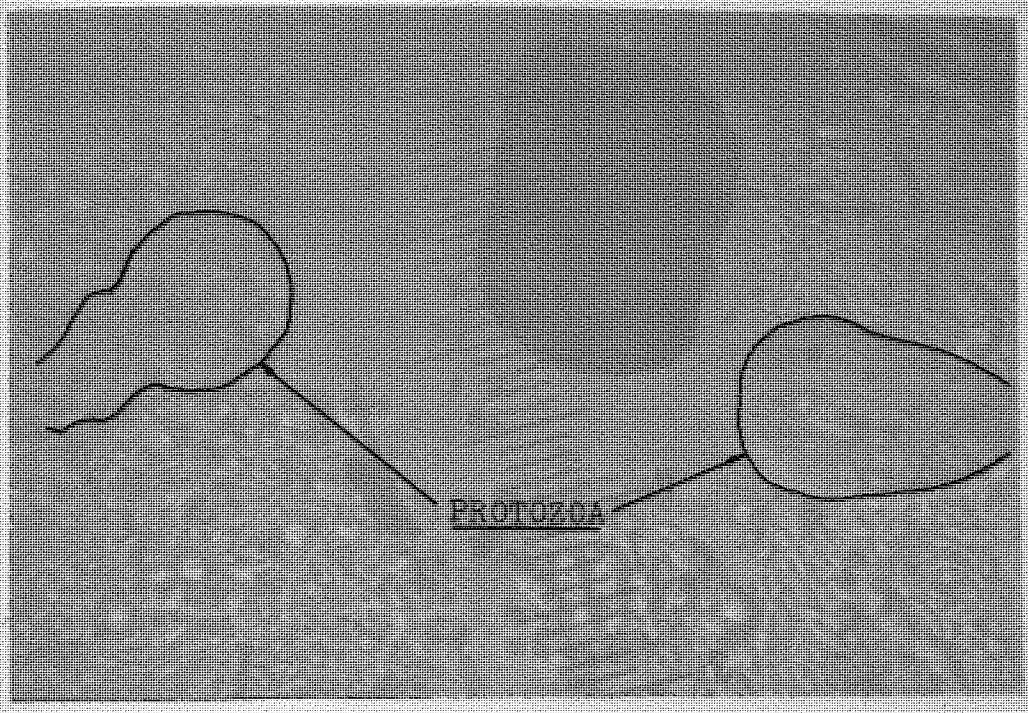

Figures 5.11a & b Micrographs of microbial film showing the restricted movement of protozoa

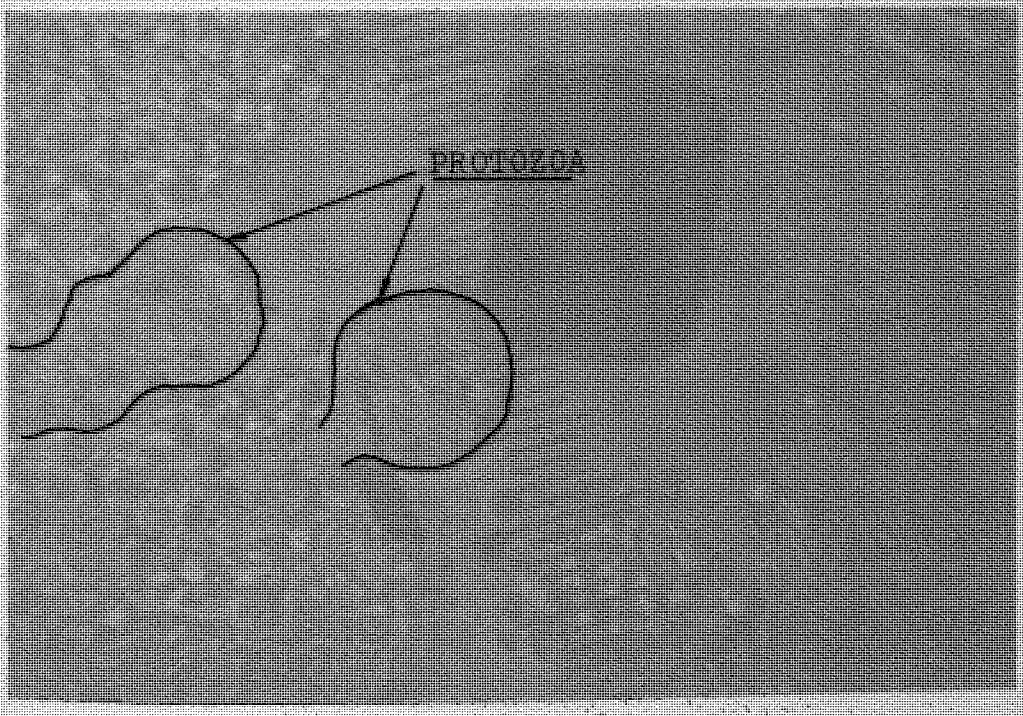

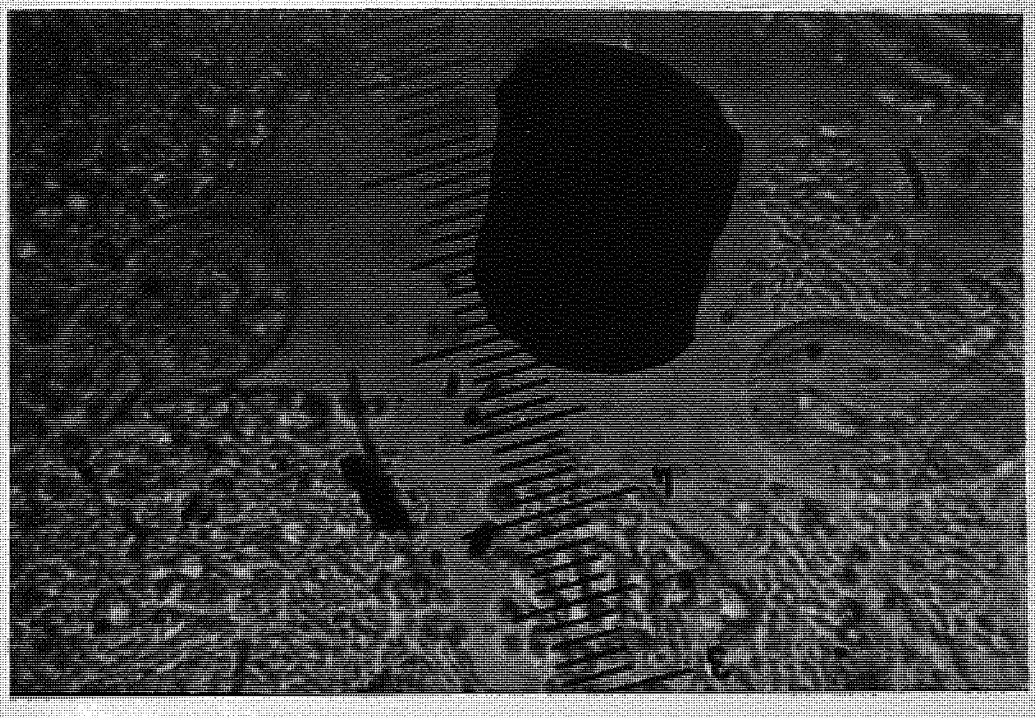

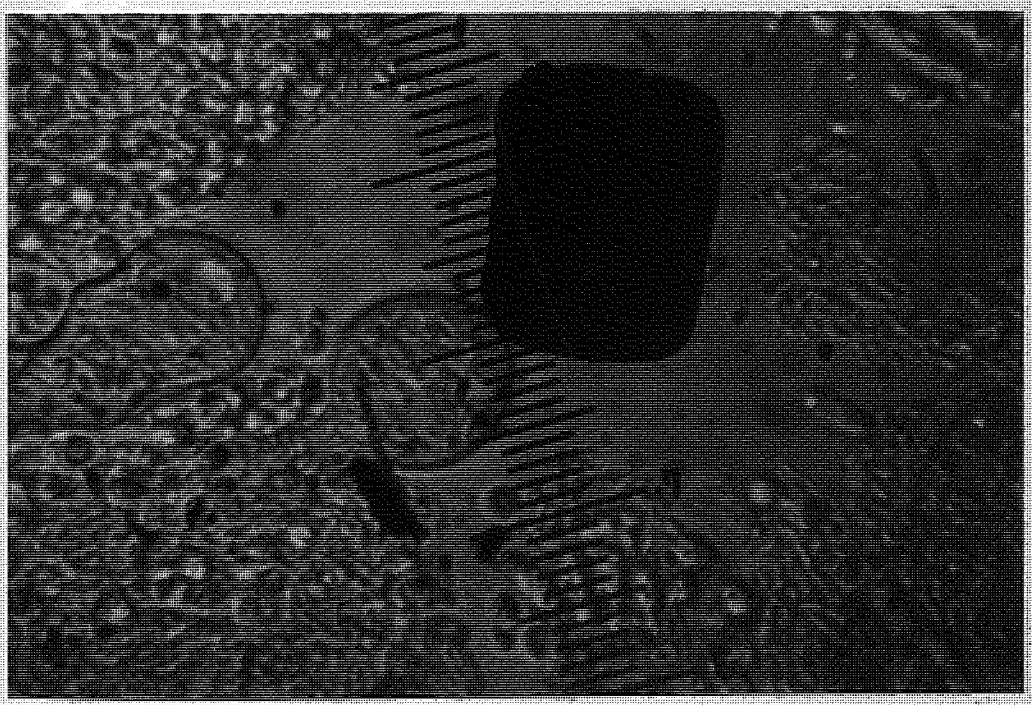

5.6. Observations Using a High Glucose Concentration (1000mg/l) with a High Carbon/Nitrogen Ratio.

In this case, the microbial film was pale brown in colour, being similar to that formed when using the low glucose concentration and standard C/N ratio. It appeared to consist of small pieces of cotton wool, about 1 to 2mm in diameter, set in a gel; the surface was nevertheless smooth and the film cohered and adhered to the perspex plane well, but was not as tough as the film formed during experiments with effluent of intermediate glusose concentration. As the film developed its behaviour was similar to that of the film formed at the intermediate glucose concentration but mould growth, film darkening and gas formation were less pronounced.

When viewed under the microscope the microbial composition was seen to be similar to that of the film formed at the intermediate glucose concentration. The impression gained by the author was that, whilst the film was very coherent, it contained fewer bacteria than were present in the film formed at the intermediate glucose concentration and the fungi were in discrete colonies. No protozoa were observed. The effluent was clear.

5.7. A Summary.

The key points described in the above section are summarised in Table (5.1) overleaf.

Table(5.1) Summary of Microbial Film Properties and Behaviour

Model Effluent	Film Properties				Overall Film Behaviour	Dry Wt. %	Microscopic Observations			Effluent condition
	Colour	Texture	Surface	Adhesion to Perspex			Bacteria	Fungi	Protozoa	
500mg/l Glucose Std. C/N	Brown	Tough	Mouldy prior to sloughing	Good	Sloughs after gas formation	1.43	Closely and firmly held	Long, twisted hyphae	None seen	Clear
1000mg/l Glucose Std. C/N	Brown	Gel-like	Apparently smooth	Good	Sloughs frequently	1.25	Closely and firmly held	Few short hyphae, many spores	Seen occasionally	Turbid
100mg/l Glucose Std. C/N	Pale brown	Soft, loose	Uneven	Poor	Shedding	0.63	Few, loosely bound	Long, twisted hyphae	Often seen	Turbid
100mg/l Glucose Low C/N	Dark brown	Like a wet powder	Apparently smooth	Poor	Shedding	1.94	Closely but loosely held	Few short hyphae many spores	None seen	Turbid
1000mg/l Glucose High C/N	Pale brown	Tough/ gel-like	Apparently smooth	Good	Sloughs	1.53	Firmly but less closely held	Long, twisted hyphae	None seen	Clear

5.8. Discussion.

Many of the physical characteristics of high- and low-rate biological filters reported in the literature and discussed in Chapter 3 have been reproduced on the inclined plane. Some of these characteristics have been quantified, and others which have not previously been reported, have been observed.

The type of tough, thick microbial films, which are reported to cause ponding, were formed when using the effluent of intermediate glucose concentration (500mg/l) with a standard C/N ratio and the effluent of high glucose concentration (1000mg/l) with a high C/N ratio. Although the film formed at the intermediate glucose concentration sloughed after 10 to 11 days on the inclined plane, the film thicknesses reached would be sufficient to cause ponding in a packed bed. Despite reports (1) that such films are predominantly fungal in composition, comparable quantities of both fungi and bacteria were found to be present during the author's work.

A predominantly fungal film was only seen when using effluent at the low glucose concentration (100mg/l) with a standard C/N ratio. This type of film was not tough due to its lack of cohesion and so would be unlikely to support "ponds" of liquid. In addition, this type of film attained, after an initial period, a constant local average thickness as a result of continuous shedding of material.

Poor cohesion and shedding were also observed with the bacterial film produced at the low glucose concentration with a low C/N ratio; again this type of film is unlikely to cause ponding. However, good cohesion is not the only condition needed to cause ponding. The bacterial film produced at the high glucose concentration with the standard C/N ratio

cohered well but sloughed every 5 days; consequently it was not possible for a thick film to develop. Ponding is, therefore, only likely to occur in the case of films that cohere well and possess a long sloughing cycle.

The microbial composition of the films was found to vary on altering the glucose concentration, whilst maintaining a standard C/N ratio. This suggests that the C/N ratio does not govern the film composition, although this is often reported to be the case (see Section 3.2). The results suggest that it is the absolute concentration of the carbon and/or nitrogen that influences the microbial film composition. It is readily apparent from the information given in Table (5.2) that fungi are present over the full range of glucose concentrations but are absent when there is a high nitrogen concentration.

Table (5.2) Effect of effluent Composition on Occurence of Bacteria and Fungi.

Glucose Concentration	C/N Ratio	Nitrogen Concentration	Most Common Organisms
High	Std.	High	Bacteria
Intermediate	Std.	Intermediate	Bacteria & Fungi
Low	Std.	Low	Fungi
High	High	Low	Bacteria & Fungi
Low	Low	High	Bacteria

It may be concluded that the high nitrogen concentration, directly or indirectly, inhibits fungal growth. It is also clear from Table (5.2) that bacteria were only absent when both the carbon and nitrogen concentrations were low: however, bacteria were predominant in the early stages

even when using this effluent, and so it is possible that bacteria will grow under these conditions in the absence of fungi. Under conditions in which there is a lack of a suitable nitrogen source, some fungi adjust their metabolism and produce different metabolic by-products (2,3). It is possible that this has happened in the author's work, the presence of the metabolic by-products and the low glucose concentration being sufficient to inhibit the rapid growth of the bacteria.

The poor cohesion and adhesion, the presence of Brownian motion and the powdery texture of the bacterial film formed when using the low glucose concentration with the low C/N ratio may be attributed to the lack of extracellular polypeptide or polysaccharide slime: this, in turn, may be due to the absence of a sufficient carbon source for slime production. Similarly, the loose texture and poor cohesion of the fungal film formed when using the low glucose concentration with the standard C/N ratio may ultimately be attributed to the low level of the carbon source and the relatively low quantity of bacteria available to produce the slime.

The tougher films were formed when fungi and bacterially produced extracellular slime were present together. A useful analogy, for descriptive purposes, can be drawn between such films and glass fibre reinforced plastic resins. The fibrous fungi, like glass fibres, have no strength as a bulk material, and the bacterially produced slime, like plastic resin, will break up easily; however, the respective materials, when combined, form much tougher composites. As suggested in Chapter 3, this composite strength may partly account for the long sloughing cycle (10 to 11 days) of such films compared to a cycle of 5 days for an essentially bacterial film held together by extracellular slime. As was also suggested

in Chapter 3, the sloughing of a predominantly bacterial film may only require a loss of adhesion between the microbial film and the packing, brought about by the reabsorption of the extracellular slime. Breakdown of the composite films (fungi and bacterial slime) is likely to be brought about by the reabsorption of the slime followed by the bacterial degradation of the fungi. The time factor for fungal breakdown is reflected in the difference between the period of the two sloughing cycles (about 5 days) and is comparable with the results of Tomlinson (4) which are also discussed in Chapter 3.

The conditions in which fungi, bacteria or the bacterial extracellular slime are absent in the microbial film have been explained above as being due to some form of direct or indirect inhibition. Fungi, bacteria and the extracellular slime may, therefore, be expected to be present unless some adverse condition exists. It is quite clear that the film strength will reach a maximum arising at a given fungal-bacterial slime combination. Although this combination has not been quantified the author anticipates that such a film would be similar in character to that formed at the intermediate glucose concentration with the standard C/N ratio. Hence, glucose concentrations lower than about 500mg/l may give films with a reduced strength due to a reduction in the bacterial slime. Similarly higher nitrogen salt concentrations may be expected to weaken the film by reducing the quantity of fungi. One practical method of reducing the concentration of the carbon source is by the use of recycle. The change in microbial film composition which may be expected to arise with recycle may explain the apparent success in preventing ponding by this method. The nitrogen salts concentration may be increased by direct addition of say chemical fertilisers or by mixing the

effluent with another effluent of a higher nitrogen concentration: for example, the domestic sewage main may be tapped to supplement the nitrogen in an industrial effluent. This latter method is favoured as the nitrates may become an additional effluent problem.

Any attempts to avoid ponding must take into account the effects of temperature. As discussed in Chapter 3, fungi are likely to become more dominant in colder months, and so, during this period, the methods suggested for reducing fungi may be less effective. Also, reabsorption of extracellular slime and fungal degradation processes will be slower at reduced temperatures and the substrate penetration depth may increase (see Section 2.5), in which case, the ponding is more likely to occur.

It was noted above that the protozoa preyed exclusively on bacteria and could not move within parts of a film which contained firmly held fungal hyphae. This restriction in movement prevents the protozoa from feeding and may explain why they were not seen in the tough, cohesive film. Protozoa were seen when using high and low glucose concentrations with standard C/N ratios, thus demonstrating that protozoa are able to grow at high and low glucose and nitrogen concentrations. They were not observed in the presence of the low glucose concentration with the low C/N ratio and at the high glucose concentration with the high C/N ratio. However, it should be noted that the inability to find any protozoa is insufficient evidence alone to suggest that the conditions were unfavourable for development of protozoa.

Effluent turbidity arising from microbes and small pieces of microbial film in suspension was most apparent under conditions in which the films did not cohere well and

were prone to shedding. Conversely, clear effluents were produced following the formation of tough, cohesive films which are most likely to cause ponding. It is, therefore, suggested that protozoa do not cause turbidity, but are only likely to occur in films which tend to give rise to turbid effluents.

Turbidity in the final effluent is undesirable and may be reduced by manipulating the conditions so that the formation of relatively tough, cohesive films is favoured; at the same time, this will tend to cause ponding. On the other hand, attempts to reduce ponding may give rise to effluents which are turbid. Consequently, a compromise position should be pursued.

5.9 References.

1) Williams, I.L. A study of factors affecting the incidence and growth rates of fungi in sewage bacteria beds. M.Sc. thesis, University of Aston in Birmingham, (1971).

2) Kristiansen, B. & Sinclair, C.G. Production of citric acid in continuous culture. Biotechnol. Bioeng. 21, p297 - 315 (1979).

3) Davies, I.W. & Sutherland, I.W. Microbial Physiology: Basic Microbiology Volume 4. Blackwell Scientific Publications, Oxford, London, Edinburgh, Melbourne.

4) Tomlinson, T.G. Some aspects of microbiology in the treatment of sewage. J. Soc. Chem. Ind. 61, p53 - 58 (1942).

CHAPTER 6

EVALUATION AND INTERPRETATION OF KINETIC PARAMETERS

6.1. Introduction.

The two bulk rate equations for the removal of the rate-limiting substrate that arise from zero-order kinetics coupled with diffusion are:-

$$(-r_a) = k_o F \qquad (2.4)$$

$$(-r_a) = \sqrt{2 k_o D C} \qquad (2.5)$$

where

C ——— concentration of the rate-limiting substrate (ML^{-3})

D ——— apparent coefficient of diffusivity of the rate-limiting substrate through the microbial film ($L^2\theta^{-1}$)

F ——— microbial film thickness (L)

k_o ——— intrinsic zero-order rate constant ($ML^{-3}\theta^{-1}$)

$(-r_a)$ ——— rate of substrate removal per unit wetted area of substrate

The zero-order rate constant, k_o, may be evaluated from an average microbial film thickness and a substrate mass balance over the inclined plane when equation (2.4) is known to apply, i.e. when the thickness of the microbial film is such that the condition $F < F_{crit}$ is satisfied. F_{crit} is defined by setting the two rate equations equal, thus:

$$F_{crit} = \sqrt{\frac{2DC}{k_o}} \qquad (2.7)$$

Under this condition, the bulk zero-order equation may apply for any substrate and the individual k_o values may be evaluated. As previously stated in section (4.5), local concentration measurements could not be used to evaluate the F_{crit} profile; instead, the limit of the exponential phase for microbial film growth was used.

6.2. Evaluation of the F_{crit} Profile on the Inclined Plane.

If experimental data are plotted as in Figure (6.1), F_{crit} cannot be evaluated with confidence because of uncertainty of the changeover from exponential to linear growth.

Figure (6.1) Microbial Film Thickness as a Function of Time.

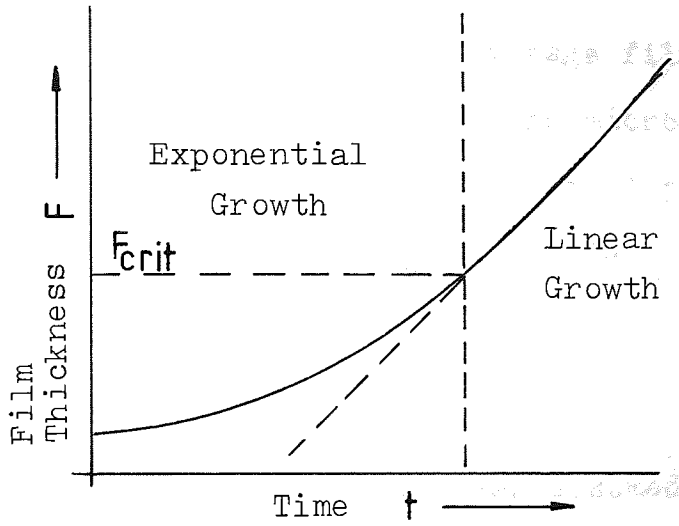

An alternative method is to plot microbial film growth rate against film thickness as shown in Figure (6.2). Such a plot should make it easier to locate F_{crit}.

Figure (6.2) Microbial Film Growth Rate as a Function of Film Thickness.

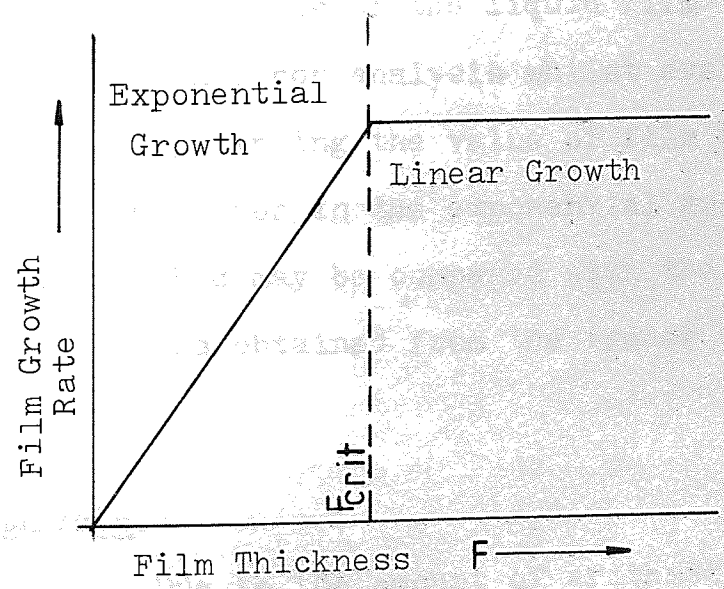

Analysis From Measurements at Single Points.

As discussed in section (5.4), if either parts of the microbial film are continuously shed or isolated patches stop growing due to liquid channelling, then the average film thickness will not provide a satisfactory measure of growth at specific points on the inclined plane; indeed, it is possible that the film at single points may be shedding and regrowing exponentially while the average film thickness is constant. However, if the change in the microbial film thickness is considered at each measurement point, periods of film loss and zero growth may be identified and data at such times can be excluded from the average.

Liquid Film Thickness Estimates.

So far, it has been assumed that the actual microbial film thickness was the distance measured using the converted micrometer, shown in Figure (4.2). However, there was a thin, flowing liquid film on top of the microbial film which was included in these measurements.

It was not possible to measure this liquid film thickness directly, since the film only formed when the microbial film covered the perspex surface of the inclined plane. However, an estimate of the liquid film thickness could be made from an error analysis whilst evaluating F_{crit}: this was achieved by finding the value of film thickness which minimised the error in the exponential growth rate. The results of this method may be compared with the values of liquid film thickness obtained from the tracer studies - see section (8.6).

Computer Analysis.

Due to the amount of arithmetic involved

in analysing data taken from many individual measurement points and the added task of estimating liquid film thickness, a computer program was used to evaluate the F_{crit} profile based on the following assumptions:

i) the liquid film thickness was uniform over the entire inclined plane surface.

ii) during the exponential phase, the growth rate was constant over the entire inclined plane,

iii) the liquid flow over the surface of the inclined plane could be modelled as a series of eight stirred tanks and an average F_{crit} in each of these sections evaluated,

iv) the F_{crit} value reached in one section did not affect values of F_{crit} in any other down-stream section.

This latter assumption could cause large errors in F_{crit} values, particularly if sloughing, as opposed to shedding, occured.

The algorithm, computer flow diagram and computer listing for the evaluation of F_{crit} profiles are presented in Appendix 2.

Results.

The results of the computer analyses are shown in Table (6.1) for the three glucose concentrations at the standard C/N ratio: each experiment was duplicated.

6.3. Evaluation of the Apparent Diffusivity of the Rate-Limiting Substrate from Values of F_{crit}.

The apparent coefficient of diffusivity of the rate-limiting substrate through the microbial film may be evaluated from F_{crit} values alone, assuming that there is plug-flow of liquid and that oxygen is not the limiting substrate. The method does not depend on the extent of substrate

Table 6.1 Results of the Computer Analysis of Microbial Film Thickness Measurements.

Glucose Concentration (mg/l)	Exponential Growth-Rate ($hour^{-1}$)	Liquid Film Thickness 'δ' (mm)	F_{CRIT} for SECTIONS							
			1	2	3	4	5	6	7	8
100	0.0125	0.10	2.24 ±1.03	2.24 ±1.47	1.70 ±0.99	1.50 ±0.69	1.70 ±0.70	2.06 ±0.89	1.10 ±0.62	1.80 ±0.76
	0.0090	0.10	2.00 ±1.34	2.28 ±1.51	1.50 ±0.93	1.60 ±1.00	1.70 ±0.69	1.60 ±0.69	1.60 ±0.43	1.10 ±0.44
500	0.0287	0.06	1.40 ±0.68	1.10 ±0.36	1.31 ±0.28	0.80 ±0.29	0.60 ±0.26	0.50 ±0.19	0.60 ±0.37	0.60 ±0.24
	0.0287	0.04	1.50 ±0.99	1.70 ±0.57	1.40 ±0.66	0.90 ±0.36	0.80 ±0.39	0.80 ±0.24	0.94 ±0.25	0.80 ±0.25
1000	0.0180	0.05	1.90 ±1.06	1.30 ±0.58	1.20 ±0.52	1.18 ±0.51	2.10 ±0.65	2.40 ±1.21	2.05 ±0.51	1.00 ±0.36
	0.0160	0.04	1.40 ±0.85	2.01 ±0.93	2.07 ±0.77	2.34 ±1.00	1.70 ±0.93	1.58 ±0.73	1.80 ±0.79	1.32 ±0.72

utilisation, and so it is not necessary to know which is the rate-limiting substrate.

Figure (6.3) Mass Balance Over the Inclined Plane.

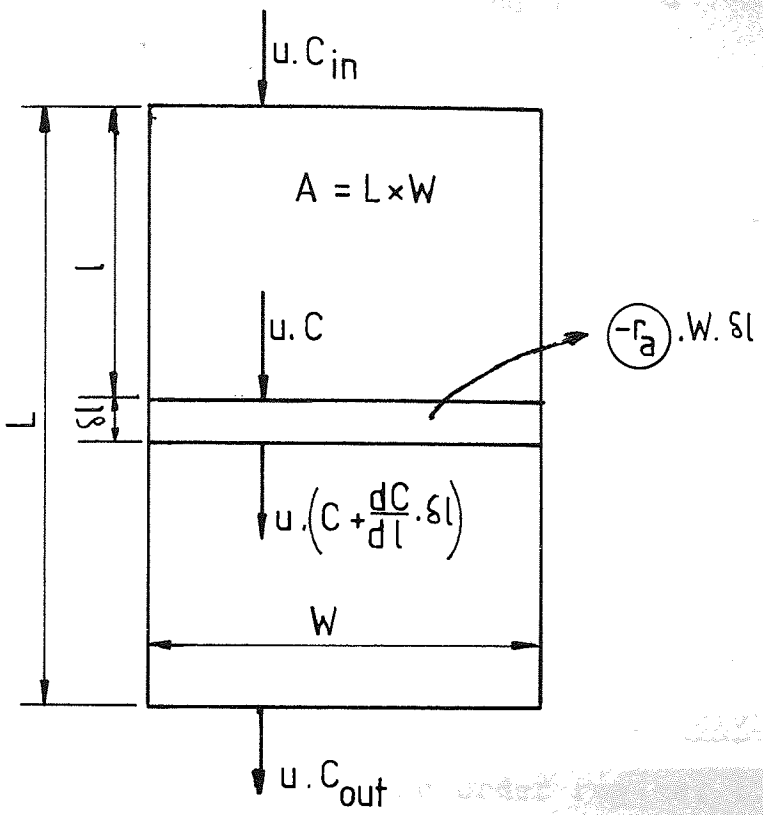

where L ——— plane length (L)

u ——— volumetric liquid flow rate ($L^3\theta^{-1}$)

W ——— plane width (L).

Mass Balance Over Element δl.

$$u.C = u\left(C + \frac{dC}{dl}.\delta l\right) + (-r_a).W.\delta l$$

$$\therefore \quad -\frac{dC}{dl} = (-r_a).\frac{W}{u}$$

In the $\frac{1}{2}$ order regime

$$(-r_a) = \sqrt{2k_o DC} = k_o F_{crit}$$

$$\therefore \quad -\int_{C_{out}}^{C_{in}} \frac{dC}{\sqrt{C}} = \frac{W}{u}\sqrt{2k_o D}\int_{L}^{0} dl$$

$$\therefore \quad 2(\sqrt{C_{in}} - \sqrt{C_{out}}) = \frac{A}{u}\sqrt{2k_o D}$$

Using the relationship

$$\sqrt{C} = \frac{k_o F_{crit}}{\sqrt{2 k_o D}}$$

$$\frac{2 k_o}{\sqrt{2 k_o D}} \left(F_{crit_{in}} - F_{crit_{out}} \right) = \frac{A}{u} \sqrt{2 k_o D}$$

Rearranging,

$$F_{crit_{in}} - F_{crit_{out}} = \frac{A}{u} D$$

or

$$D = \frac{u}{A} \left(F_{crit_{in}} - F_{crit_{out}} \right) \qquad (6.1)$$

$F_{crit_{in}} - F_{crit_{out}}$ may be most accurately evaluated from a linear regression of all the F_{crit} values along the length of the plane. Calculated values of D using this method are shown in Table (6.4).

6.4. Evaluation of the Zero-Order Rate Constant.

Method 1. Independently of Substrate Diffusivity.

In the zero-order regime, i.e. when all the film thickness measurements are below a value corresponding to F_{crit}, the rate of substrate utilisation is given by equation (2.4):-

$$(-r_a) = k_o F \qquad (2.4)$$

A mass balance over the inclined plane (see Figure (6.3)) then leads to:-

$$-\int_{C_{out}}^{C_{in}} dC = \frac{k_o \bar{F} W}{u} \int_{L}^{0} dl$$

$$\therefore \quad C_{in} - C_{out} = \frac{k_o \bar{F} A}{u}$$

where $\bar{F}$ ——— mean microbial film thickness over the entire plane $= (\bar{F}_m - \delta)$ (L)

$\bar{F}_m$ ——— mean measured film thickness over the entire plane (L)

δ ——— liquid film thickness from Table (6.1) (L).

Rearranging,

$$k_o = \frac{(C_{in} - C_{out})}{(\bar{F}_m - \delta)} \frac{u}{A} \qquad (6.2)$$

Hence, the zero-order rate constant can be found from substrate concentrations and film thickness measurements without knowing the substrate diffusivity and the rate-limiting substrate.

Method 2. Using a Known Substrate Diffusivity.

The zero-order rate constant, k_o, may also be evaluated from a measured value of diffusivity, the F_{crit} value at the inlet to the plane and the inlet substrate concentration for a specified rate-limiting substrate, using equation (2.7).

Since

$$F_{crit_{in}} = \sqrt{\frac{2 D C_{in}}{k_o}} \qquad (2.7)$$

$$k_o = \frac{2 D C_{in}}{(F_{crit_{in}})^2} \qquad (6.3)$$

The value of $F_{crit_{in}}$ may be more accurately evaluated from a linear regression analysis of all the F_{crit} values. The values of k_o for the rate-limiting substrates are presented in Table (6.5), subsequent to the identification of the rate-limiting substrates.

k_o Values Using Method 1.

The values of k_o at the different inlet glucose concentrations were expected to be different due to the changes in the microbial film composition (see Chapter 5). At film thicknesses less than the corresponding F_{crit} values set out in Table (6.1), the values of k_o for glucose obtained using equation (6,2) were found to be independent of the film thickness with both the intermediate and high glucose concentrations. However, the k_o values for glucose at the low

glucose concentration were found to vary according to the average film thickness as shown in Figure (6.4).

Figure (6.4) Variation of k_o for Glucose with Film Thickness: Low Glucose Concentration.

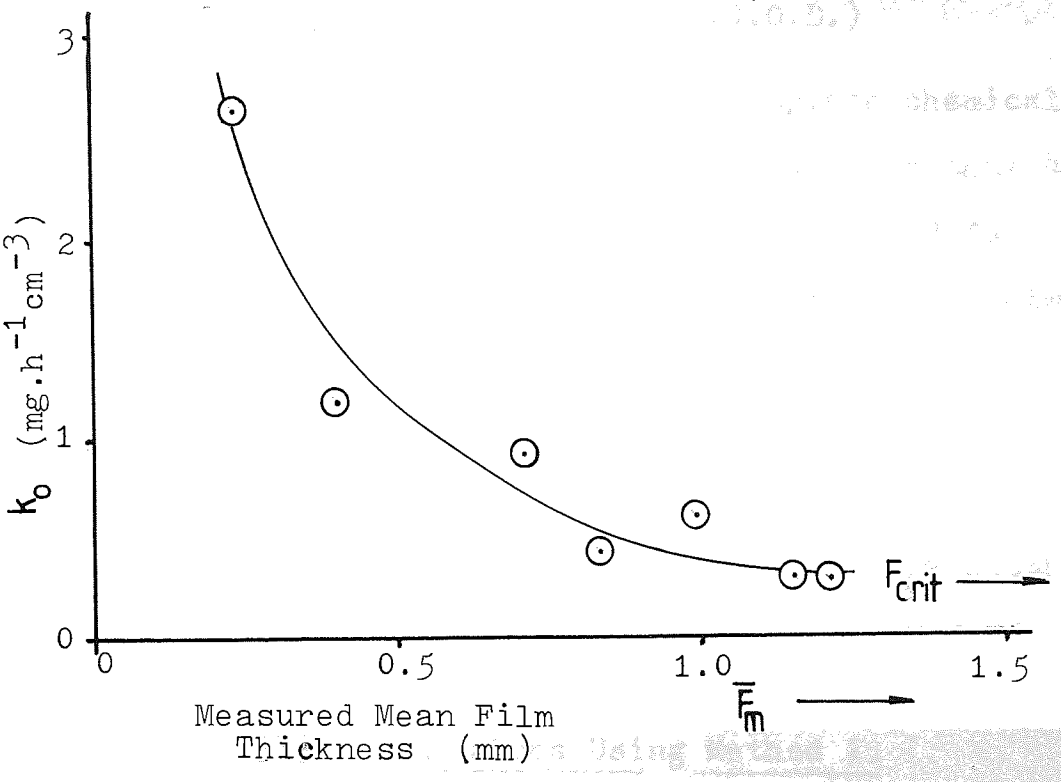

This variation in k_o may be due to the steadily changing microbial composition observed at the low glucose concentration (see section (5.4)). The lower values of k_o in Figure (6.4) will be assumed to be appropriate since the F_{crit} values at this particular feed concentration are in the range 1 to 2.5mm. The values of k_o for glucose at the three concentrations are summarised in Table (6.2).

Measurements of the concentration of nitrogen as nitrates/nitrites revealed that the nitrate/nitrite concentration was not changed significantly over the length of the inclined plane at any glucose concentration. This also indicated the absence of any nitrifying bacteria. The combination of poor analytical reliability and the restriction that the film thickness be less than F_{crit} meant that there were insufficient data available to evaluate k_o for nitrogen as

k_o for oxygen was estimated from the value of k_o for glucose using an empirical relationship taken from the literature (1).

Assume

$$\text{Biological Oxygen Demand (B.O.D.)} \simeq \frac{2}{3} \text{ Chemical Oxygen Demand (C.O.D.)} \quad (6.4)$$

Since 6 moles of oxygen are required for complete chemical oxidation of one mole of glucose, it may be assumed that 4 moles of oxygen per mole of glucose will be required for biological oxidation. On this basis, the relationship between k_o for oxygen and glucose on a weight basis is:

$$k_o \text{ oxygen} \simeq k_o \text{ glucose} \times 0.71 \quad \text{——————} \quad (6.5)$$

k_o values for oxygen based on this relationship are shown in Table (6.2).

Table (6.2) k_o Values Using Method 1.

Inlet glucose concentration (mg/l)	k_o for glucose ($mg.h^{-1}cm^{-3}$)	Estimated k_o for oxygen ($mg.h^{-1}cm^{-3}$)
100	0.27	0.19
500	2.7 ± 0.4	1.9 ± 0.3
1000	2.1 ± 0.6	1.5 ± 0.4

6.4.1 Identification of the Rate-Limiting Substrates.

A comparison of predicted and measured F_{crit} values may be used to aid the identification of the rate-limiting substrates and demonstrate the significance of apparent diffusivities. Having identified the rate-limiting substrate, the k_o values using Method 2 may be evaluated and compared to those obtained using Method 1. This comparison

may confirm the zero-order/½' order kinetics and the identification of the rate-limiting substrate.

The F_{crit} profiles may be predicted from values of k_o using Method 1 and published values of the diffusivity coefficients in water using equations (2.7) and (6.1). The values of diffusivity coefficients for oxygen (2), glucose (3) and the salts in water are shown in Table (6.3). The diffusivity coefficients of the salts were estimated using the Nernst equation (2,3). It should be noted, however, that the diffusivities of salt mixtures in solution will differ from the diffusivities of the pure salts.

Table (6.3) Diffusivities in Water.

Compound	Diffusivity ($cm^2 s^{-1}$)
Glucose	0.673×10^{-5}
NH_4NO_3	1.93×10^{-5}
$(NH_4)_3PO_4.3H_2O$	1.38×10^{-5}
O_2	2.73×10^{-5}

The dissolved oxygen concentration at the surface of the microbial film was taken to be that for air-saturated water; at the operating temperature this is 8.8mg/l (4).

Predicted F_{crit} profiles for the cases where either glucose or oxygen are limiting are plotted in Figures (6.5),(6.6) and (6.7): diffusivities equal to those in water and the k_o values given in Table (6.2) were used in the calculation. Also shown are the measured F_{crit} values listed in Table (6.1); regression lines through the measured F_{crit} values are shown in Figures (6.5) and (6.6), but, due to the spread in the results, no regression analysis was performed

Figures(6.5a&b) Critical Film Thicknesses .vs. Inclined Plane Section with a Low Glucose Concentration

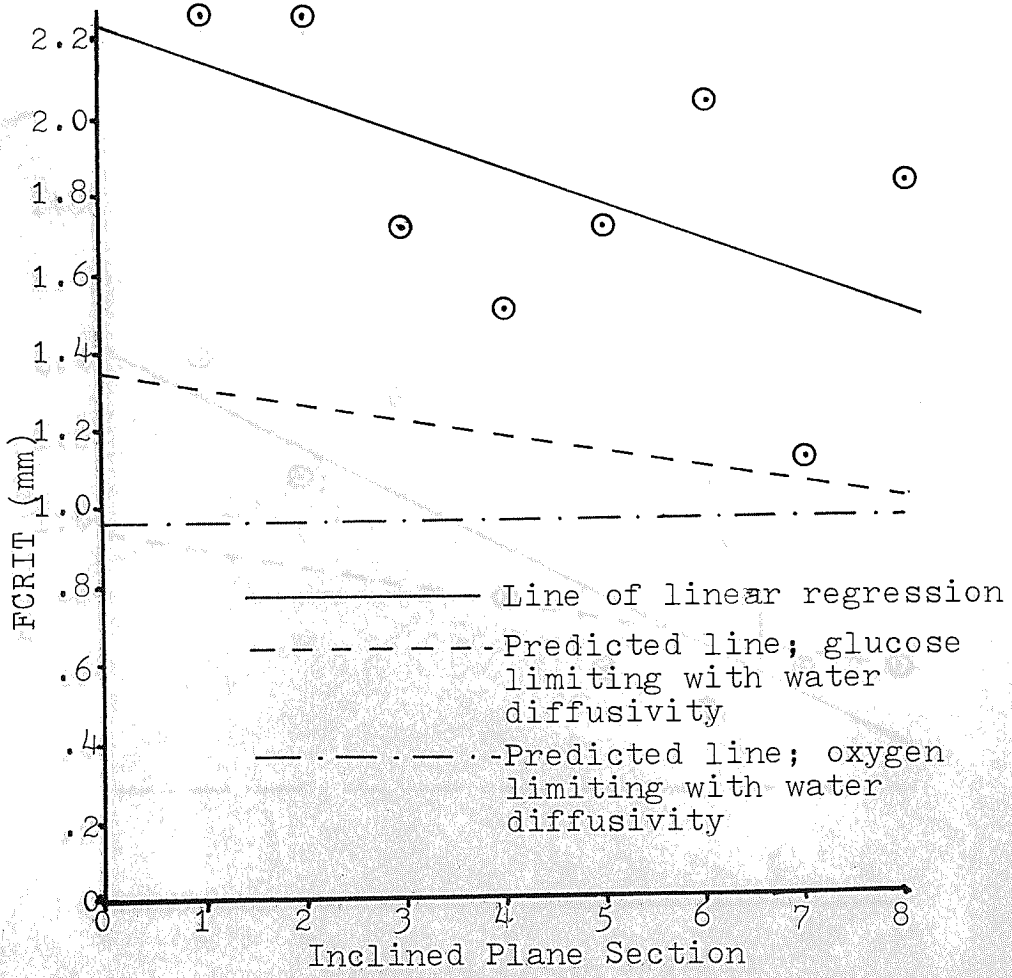

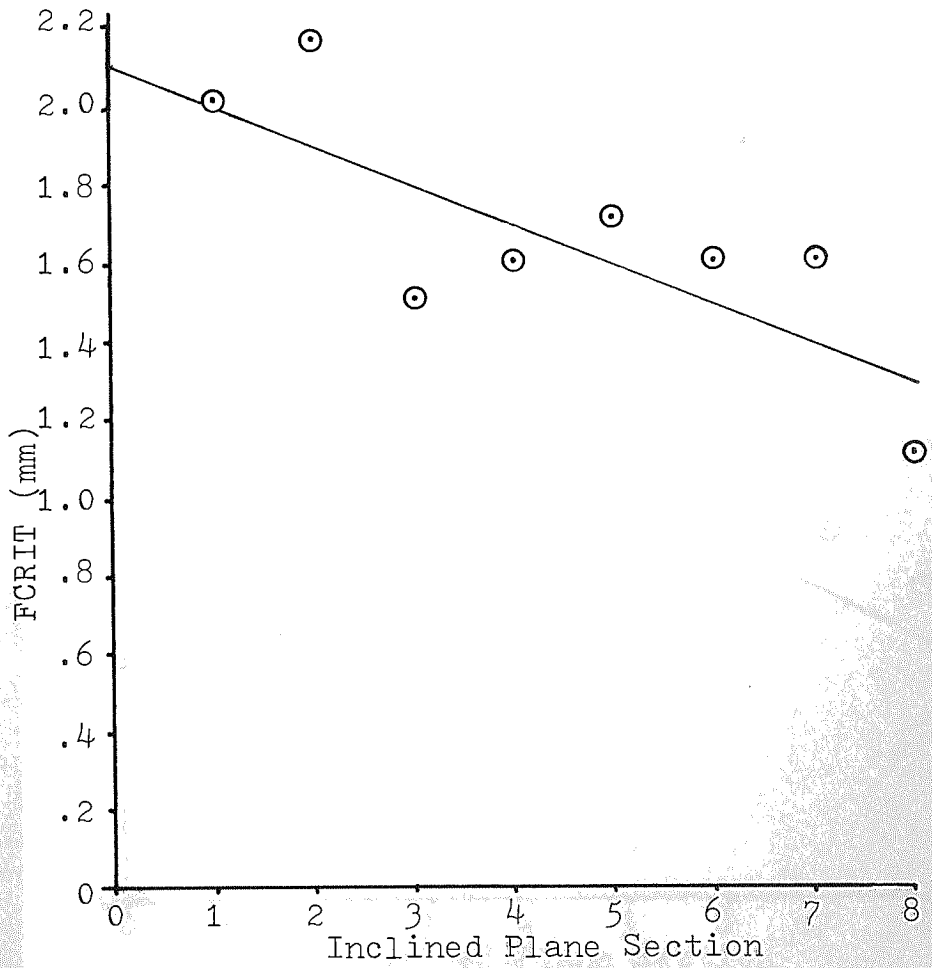

Figures(6.6a&b) Critical Film Thicknesses .vs. Inclined Plane Section with an Intermediate Glucose Concentraion

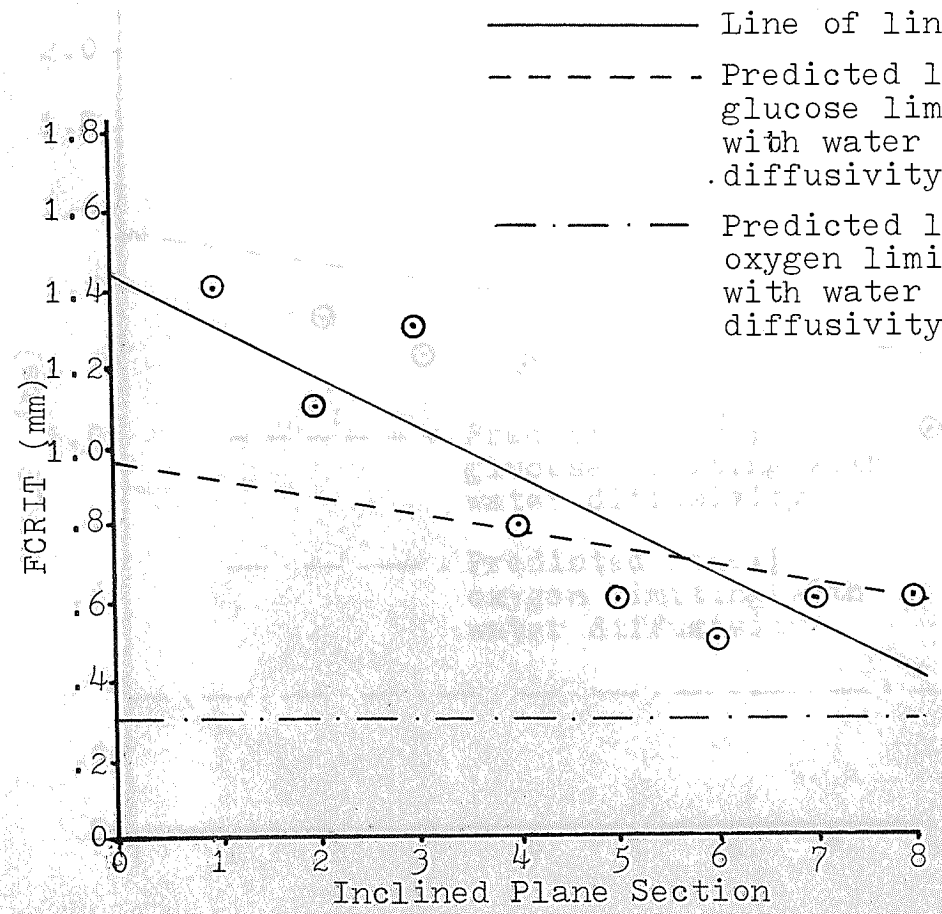

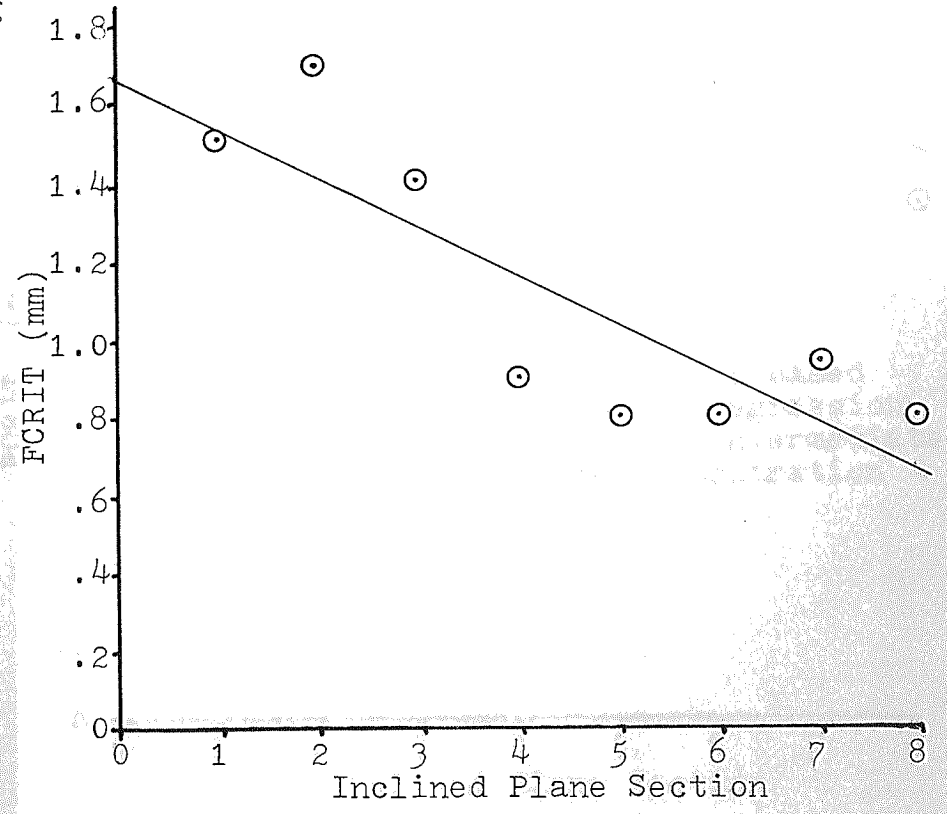

Figures(6.7a&b) Critical Film Thicknesses .vs. Inclined Plane Section with a High Glucose Concentration

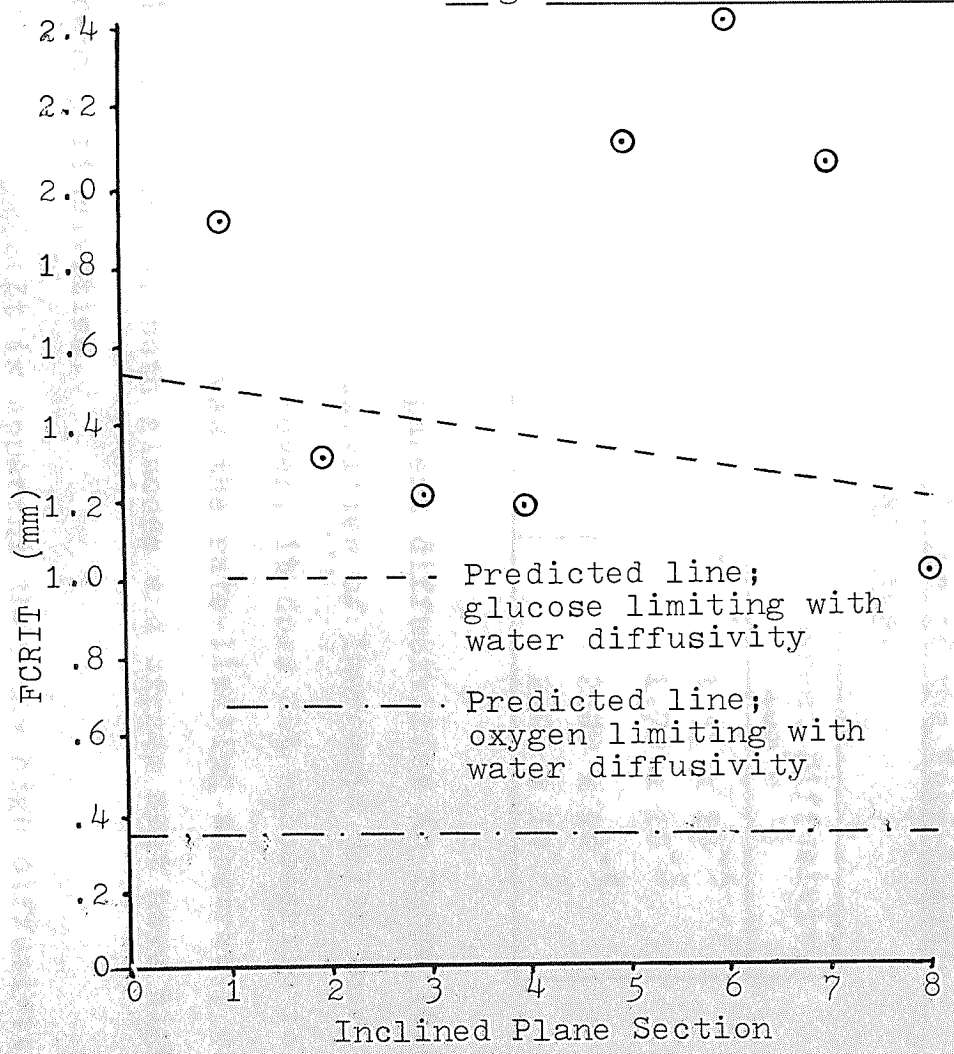

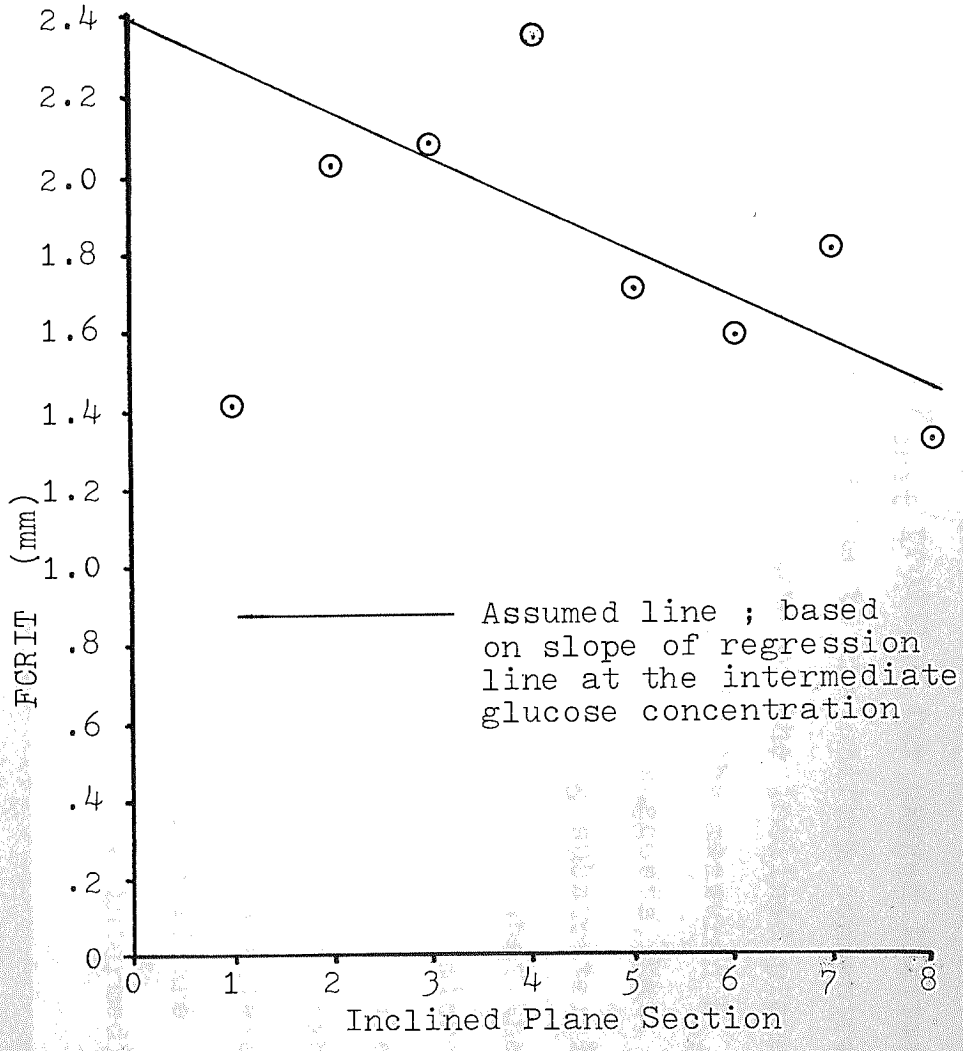

on the data shown in Figure (6.7).

It will be noted in Figures (6.5),(6.6) and (6.7) that the predicted F_{crit} profiles for oxygen limitation are horizontal lines. This is due to the uniform concentration of dissolved oxygen along the length of the inclined plane. Hence, the existence of negative slopes in the measured F_{crit} profiles, shown in Figures (6.5) and (6.6) suggests that, in these cases, oxygen was not the rate-limiting substrate. It is also apparent in Figures (6.5),(6.6) and (6.7) that the diffusivities of both oxygen and glucose through the microbial films must be considerably higher than in water, since the measured F_{crit} profile is the minimum any compound can exhibit. The diffusivities of the rate-limiting substrate calculated from the measured F_{crit} profile using equation (6.1) are shown in Table (6.4) for the cases involving the intermediate and low glucose concentrations.

Table (6.4) Apparent Diffusivities of the Rate-Limiting Substrates.

Glucose Concentration (mg/l)	Apparent Diffusivity ($cm^2 s^{-1}$)
Low (100)	1.51×10^{-5}
	1.70×10^{-5}
Intermediate (500)	2.09×10^{-5}
	2.04×10^{-5}

The apparent diffusivities in Table (6.4) are similar to the diffusivities of inorganic salts in water shown in Table (6.3). However, it does not necessarily follow that an inorganic salt was the rate-limiting substrate, since, as discussed above, both glucose and oxygen must have high apparent diffusivities.

It is apparent that the high diffusivities

of glucose and oxygen which must exist are not related to the presence of high concentrations of fungi: the apparent diffusivity of the rate-limiting substrate is higher at the intermediate glucose concentration than it is at the low glucose concentration which resulted in the formation of a film containing a higher proportion of fungi. The apparent diffusivity of the rate-limiting substrate, although not quantified, must also be of the same order of magnitude at the high glucose concentration which produced a film having very little fungi present.

It is interesting to note that high diffusivities in polymer solutions have been reported by several workers, and it has been shown that the diffusivity of a dissolved gas can increase up to a maximum value with increasing polymer concentration (5). It has been suggested that molecular realignment within the polymer solutions is responsible for the increased diffusivities of the non-polar solutes (5). These findings may offer some explanation for the author's results, bearing in mind that the lower apparent diffusivity arose at the low glucose concentration, when the microbial film contained less polysaccharide polymer (see sections (5.7) and (5.8)). It is unlikely that the diffusivities of the inorganic salts will increase with an increasing polymer concentration which brings about a realignment of the water molecules, since the relatively high diffusivities of ionic compounds in aqueous solutions are due to the polar structure of water. If the rate-limiting substrate was the same at both the low and intermediate glucose concentrations, it is therefore unlikely to have been an inorganic salt. It is therefore suggested that glucose was the rate-limiting substrate at the low and intermediate glucose concentrations

and that the diffusivities in Table (6.4) are the apparent diffusivities of glucose.

The poor quality of the F_{crit} profiles at the high glucose concentration (see Figure (6.7)) may be attributed to the lack of film thickness measurements once F_{crit} was exceeded: film break-away occured shortly after F_{crit} was exceeded, as is apparent from the short sloughing cycle (see section (5.3)). However, if it is assumed that the diffusivity of glucose reached a maximum value at the intermediate glucose concentration, then the slope of the F_{crit} profiles at both the high and intermediate glucose concentrations should be the same; this also assumes oxygen was not limiting at the high glucose concentration. Although it is meaningless to place such a line on Figure (6.7a) this has been done in the case of Figure (6.7b). In this case it may be reasonable to assume that glucose was limiting, although some supporting evidence is necessary.

k_o Values Using Method 2.

Having tentatively concluded that glucose was the rate-limiting substrate, values of k_o can be evaluated from the F_{crit} profile using equation (6.3) and are listed in Table (6.5); the value given for the high glucose concentration was obtained from the "assumed" F_{crit} profile.The values of k_o for glucose obtained using Method 1 are included in Table (6.5) for comparison.

It will be seen in Table (6.5) that the two different methods of evaluating the k_o values have given similar results. This tends to confirm the identification of the rate-limiting substrate as being glucose at all three glucose concentrations and the validity of the F_{crit} profile used at the high glucose concentration.

Table (6.5) k_o Values For Glucose.

Inlet Glucose Concentration (mg/l)	k_o Values ($mg.h^{-1}cm^{-3}$)	
	Method 1	Method 2
Low (100)	0.27	0.22 0.24
Intermediate (500)	2.7	3.6 3.5
High (1000)	2.1	2.6

The fact that the Method 1 k_o values based on the intermediate and high glucose concentrations are lower than the Method 2 values may be due to liquid channelling and partial wetting of the microbial film: as well as reducing the effectiveness of the inclined plane as a biological filter this would also have affected glucose sampling. The Method 2 k_o values are based on film thickness measurements and are not influenced by periods of partial wetting and are hence considered to be the more reliable. The fact that the Method 2 k_o value based on the low glucose concentration is lower than the Method 1 value may be due to a further reduction in k_o with increasing film thickness (see Figure (6.4)). Since the average film thicknesses are relatively constant and above the F_{crit} values at this glucose concentration (see Section (5.4)), the lower Method 2 k_o value is considered to be the most appropriate.

6.5. Minimum Oxygen Diffusivities.

Having concluded that oxygen transfer was not limiting the growth of the microbial films, a minimum diffusivity for oxygen may be estimated for each experiment. The depth of penetration of oxygen must have been no less than the maximum F_{crit} value measured in each experiment. The

maximum F_{crit} value in each experiment may be taken as that at the inclined plane inlet from the F_{crit} profiles (see Figures (6.5),(6.6) and (6.7)). The estimated values of the minimum oxygen diffusivities calculated using equation (6.3) and based on the k_o values for oxygen in Table (6.2) and a dissolved oxygen concentration of 8.8mg/l (air saturated) are presented in Table (6.6).

Table (6.6) Minimum Oxygen Diffusivities.

Glucose Concentration (mg/l)	Minimum Oxygen Diffusivity (cm^2s^{-1})	Minimum Diffusivity / Diffusivity in Water
Low (100)	1.25×10^{-4}	4.6
Intermediate (500)	1.02×10^{-3}	37
High (1000)	1.68×10^{-3}	62

6.6 Microbial Film Exponential Growth and Yield Coefficients.

The exponential growth rate constants, S , of the microbial film shown in Table (6.1) show a good reproducibility but with large differences between the different glucose concentrations. Before comparisons between these growth rate constants can be made it is important to consider the quantity of water physically held within the film. This may be done using the Dry Weight%'s shown from Table (5.1).

An arbitrary term that allows the growth rates of the micro-organisms at the different glucose concentrations to be compared is given by the product of the film growth rate and the Dry Weight %; the values obtained are shown in Table (6.7).

In the same way that the film growth rates

can not be compared directly the volumetric yields Y_{vm} as described by equation (2.21) can not be compared directly. It is the dry mass yields Y_{dm} as described by equation (2.13) which should be used for comparison.

Y_{vm} is given by equation (2.14):-

$$Y_{vm} = \frac{\text{Rate of Film Growth}}{\text{Rate of Substrate Removal}} = \frac{(+r_g)}{(-r_a)} \qquad (2.14)$$

Hence for exponential film growth i.e. zero-order kinetics,

$$Y_{vm} = \frac{(+r_g)}{(-r_a)} = \frac{S\cancel{F}}{k_o\cancel{F}} \qquad (cm^3 mg^{-1})$$

also

$$Y_{dm} = \frac{1000mg}{cm^3} \times \frac{DryWt\%}{100\%} \times Y_{vm} \qquad (2.13)$$

The values of Y_{vm} and Y_{dm} obtained are shown in Table (6.7) which are based on k_o values obtained using the Method 2.

Table (6.7) Exponential Growth Parameter and Yield Coefficients.

Inlet Glucose Concentration (mg/l)	$S \times \frac{\text{Dry Weight \%}}{100\%}$	Y_{vm} $cm^3 mg^{-1}$	Y_{dm} $mg.mg^{-1}$
Low (100)	7.9×10^{-5} 5.7×10^{-5}	0.054 0.039	0.34 0.25
Intermediate (500)	4.1×10^{-4}	0.0081	0.12
High (1000)	2.3×10^{-4} 2.0×10^{-4}	0.0069 0.0062	0.09 0.08

6.7 Discussion.

The k_o values obtained using the Method 1 are based on the assumption that bulk zero-order kinetics apply and are quantified using concentration and microbial film thickness measurements. The k_o values obtained using the Method 2 are based on the assumption that zero-order intrinsic kinetics apply with a diffusion limitation and are quantified using the inlet concentrations and by locating the transition between bulk zero-order and $\frac{1}{2}$' order kinetics. Since the two methods of evaluating k_o utilise different characteristics of the same kinetic model and different analytical techniques, the confirmation of the k_o values tends to endorse the kinetic model.

The rate-limiting substrate has been identified as glucose in all three experiments. The k_o values for glucose are clearly dependent on the microbial film composition which is in turn affected by the composition in the liquid phase. Hence, changes in the k_o values with filter depth may be apparent on particularly deep high-rate biological filters. It should be noted that no significant differences were observed in the microbial film composition across the inclined plane, which represents 8ft of packing depth (see section (4.2.1.)). Hence a sequence of average k_o values may adequately describe a deep filter's performance; more elaborate models are not required for single substrate limitation. The diffusivity of glucose is also affected by the microbial film composition, although the changes in the diffusivity were relatively small as compared to the changes in k_o values. Hence an average diffusivity over a deep filter should be appropriate.

The diffusivities of glucose and oxygen through the microbial films obtained are considerably higher

than through water. As previously discussed in section (6.4.1) this is not related to the presence of fungi and is most probably due to the presence of the bacterially-produced extracellular slime. Tomlinson and Snaddon (6), who put forward the hypothesis of fungal "hyphal streaming" as the cause of the high diffusivities, did not observe high diffusivities with predominantly bacterial films. However, in their work, the predominantly fungal films were produced using a synthetic medium of glucose and the predominantly bacterial films were produced using domestic sewage. Since domestic sewage contains relatively small quantities of sugars, it is most likely that the composition and characteristics of a bacterial slime produced from sewage will differ from those produced from glucose. In addition, it was noted in section (5.8) that the characteristics of a so-called predominantly fungal film were only reproduced in the author's work by a film containing comparable quantities of both fungi and bacteria. It is therefore suggested that hyphal streaming was not the cause of Tomlinson and Snaddon's results (6), but it was a bacterial slime produced from glucose which gave the high apparent diffusivities and the bacterial slime produced from domestic sewage did not give rise to high apparent diffusivities.

The diffusivity of oxygen through the predominantly fungal film in Tomlinson and Snaddon's work (6) was ten times that through water. Due to order of magnitude differences in the Dry Weight % of the microbial films arising from the different geometries of the experimental equipment, oxygen diffusivities obtained by these workers can not be compared directly to those obtained here. However, Tomlinson and Snaddon do refer (6) to data taken from biological filters in which oxygen diffusivities in excess of their laboratory

measured values were most probable. In addition, the k_o values for oxygen used in this thesis (see Table (6.2)) were estimated and are considerably higher than Tomlinson and Snaddon's (6) measured values; had the lower values of k_o been used in this work, the minimum oxygen diffusivities would have been nearer to those of Tomlinson and Snaddon's.

It will be seen in Table (6.7) that the predominantly fungal films obtained using the low glucose concentration (100mg/l) converted the most glucose into biomass (on a dry basis) and produced biomass (on a dry basis) at the lowest rate. The predominantly bacterial films produced using a high glucose concentration (1000mg/l) converted the least glucose into biomass (on a dry basis). These findings are in accord with published observations (see section (3.2)). The most rapid production of biomass (on a dry basis) occured using an intermediate glucose concentration (500mg/l); this is due to the inhibition of microbial growth that was apparent when using the low and high glucose concentrations (see section (5.8)).

6.8 References.

1) Quirk, Lawler & Matusky, Engineers. Whey effluent packed tower trickling filtration. Report for the Office of Research and Monitoring Environmental Protection Agency. Project no. 12130DUJ (1971).

2) Perry & Chilton (Editors). Chemical Engineers Handbook. 5th edition. McGraw - Hill, New York, London.

3) C.R.C. Handbook of Physics and Chemistry. 60th edition 1979 - 1980. Chemical Rubber Company, Florida, U.S.A.

4) Starke & Wallace. Chemistry Data Book S.I. edition. John Murray, London (1970).

5) Mashelkar, R.A. & Soylu, M.A. Diffusion in flowing films of dilute polymeric solutions. Chem. Eng. Science 29, p1089 - 1099 (1974).

6) Tomlinson, T.G. & Snaddon, D.H.N. Biological oxidation of sewage by films of micro-organisms. Air & water Pollut. Int. J. 10, p865 - 881 (1966).

CHAPTER 7

HYDRAULICS

7.1. Introduction.

The diffusion/reaction kinetic models discussed in Chapter 2 express the bulk rate of substrate removal in terms of " unit wetted surface area", this being the surface area of microbial film in physical contact with the flowing liquid. Since the biological filter is not totally submerged, the wetted surface area may be expected to change with flow-rate as in the case of packed gas-absorption columns (1). In fact, it has been shown that wetted surface area increases with increasing flow (2). As with most chemical reactor systems, the flow-rate through a biological filter will also affect the mass balance and may affect the degree of liquid mixing. The effect of liquid flow on the microbial film composition, as discussed in Chapter 3, will not be regarded as a hydraulic parameter.

As mentioned in Chapter 2 , if kinetic data are used to estimate the wetted surface area and/or liquid mixing, it is impossible to state whether the resulting overall model is a true representation or a modification of an inadequate kinetic model to fit the recorded data. For this reason, an independent method of evaluating the hydraulic parameters, such as tracer analysis, should be relied upon.

Based on the assumption that the liquid film thickness does not decrease with increased flow-rate, it follows logically that the increased wetted area must be accompanied by an increased liquid hold-up. Many workers have used this assumption to relate liquid hold-up , measured via mean residence times of tracers, to filter performance e.g. (3,4). The resulting model usually involves an empirical power law relationship between filter performance and flow rate e.g. (3,4). However, in the evaluation of the liquid hold-up, by tracer analysis, the liquid within the microbial film is

also included. The liquid in the microbial film may well exceed the volume of the flowing liquid film; hence, the relationship between liquid hold-up and wetted surface area may be difficult to evaluate. Heinrich (5), in a set of laboratory studies on nitrification rates in biological filters, has demonstrated that performance is dependent on wetted surface area and is not related to retention time; the studies compared different support media which were used to change the surface area but not the retention time.

In the situation where zero-order kinetics apply, as discussed in Chapter 2 , the bulk rate of substrate removal per unit wetted surface area is proportional to the microbial film thickness. Hence, the overall rate of substrate removal, where zero-order kinetics apply, may be closely proportional to the total liquid hold-up. It is also a feature of zero order kinetics, in any reactor system, that liquid mixing has no bearing on performance.

7.2. Preliminary Experimental Work.

Tracer Studies With Dyes.

Some preliminary experiments were carried out on the inclined plane rig to investigate liquid mixing and channelling and to observe how well the microbial film was wetted by the flowing liquid. With organic dyes as tracers, it was seen that a thin, developing microbial film was equally-well wetted and no liquid mixing or channelling was apparent. After a thicker, older microbial film had formed (in excess of about 2mm) "non-wetted" areas appeared and channelling became apparent. Figures7.1 and 7.2 show the near plug-flow front of dye with the thinner microbial film and the channelling of dye in the presence of the thicker microbial film.

Figure 7.1 Plug flow of dye tracer with a thin microbial film

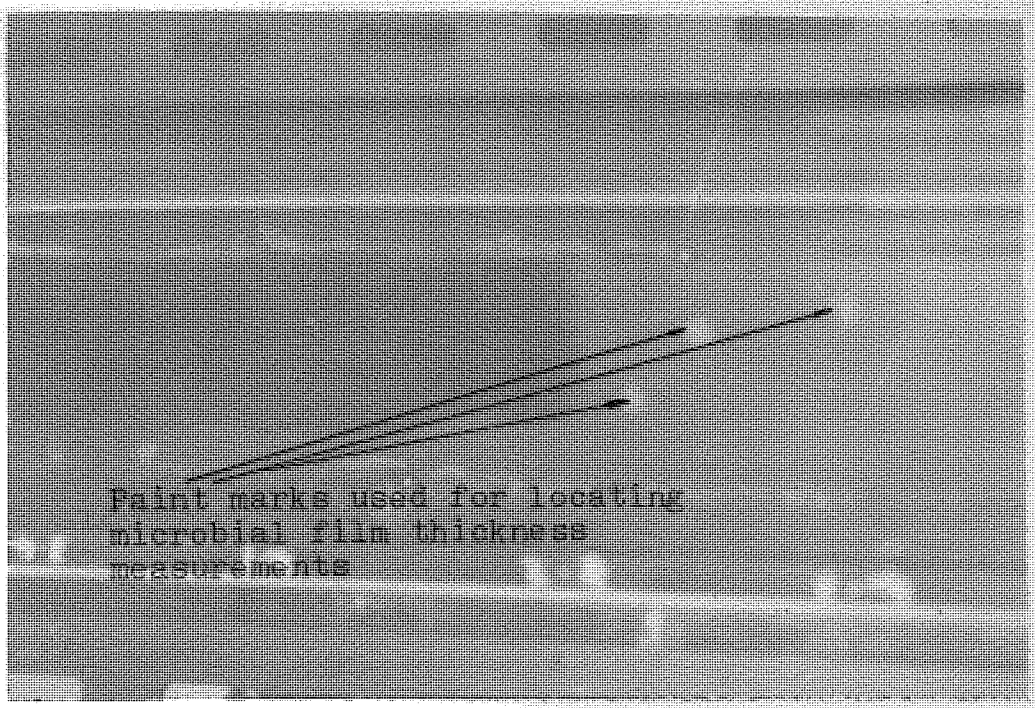

Figure 7.2 Channelling of dye tracer with a thick microbial film

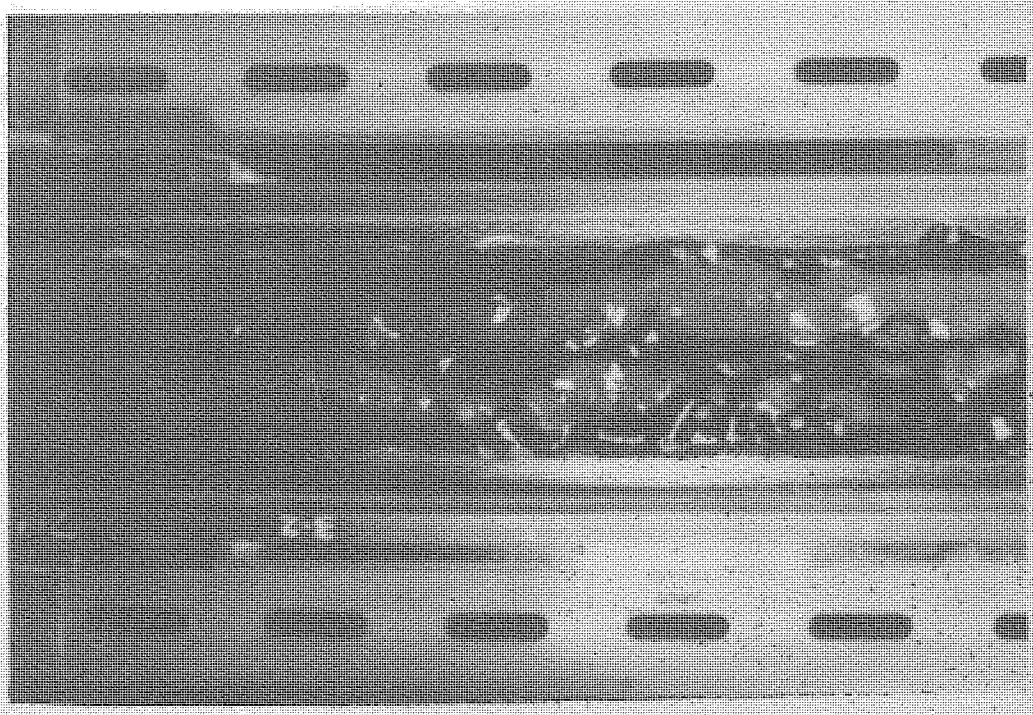

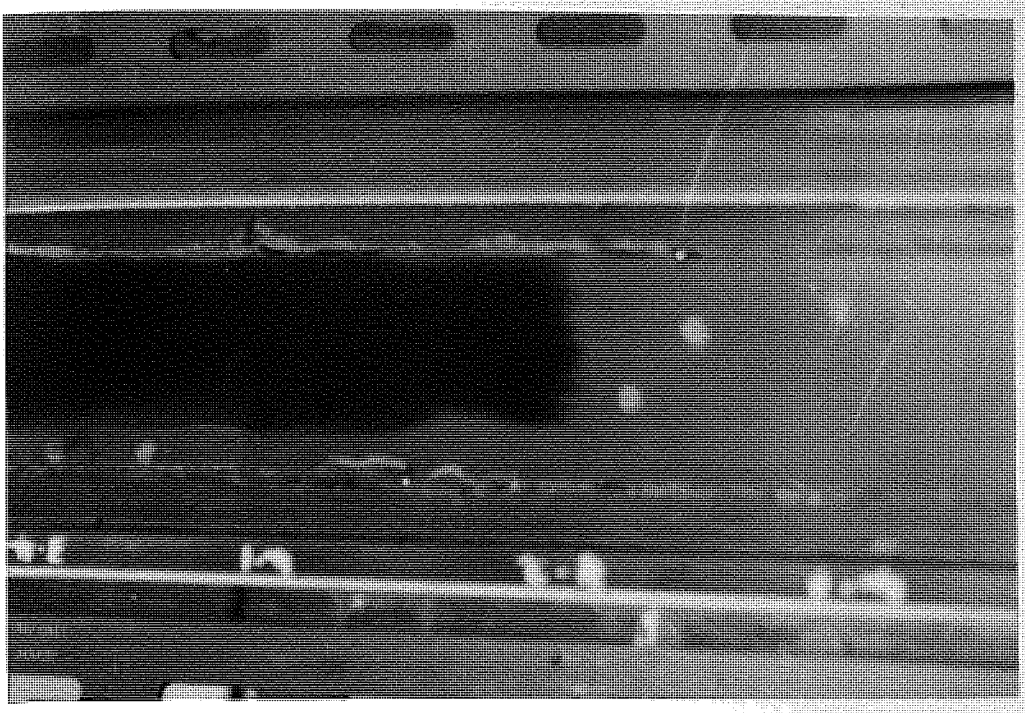

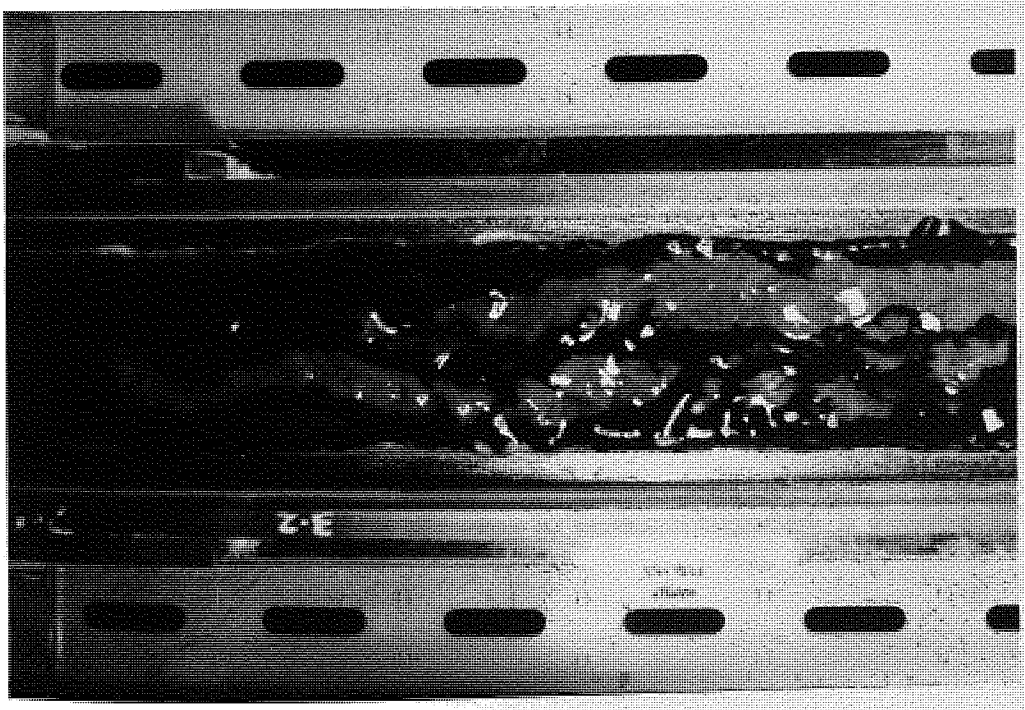

The use of dyes as tracers was then terminated as they tended to permanently stain the microbial film and made further experiments impossible.

Mean Residence Time Studies with Sodium Chloride as Tracer.

Quantitative experiments were started using sodium chloride as a tracer, initially to further investigate the power law relationship for liquid flow-rate against performance and to gain some insight into possible alternative methods of describing liquid mixing and channelling. The tracer was introduced as a step-change, for experimental ease, and the changes in outlet concentration with time were estimated by means of conductivity measurements. The method of calculating mean residence time from response data is shown in Appendix 3.

It became apparent that the mean residence time was really a measurement of the total microbial film and liquid film present divided by the liquid flow-rate. This was established by comparing the tracer results to microbial film thickness measurements made in the kinetic studies. Tracer methods which accounted for the shape of the response curve were then considered necessary.

The technique based on the use of sodium chloride and conductivity measurements was then discarded for the following reasons:

(i) the need for a range of concentrations of at least three powers of ten to adequately study the shape of the response curve, and

(ii) the related need to use relatively high levels of sodium chloride to overcome the background conductivity of the medium.

Experience showed that the salt concentrations required

affected microbial activity and could destroy the microbial film.

7.3. Final Choice of Tracer System

The requirements for a suitable tracer system are considered to be the following:

(i) non-biodegradable

(ii) water soluble

(iii) non toxic to micro-organisms

(iv) non-reactive with substrates in the effluent/model effluent

(v) non-volatile

(vi) readily measured over a wide concentration range (at least three powers of ten) at relatively low concentrations.

(vii) inexpensive.

Sheikh (6) has studied tracer techniques suitable for use in biological filters. In his study, he took account of the changes in microbial film characteristics by allowing his pilot-scale, low-rate filters to settle down for a period of weeks between each change in flow-rate. His final recommendation of tracer was radio-active bromine 82, as NH_4Br; the concentration was measured by a gamma scintillation counter.

The use of radio-active tracer was prohibitively expensive and the necessary procedures would have restricted available time. In this project, the bromide ion, introduced as KBr, was used as a tracer, its concentration being measured by means of a specific-ion electrode. The Orion specific bromide electrode (model 94-35A) connected to a Corning pH/mV meter used for this purpose was capable of measuring bromide concentrations quickly, in the range 10^{-5} to 1 molar. However,

this system did have the draw-back of lacking precision when the response measurement approached that of the inlet concentration, a change of only 1mV corresponding to a change from 98% to 100%, a result of 100% being theorectically impossible. The system was later modified by combining the Corning pH/mV meter with a more accurate Fluke digital voltmeter (model type 8300A); this combination could measure to $\pm$ 0.01mV.

The tracer was again introduced as a step-change in concentration by switching from one feed line to another. Samples were taken from the outlet as often as practically possible and each sample was measured separately. The sample size was between 2 and 5 cm^3. It was found necessary to recalibrate the system each time it was used; a typical log:linear calibration plot for the electrode is shown in figure A6.2 of Appendix 6.

7.4. Analysis of Experimental Data.

7.4.1. The Method of Sheikh

Sheikh's method (6) for analysing the experimental data was to plot the integrated pulse response on log:normal probability scales. His results took the form of straight lines which could be described by two characteristic points t_{16} and t_{50}, these being the times for 16% and 50% of the pulse tracer to emerge at the outlet. Sheikh then used the points t_{16} and t_{50} to empirically relate flow-rate to filter performance.

The log:normal probability plot was applied to the response data from the inclined plane; the results for a thin, developing microbial film and an older, thicker film are shown in figure 7.3.

Figure(7.3) Inclined Plane Tracer Responses
Showing Error Bands

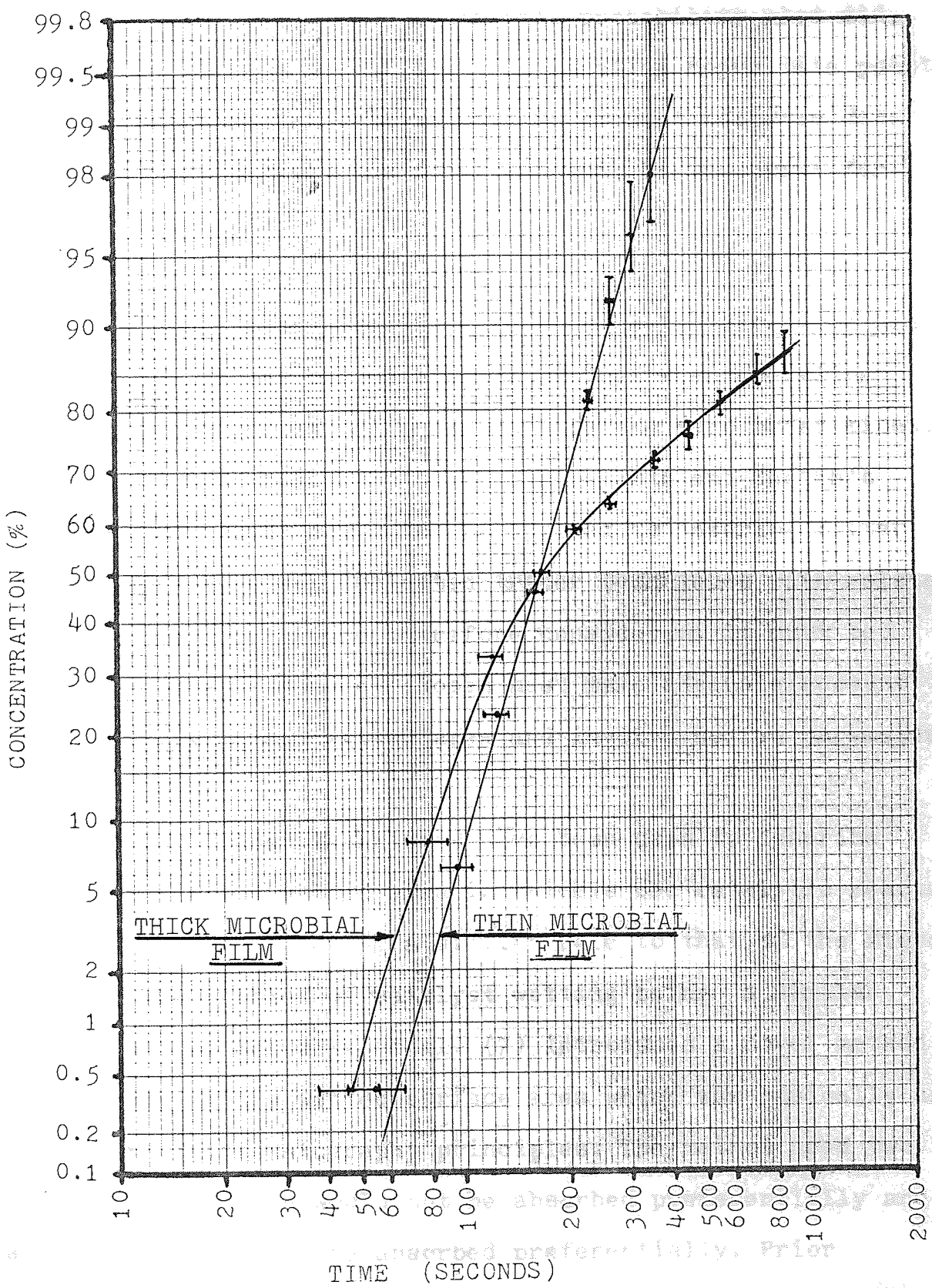

It will be noted that the straight line plot arises with the thinner microbial film and not with the thicker film. It was concluded that the method of Sheikh (6) would be inappropriate for high flow-rate conditions while a thick microbial film exists. The log:normal probability plot did, however, serve as a useful tool for locating rogue data points and extrapolating data. It is used to present response data because it exaggerates the front and tail of the curve for critical visual inspection.

7.4.2. Related Tracer Studies with Trickle Bed Catalytic Reactors.

It has been demonstrated that when operating with a thick microbial film and outside the zero order kinetic regime that mean residence time measurements and Sheikh's graphical technique could not be applied to describe filter performance. More sophisticated tracer techniques with related mathematical models were therefore considered. It must be remembered that the model chosen must take adequate account of liquid mixing and wetted area and involve as few parameters as possible.

Tracer techniques have been used to describe liquid mixing and wetted area in trickle bed catalytic reactors, with the catalyst playing a similar role to that of the microbial film and the problem of catalyst wetting being a similar consideration. Schwartz et al. (7) introduced a novel method of determining the wetted surface area which was basically an extension of chromatography principles. The method used two tracers - one which would not be absorbed preferentially and a second which would be absorbed preferentially. Prior knowledge of the absorption characteristics of the two tracers could be used to determine the wetted area through which the

second tracer was preferentially absorbed. The disadvantage of this method is that two suitable tracers with the required absorption characteristics may be particularly hard to find with regard to absorption into a microbial film.

A second, but less elaborate, tracer method applied to trickle bed reactors has been described by Colombo et al. (8). This method compares the tracer response when the reactor is operating as a trickle bed to that when the packing is totally submerged. The differences in the rates of uptake of the tracer can be attributed to the differences in wetted surface area; under totally submerged conditions the wetted surface area is a known quantity.

This latter method could not be adopted for use with biological filters as the microbial film could not withstand being totally submerged. However, the principle of comparing responses when the wetted surface area was a known quantity to those when it was an unknown quantity was adopted. The method compared response data from the inclined plane when the microbial film was "well wetted" to response data from the Biopac rig and the inclined plane when channelling existed. Early experience with dye tracers was relied upon to judge when the microbial film may have been "well wetted". A new mathematical model was developed for analysing the response data.

7.4.3. Tanks-in Series Models.

Because of the relative complexity of the kinetics and the method in which the microbial film thickness measurements were to be made, it was decided to model the liquid mixing as a series of well mixed tanks, as opposed to a differential model.

A Simple Series of Uniform Stirred Tanks.

A simple tanks-in-series model, as shown in figure 7.4, may be used to describe the liquid flow when there is little or no uptake of the tracer into the microbial film, as may be expected while the microbial film is thin.

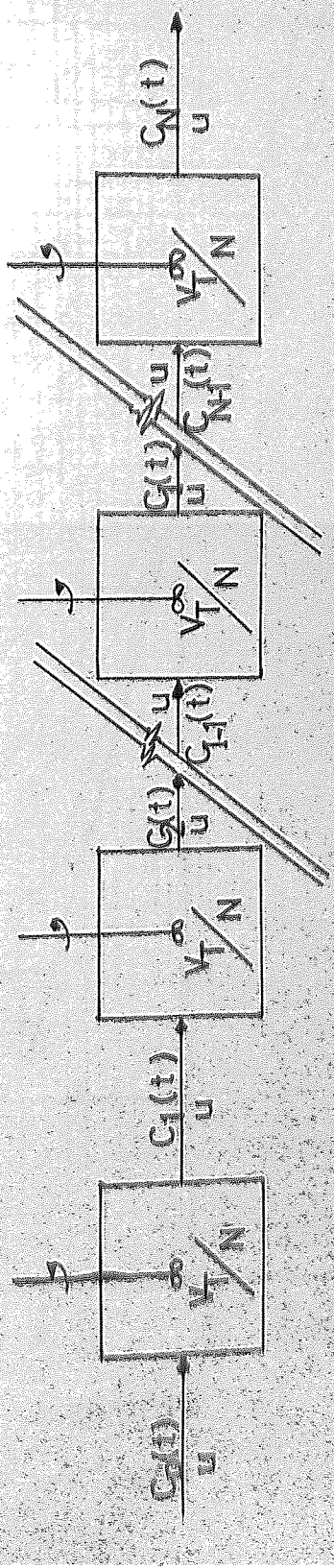

Figure 7.4 A Simple Series of Uniform Stirred Tanks

Figure(7.5) Inclined Plane Tracer Response for a Thin Microbial Film and Simple Tanks in Series

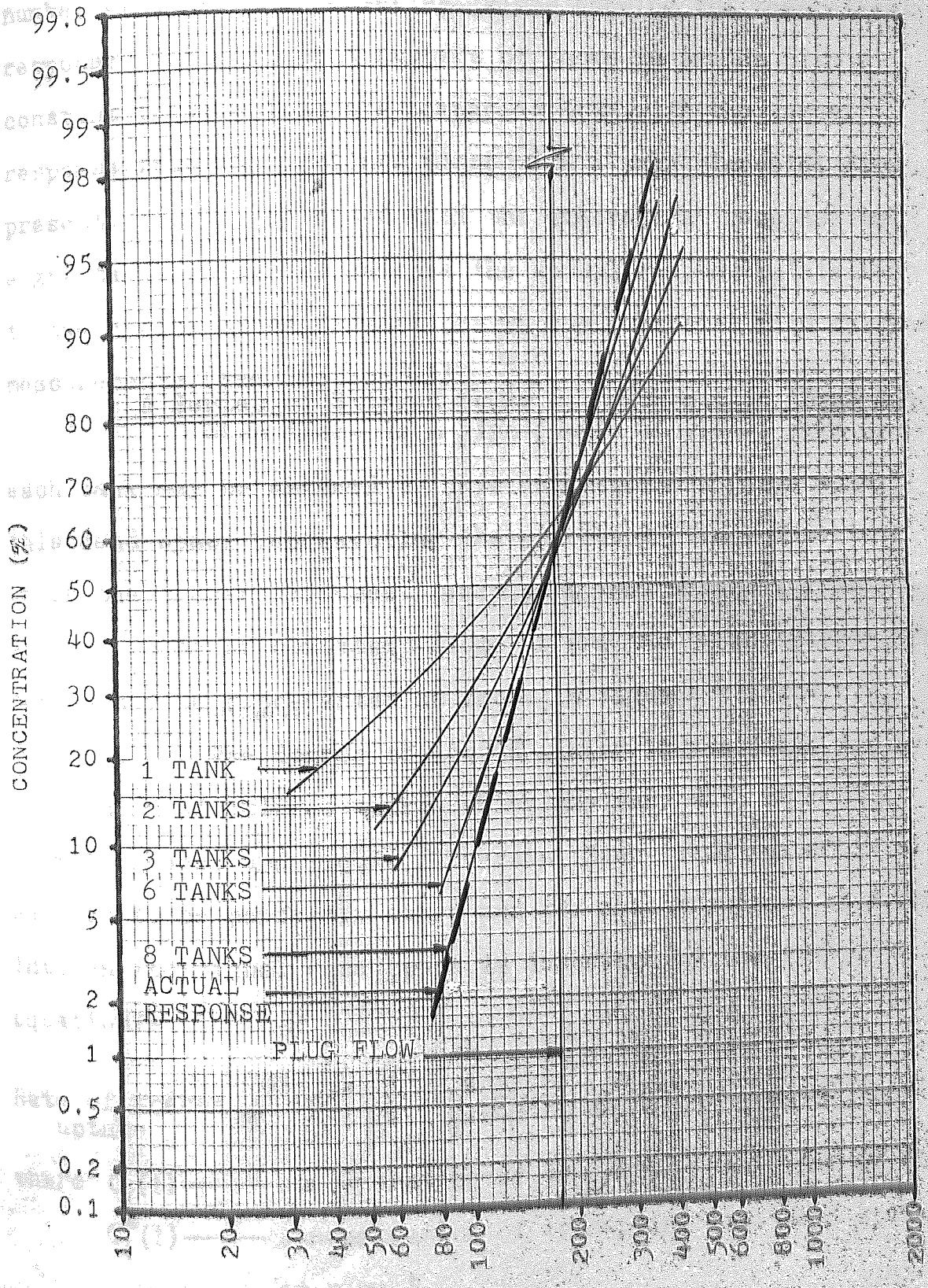

The analytical solution for a response to a step change in the inlet concentration is shown in Appendix 3. Each tank is of uniform volume and is assumed to be well mixed, the degree of liquid mixing being indicated by the number of tanks in the series. Plots showing the theoretical responses for different numbers of tanks-in-series with a constant total volume are compared in Fig 7.5 with the actual response from the inclined plane with a thin microbial film present. It will be noted that the theoretical response to eight tanks-in-series matches the actual response; this led to the choice of eight sections for the microbial film thickness measurements (see Section 4.5).

A Series of Stirred Tanks with Associated 'Dead Spaces'.

When there is a significant microbial film present each tank may be assumed to have an associated 'dead space', this dead space representing the microbial film volume into which the tracer diffuses. Again, each well mixed tank is assumed to be of constant volume as are the 'dead spaces'. The series may be represented as shown in figures 7.6 and 7.7.

The degree of liquid mixing is accounted for by the number of stirred tanks, which may vary with microbial film thickness and liquid flow-rate. Each 'dead space' is also assumed to be perfectly mixed and the rate of uptake of tracer into an individual dead space is described by the equation:-

$$\text{Rate of tracer uptake} = \frac{dC_i^*}{dt} = \frac{u^*}{V^*}(C_i(t) - C_i^*(t)) \qquad 7.1$$

where $C_i(t)$ —— concentration of tracer in 'i th' tank at time t

$C_i^*(t)$ —— concentration of tracer in 'i th' dead space at time, t

u^* —— hypothetical flow rate into and out of 'dead space'

V^* —— volume of 'dead space'.

Figure 7.6 Ideal Tanks-in Series Model with Associated 'Dead Spaces'

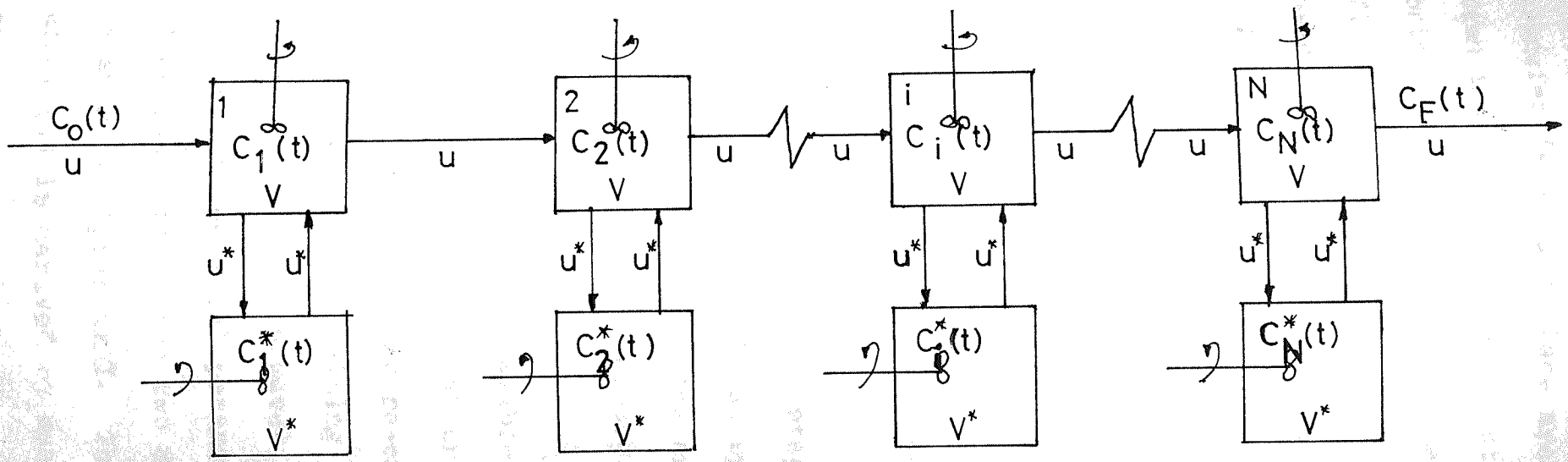

Figure 7.7 Pictorial Representation of Tanks-in-Series Model in Relation to Inclined Plane

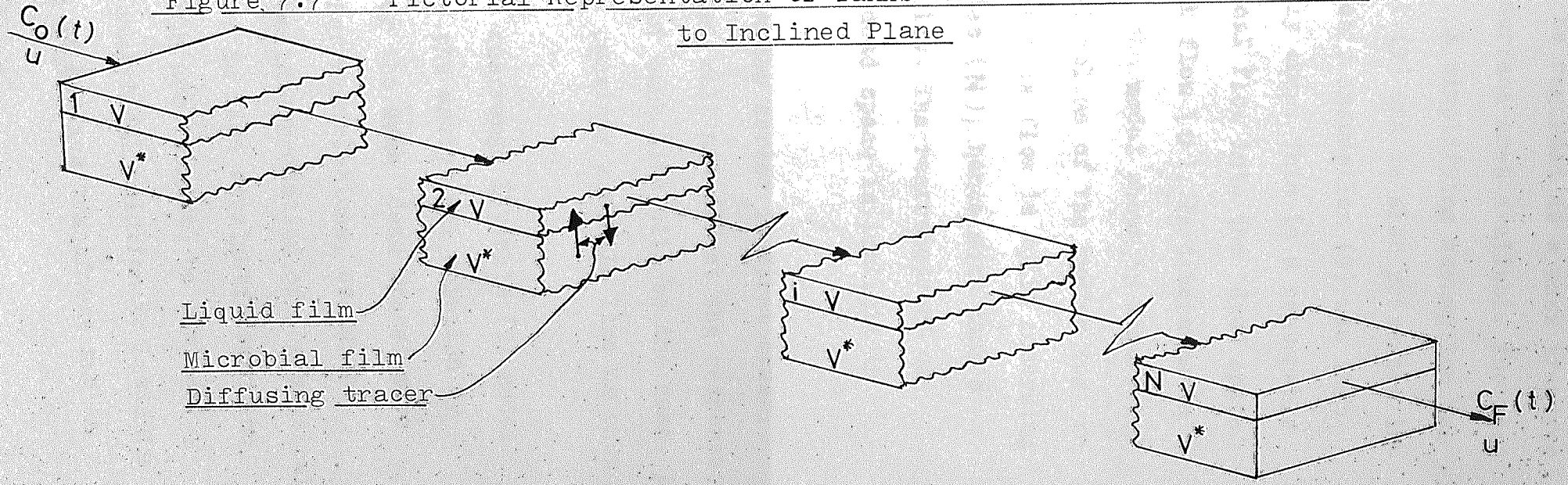

The term u^*/v^* may be regarded as a mass transfer coefficient multiplied by the surface area available for mass transfer (wetted surface area). A simplifying assumption has been introduced by Levich et al.(9) and is also presented in brief in Levenspiel (10). Levich's assumption (9) was that fluid enters any dead space only once. This is a reasonable assumption while the hypothetical flow into the 'dead space' (u^*) is much less than the bulk flow (u). In diagrammatic form this assumption leads to the model shown in figure 7.8 It will be noted that the total volume of the system must be the same as in figure7.6 and the bulk flow is split according to the number of tanks-in-series (N); hence each tank's volume is adjusted proportionally. The rearrangement of returning flow (u^*) from each dead space is implicit in Levich's assumption (9).

Since each step in the series is first order, the location of the 'dead space' will not affect the response; hence the response at the end of each line will be the same. It is therefore only necessary to consider a single line as shown in figure 7.9.

It is possible to rearrange Levich's (9) model without adding undue labour to the analytical solution by allowing the liquid to re-enter the same 'dead space' more than once, but maintaining other restrictions, as may be shown in figure7.10. However, the interpretation of the physical meaning of the model parameters is less straightforward and, after inspection, the two models are found to be similar, as shown in Appendix 3. The analytical solution to Levich's model (9) is derived by means of Laplace transforms and is presented in Appendix 3.

Figure 7.8 Levich's Hydraulic Model.

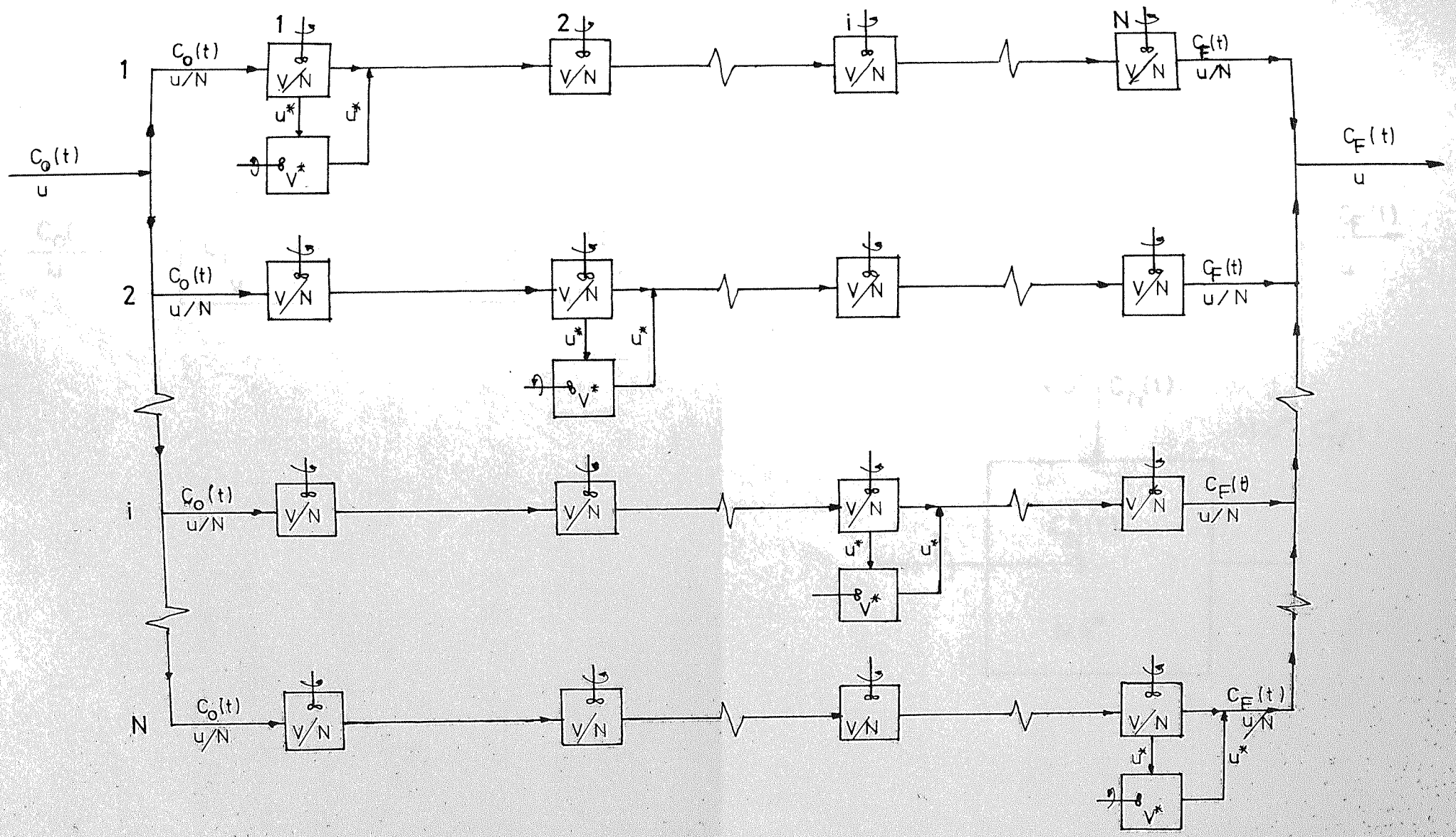

Figure 7.9 Series of Uniform Stirred Tanks with Single 'Dead Space'

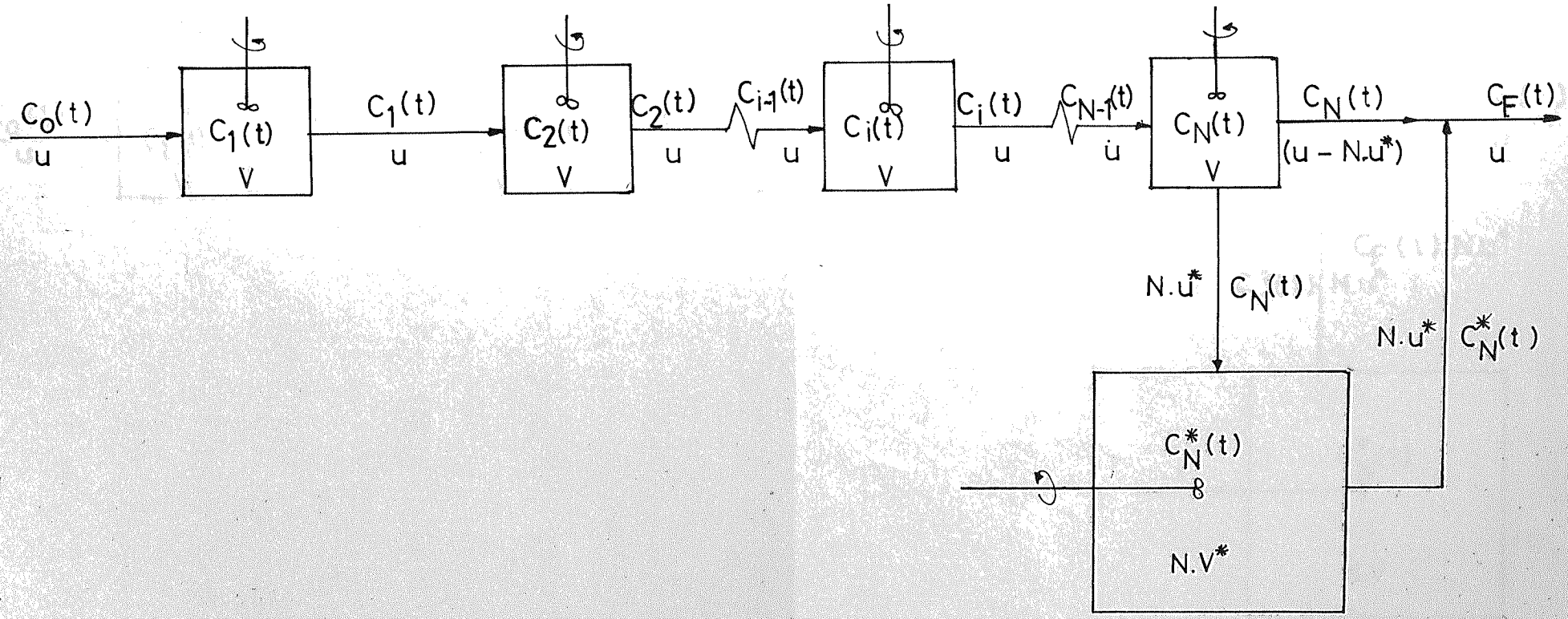

Figure 7.10 Stirred Tank Model with Re-entry Considered.

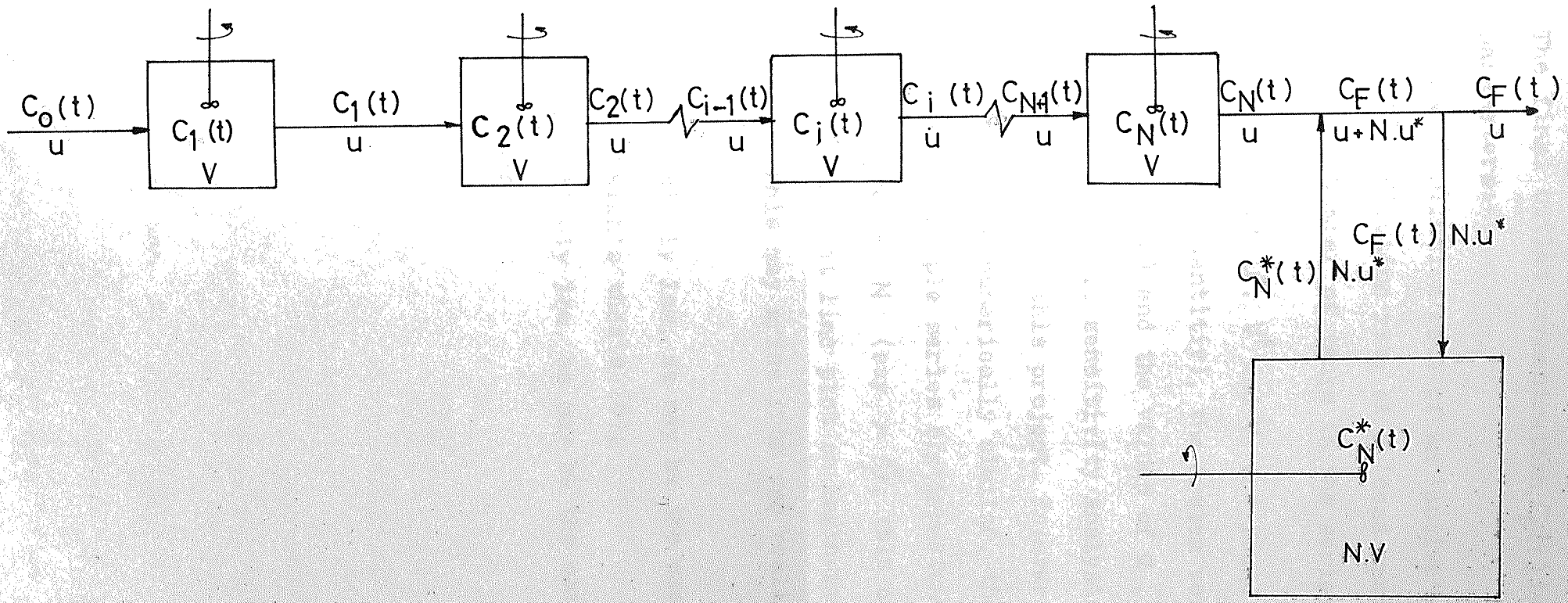

Model Sensitivity.

The final outlet concentration, $C_F(t)$, is a function of the three parameters:-

(i) $a = u/V$ Dilution rate of an 'active' tank (θ^{-1})

(ii) $b = u^*/V^*$ Dilution rate of a 'dead space' (θ^{-1})

(iii) N Number of tanks in the series.

The values of u^*, V^* and V are found from the bulk flow u (a known quantitiy), the system volume V_T (measured via response data) and the values of a, b and N

To present a full sensitivity analysis of the model is beyond the scope of this project. However, it may be seen that if a and b are numerically similar, the analysis simplifies to that of a simple series of stirred tanks with no 'dead spaces'. For a large N (say > 5), this condition will subsequently give a straight line plot on log:normal probability scales. This may arise from two realistic situations:

(i) u being relatively low, as may be the case in a low-rate filter, as in Sheikh's thesis (6);

(ii) V^* being relatively low, as may be the case when the microbial film is thin.

7.5 References.

1) Porter, K.E. & Smith, E.L. Plastic Media. Paper presented to the Institution of Water Pollution Control, at the University of Aston in Birmingham, March, 1978.

2) Atkinson, B & Williams, D.A. Trans. Inst. Chem. Engrs. 49, p219 (1971).

3) Balakrishnan, Eckenfelder and Brown. Water and Wastes Engineering. Volume 6 No. 1. Reuben H. Donnelly Corporation, (1969).

4) Sinkoff, M.D., Porgess, R. & McDermott, J.H. Mean residence time of a liquid in a trickling filter. J. Sanitary. Eng. 85, p51 (1959).

5) Heinrich, D. Laboratory study to clarify the effect of surface area and ret ntion time on nitrification in a fixed bed reactor. Gas - U Wasserbach 121 (5), p230 - 234 (1980).

6) Sheikh, M.I. Organic and liquid retention times in percolating filters. Ph. D. Thesis, University of Newcastle, (1968).

7) Schwartz, J.G., Weger, E. & Dudukovic, M.P. A new tracer method for determination of liquid - solid contacting effeciency in trickle bed reactors. A. I. Ch. E. Journal 22, p894 - 904 (1976).

8) Colombo, A.J., Baldi, G. & Sicardi, S. Solid - liquid contacting effectiveness in trickle bed reactors. Chem. Eng. Science 31, p1101 - 1108 (1976).

9) Levich, V.G., Markin, V.S. & Chismadzhez, Y.A. Chem. Eng. Science 22, p1357 (1967).

10) Levenspiel, O. Chemical Reaction Engineering. 2nd edition. Wiley & Sons, New York. (1966).

CHAPTER 8

EVALUATION AND INTERPRETATION OF THE HYDRAULIC MODEL PARAMETERS

8.1 Introduction.

The optimum combination of the hydraulic model parameters, a, b and N, will in both models give rise to the minimum difference between the actual response and that predicted by the model. Due to the algebraic complexity of the models an exhaustive method of comparing the predicted response curves (based on the use of all reasonable combinations of the parameters) and actual response curves was adopted. A computer program was developed for this purpose, the flow diagram and detailed explanation of the method being given in Appendix 4.

In the situation where the predicted response data from a model corresponds exactly to the actual data the method of comparison is of no consequence. However, in the more probable situation where the model merely approximates to tha actual data the method of comparison may be of considerable importance. Given that a model is not exact, then it is possible to choose which sections of the actual response curve should be most closely matched by the theoretical curve. It is for this reason that two different comparison methods were used simultaneously with each model.

8.2 Optimisation Methods.

Method 1.

The optimum combination of the hydraulic parameters was taken to be the one that yielded the minimum sum of errors, according to equation (8.1)

$$\text{Sum of errors} = \sum_{t=0}^{T} \frac{[C_F(t) - C(t)]^2}{[C(t)]^2} \qquad (8.1)$$

where $C(t)$ ——— actual concentration at time, t $(M.L^{-3})$

$C_F(t)$ ——— predicted concentration at time, t $(M.L^{-3})$

T ——— duration of tracer experiment (θ).

The use of the concentration difference squared gave emphasis to the larger errors, as does a "least squares" method. The introduction of the term $[C(t)]^2$ into the denominator put more weighting on points at the front end of the response curve where, otherwise, the errors were numerically small and where there were fewer data points.

Method 2.

The sum of errors was defined by equation (8.2).

$$\text{Sum of errors} = \sum_{t=0}^{T} \frac{[C_F(t) - C(t)]^2}{C(t)} \qquad (8.2)$$

In this case, emphasis was still given to the front of the curve, but to a lesser extent than when applying Method 1.

The effect of using the two methods on the optimum predicted response curves is demonstrated by the curves in Figures (8.1) and (8.2). Method 1 is seen to provide a closer fit at the front of the curve and Method 2 gives a better fit at the tail of the curve. However, situations arose where both methods gave the same results.

A third method of optimization was also tried, taking the denominator as unity. This gave visually unsatisfactory results due to the particularly poor correlation at the front end of the curve.

Figure(8.1) Biopac 50 Tracer Response, Using Method 1 Error Analysis ($u = 1.31 cm^3 s^{-1}$)

——— Actual Response

– – – – Predicted Response (Method 1)

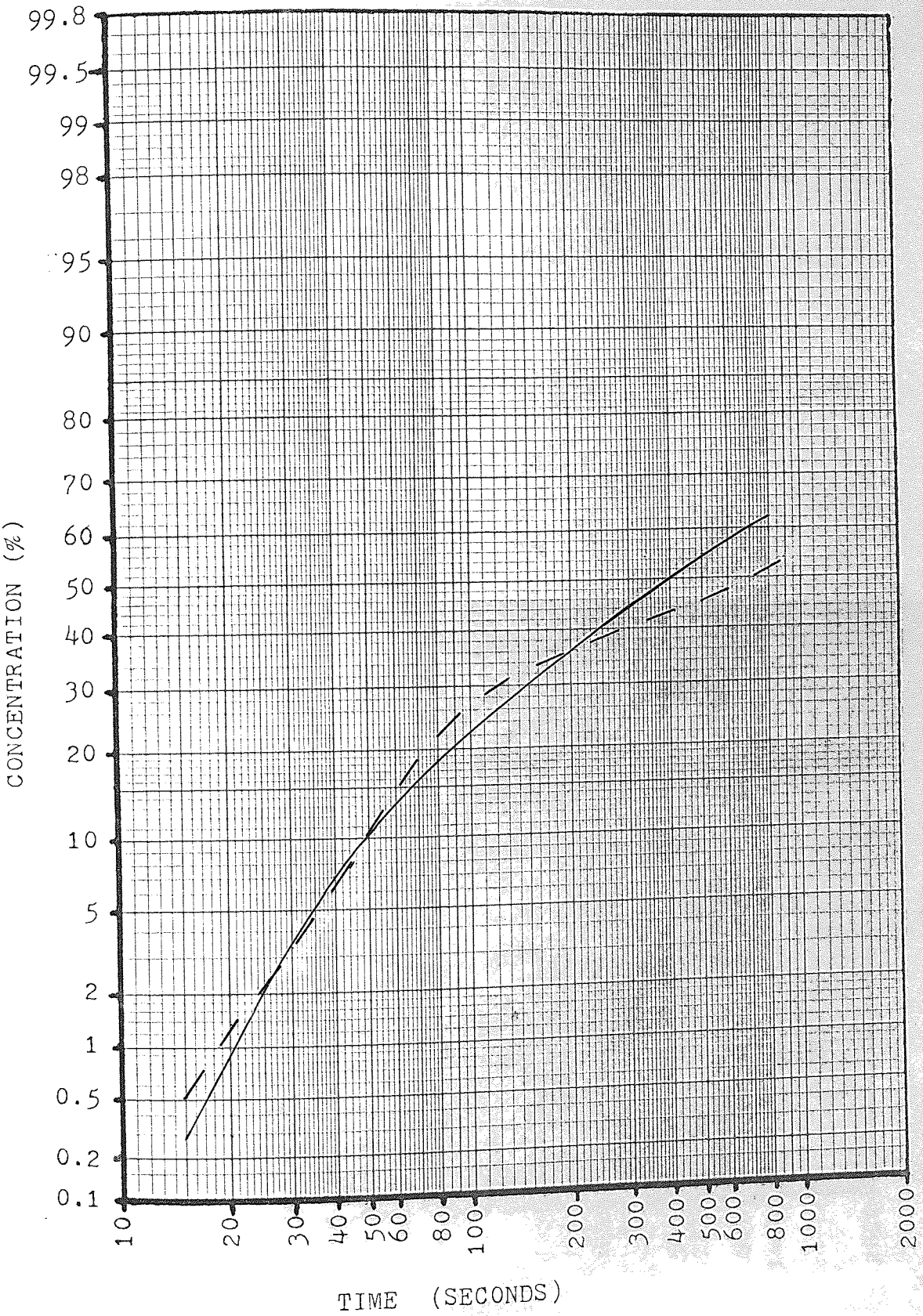

Figure (8.2) Biopac 50 Tracer Response, Using Method 2 Error Analysis ($u = 1.31 cm^3 s^{-1}$)

———— Actual Response

— — — — Predicted Response (Method 2)

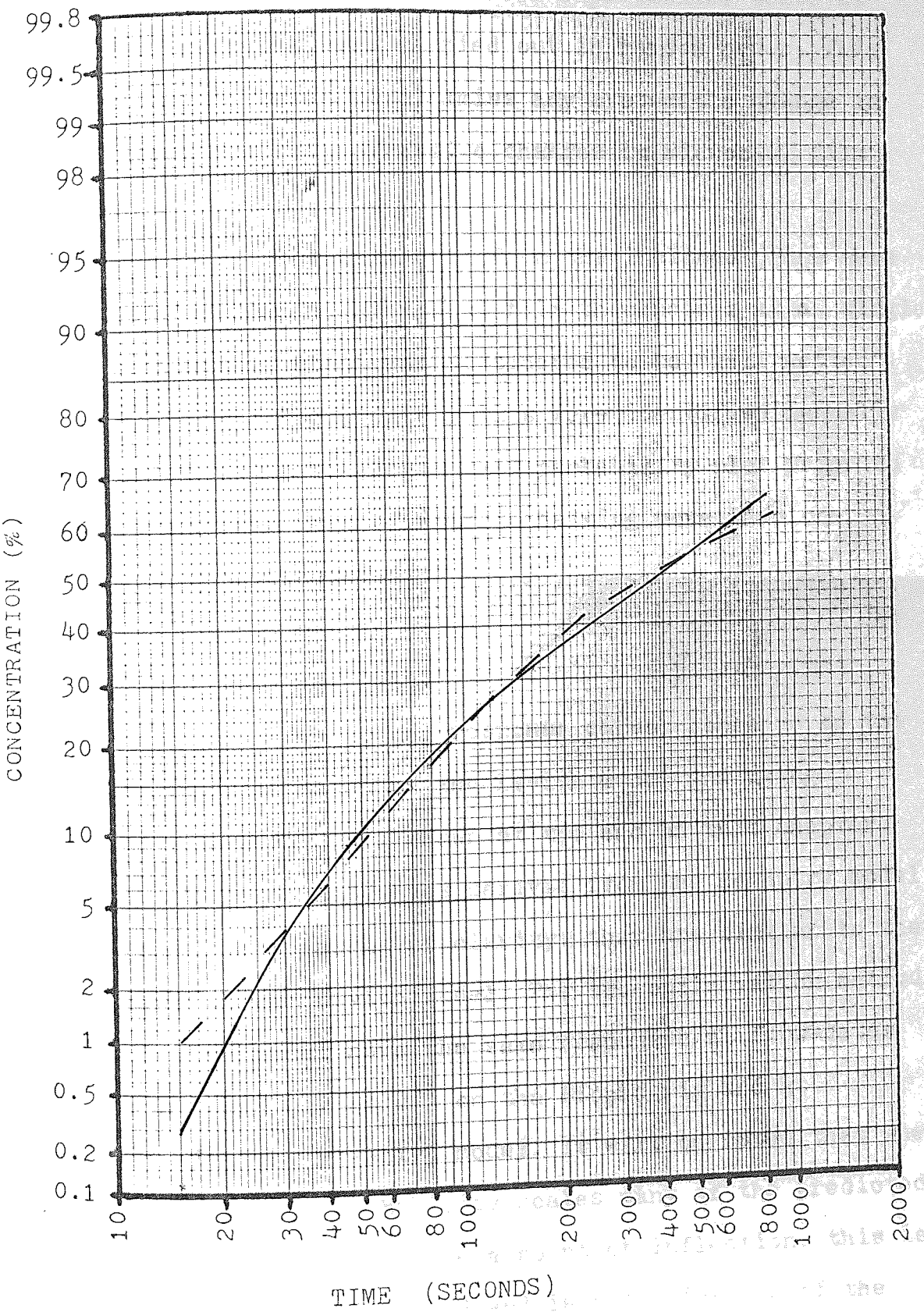

8.3 Experimental Data.

Response data from the Biopac rig, described in Section (4.7), were obtained for different liquid flow-rates. Since the microbial film was growing and the tracer was allowed one day to flush out between experiments, tests at different flow-rates were carried out in random order. This procedure was followed to minimise any systematic change in response data due to progressive changes in microbial film thickness.

Response data from the inclined plane were obtained for different microbial film thicknesses at a single flow-rate when the plane was considered to be "well wetted".

Rogue data points were identified manually and corrected using the log:normal probability plot prior to computer analysis. Sets of data containing more than one rogue point were discarded.

8.4 Predicted Response Data.

The actual response curves compared to the predicted response based on the Levich model and using Optimisation Method 2 are shown at the end of this chapter. The predicted response curves derived from the Re-entry model are not shown for reasons of clarity: they are similar to the curves based on the Levich model. The two optimization methods with the Levich model gave the same responses at flow-rates of $5.15 cm^3 s^{-1}$ and $0.75 cm^3 s^{-1}$ on the Biopac rig and at $5.15 cm^3 s^{-1}$ with the Re-entry model. It will be noted that when using the log:normal probability scales many of the predicted response curves appear to have a point of inflection; this is in fact due to the scales used and is not a feature of the model. The major feature of both models is that the tail of

the predicted curve is lower than that of the actual response curve: most liquid mixing models which do not take account of absorption show the reverse trend.(1)

8.5 Evaluation of Specific Wetted Surface Area, a Function of Liquid Irrigation Rate.

8.5.1 Mass-Transfer per Unit Wetted Area.

Table (8.1) shows the tracer mass transfer parameters $\left(\frac{U^*}{V^*}\right)$ arising from analysis of data from the inclined plane using the two hydraulic models and optimization methods. In the case of both hydraulic models, optimization method 2 is seen to give the more consistent results, although the arithmetic mean is the same in all cases, being $0.00040s^{-1}$. The mass-transfer parameter may then be evaluated using equation (8.3) and assuming the total available area of the inclined plane to be wetted.

$$\frac{\text{Mass Transfer}}{\text{Wetted Area}} = \frac{0.00040s^{-1}}{5cm \times 244cm} \qquad (8.3)$$

$$= \underline{3.279 \times 10^{-7} s^{-1} cm^{-2}}$$

8.5.2 Irrigation Rate.

Irrigation rate, like superficial velocity, is the volumetric flow rate per unit area of bed. The cross-sectional area of the Biopac rig is taken as the mean of a single piece of packing with its axes horizontal and vertical as illustrated in Figure (8.3). The irrigation rate on a full scale system is more conveniently expressed in the terms $(m^3 m^{-2} h^{-1})$. A specified irrigation rate will, for a given volumetric flow-rate, set the cross-sectional area of the bed.

Table(8.1)Mass Transfer Terms from the Inclined Plane at Various Liquid Hold-ups

Liquid Hold-up V_T (cm^3)	Levichs' Model (u^*/V^*)		Re-entry Model $(u^*/V^*)(u/(Nu^*+u))$	
	Method 1	Method 2	Method 1	Method 2
75	0.00015	0.00040	0.00016	0.00040
175	0.00052	0.00042	0.00059	0.00040
251	0.00044	0.00034	0.00040	0.00034
350	0.00048	0.00042	0.00044	0.00045
Mean	0.00040	0.00040	0.00040	0.00040
Std. Dev.	0.00017	0.00004	0.00018	0.00005

Figure (8.3) Plan Area of Biopac 50 Rig.

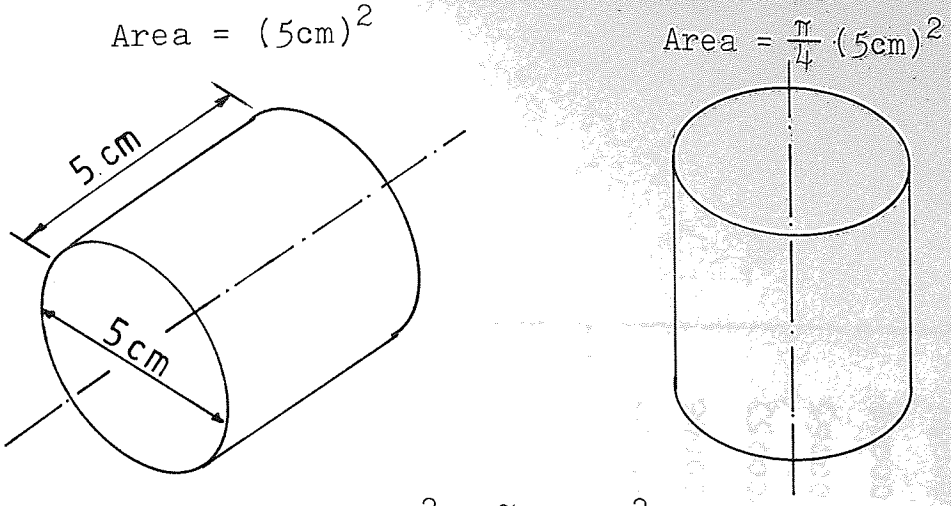

$$\text{Mean Area} = \frac{(5cm)^2 + \frac{\pi}{4}(5cm)^2}{2}$$

$$= \underline{\underline{22.3cm^2}}.$$

8.5.3 Specific Wetted Surface Area.

The specific wetted surface area is the surface area available for mass-transfer per unit volume of packed bed. The volume of the Biopac 50 rig is taken at its cross-sectional area ($22.3cm^2$) multiplied by its depth (80cm) or 1784 cm^3. Hence, the specific wetted areas from the Biopac 50 tracer experiments are given by equations (8.5) and (8.6) using the tracer mass-transfer parameters presented in Table (8.2).

$$\text{Specific Wetted Area } (cm^{-1}) = \frac{\left(\text{Total Wetted Area (Biopac experiment)}\right) cm^2}{1784cm^3} \quad \text{---(8.5)}$$

$$\text{Total Wetted Area (Biopac Experiment) } (cm^2) = \frac{\left(\text{Tracer Mass Transfer Parameter (Biopac Experiment) } s^{-1}\right)}{3.279 \times 10^{-7} s^{-1} cm^{-2}} \quad \text{---(8.6)}$$

Assuming that zero flow will give zero wetted area, the volumetric flow-rate ($cm^3 s^{-1}$) can be plotted against the tracer mass-transfer parameter (s^{-1}) for the two hydraulic

Table(8.2) Mass Transfer Terms from the Biopac 50 rig at Various Flow-rates

Liquid Flow-rate ($cm^3 s^{-1}$)	Levich's Model		Re-entry Model	
	Method 1	Method 2	Method 1	Method 2
0.75	0.00036	0.00036	0.00037	0.00034
1.30	0.00054	0.00045	0.00052	0.00046
1.95	0.00060	0.00054	0.00059	0.00053
2.60	0.00066	0.00063	0.00066	0.00065
3.90	0.00066	0.00069	0.00066	0.00069
5.15	0.00066	0.00066	0.00067	0.00067

models: these plots can then be rescaled to provide more practical plots of irrigation rate ($m^3m^{-2}h^{-1}$) against Specific Wetted Surface Area (m^2m^{-3}) as shown in Figures (8.4) and (8.5).

8.6 Liquid Film Thicknesses From Hydraulic Parameters.

As discussed in section (6.2), the thickness of the liquid film (δ) may be estimated during evaluation of the kinetic parameters from film thickness measurements and compared to those evaluated from the hydraulic parameters.

To summarise:

$$\text{hydraulic parameter } a = \frac{u}{V}$$

and

$$\text{total flowing liquid volume} = N.V$$

where u ——— bulk liquid flow-rate ($L^3\theta^{-1}$)

N ——— number of stirred tanks

V ——— volume of each active tank (L^3).

Assuming the liquid film thickness is uniform:

$$\text{Liquid film thickness} = \frac{\text{total volume}}{\text{wetted surface area}} = \frac{N.(u/a)}{\text{wetted surface area}} \quad \text{——(8.7)}$$

Tables (8.3) and (8.4) show the liquid film thicknesses evaluated from the hydraulic parameters for the inclined plane and Biopac 50 rig respectively.

8.7 Liquid Mixing.

The degree of liquid mixing is quantified by the number of tanks, N, in the series - the fewer the tanks the higher the level of mixing. Tables (8.3) and (8.4) show

Figure 8.4 Irrigation Rate .vs. Specific Wetted Surface Area on Biopac 50 (Based on the Levich Model)

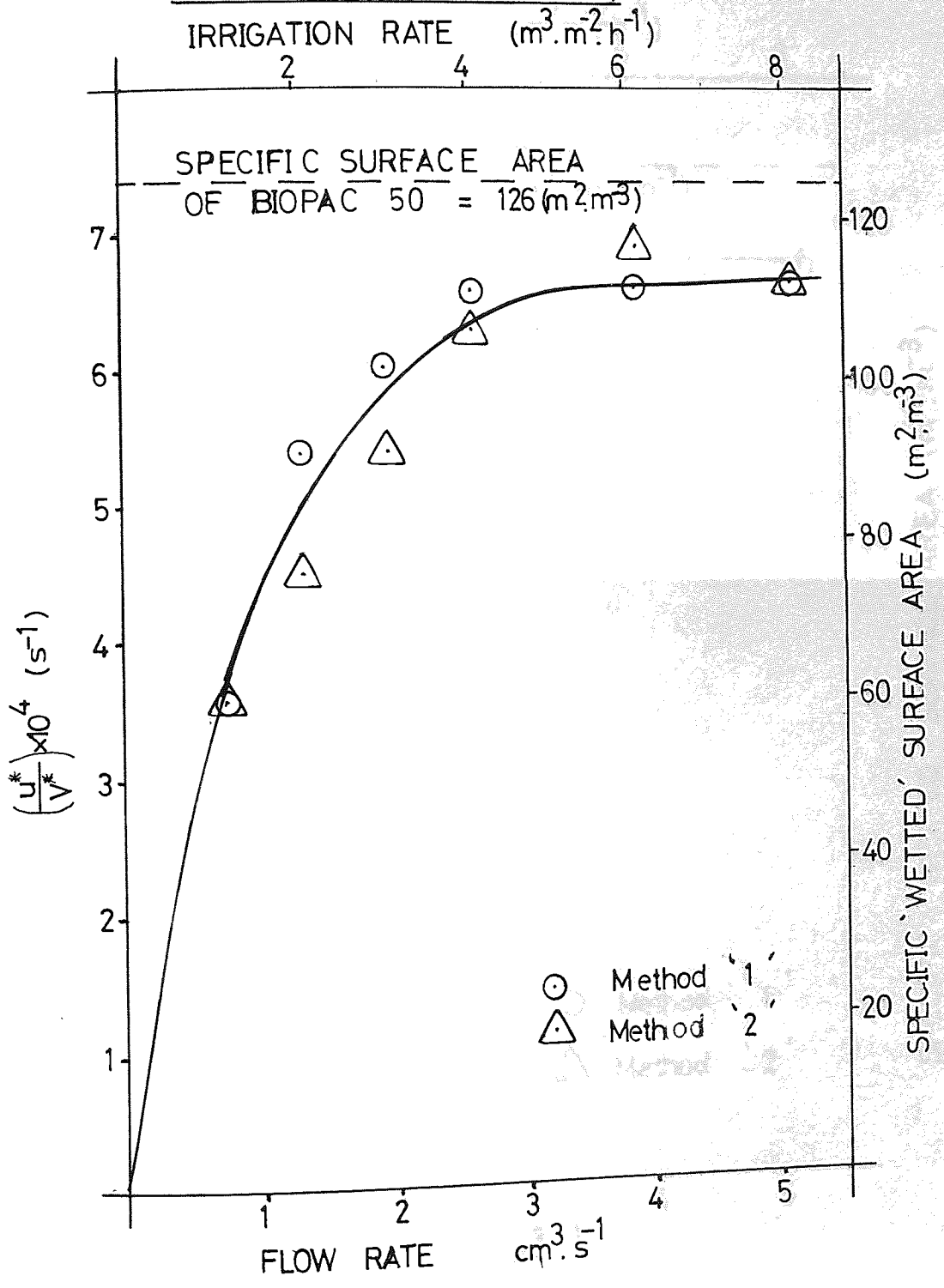

Figure 8.5 Irrigation Rate .vs. Specific Wetted Surface Area on Biopac 50 (Based on the Re-entry Model)

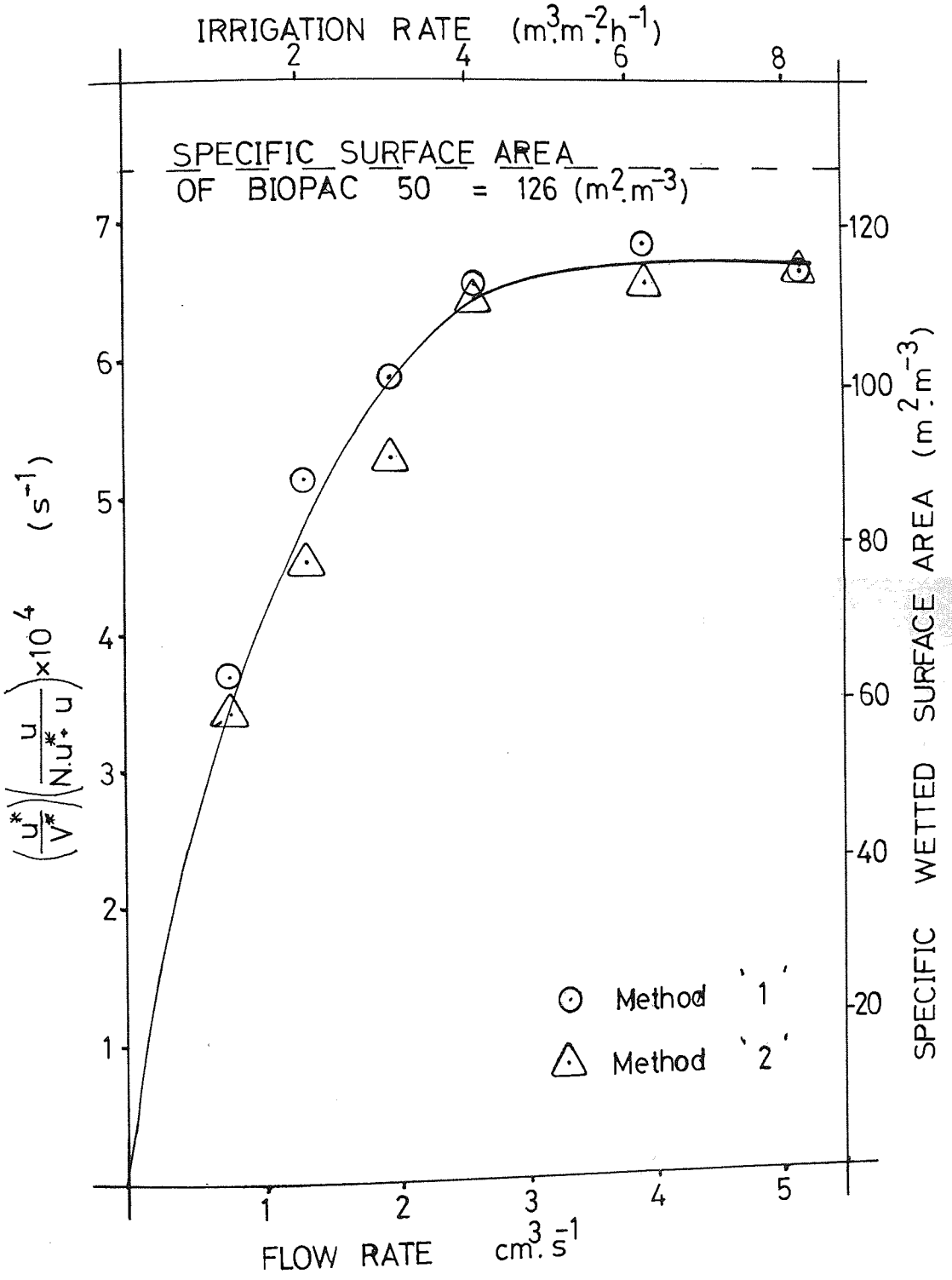

Table(8.3) Inclined Plane Liquid Film Thicknesses from Hydraulic Parameters

Liquid Hold-up V_T cm^3	Levichs' Model						Re-entry Model					
	Method '1'			Method '2'			Method '1'			Method '2'		
	N	a	δ (mm)	N	a	δ (mm)	N	a	δ (mm)	N	a	δ (mm)
75	11	0.079	0.29	10	0.077	0.27	11	0.079	0.29	10	0.077	0.27
175	4	0.035	0.23	2	0.014	0.29	4	0.035	0.23	2	0.014	0.29
251	5	0.040	0.26	3	0.019	0.32	5	0.040	0.26	3	0.019	0.32
350	11	0.078	0.29	6	0.034	0.36	11	0.076	0.30	6	0.034	0.36
Mean	—	—	0.27	—	—	0.31	—	—	0.27	—	—	0.31
Std.Dev.	—	—	0.029	—	—	0.039	—	—	0.032	—	—	0.039
Overall Mean = 0.29							Overall Std.Dev. = 0.038					

Table(8.4) Biopac 50 Liquid Film Thicknesses from Hydraulic Parameters

Liquid Flow-rate cm^3s^{-1}	Liquid Hold-up V_T cm^3	Levichs' Model						Re-entry Model					
		Method '1'			Method '2'			Method '1'			Method '2'		
		N	a	δ (mm)	N	a	δ (mm)	N	a	δ (mm)	N	a	δ (mm)
0.75	1025	2	0.018	0.76	2	0.018	0.76	2	0.016	0.74	2	0.016	0.76
1.30	1740	4	0.058	0.54	2	0.016	1.18	4	0.054	0.61	2	0.016	1.16
1.95	1052	3	0.050	0.64	2	0.028	0.85	3	0.050	0.65	2	0.028	0.86
2.60	1628	5	0.082	0.79	4	0.062	0.87	5	0.082	0.79	4	0.062	0.85
3.90	1049	1	0.022	0.88	1	0.022	0.84	1	0.022	0.88	1	0.022	0.84
5.15	1478	1	0.036	0.71	1	0.036	0.71	1	0.036	0.70	1	0.036	0.70

the number of tanks obtained using both hydraulic models and optimizations for the inclined plane and Biopac rig respectively.

8.8 Discussion.

It is apparent from Figures (8,4) and (8.5) and Tables (8.1) and (8.2) that the two hydraulic models - the Levich and the Re-entry Models - give rise to essentially the same results. The author favours the Levich Model because it is easier to interpret the model parameters.

As previously discussed in section 8.2, the two Optimization Methods on both models often gave the same or similar predicted response curves. The figures in Table (8.1) suggest that Optimization Method 2 gives the more consistent results. However, as will be seen from Figures (8.4) and (8.5) a better fit is obtained by combining the two methods.

It will be noted that the liquid film thicknesses δ calculated from the hydraulic parameters on the inclined plane and presented in Table (8.3) are higher than those calculated from kinetic data and shown in Table (6.1). The values of δ obtained from the kinetic parameters are based on actual film thickness measurements and are thus considered to be more reliable. However, the values of δ obtained from the kinetic studies were derived from data collected during the exponential growth phase i.e. while the microbial and liquid films were relatively thin and uniform. By contrast, the values of δ obtained from the hydraulic model parameters were generally based on data obtained when the microbial and liquid films were thick and uneven. The possibility and consequences of the hydraulic model over-estimating the values of δ are discussed later.

It is apparent from Figures (8.4) and (8.5) that a minimum irrigation rate is necessary to make full use of the available surface area. It will also be noted that the surface area of the film was less than that of the packing; this was due to the fact that the microbial film built up in the corners and points of contact between adjacent packing elements. The minimum irrigation rate to make full use of the available surface area found here was about $4m^3m^{-2}h^{-1}$. This is considerable higher than the range of 0.7 to $1.5m^3m^{-2}h^{-1}$ reported in the literature (2). However, the values reported in the literature have no theoretical base and may arise from cost considerations, since it may be cheaper to build and operate a bed with a greater volume than the minimum figure but of a limited height. Alternatively, the high minimum irrigation rate could have arisen from the use of a small experimental rig with a symmetrical packing configuration. Whatever the explanation, it is advisable to carry out further tracer experiments on a larger pilot plant using randomly dumped packing. Some care should be taken in sizing such a pilot plant for this purpose and is discussed below.

The degree of liquid mixing, as quantified by the number of theoretical stirred tanks, N, is shown in Tables (8.3) and (8.4). For a particular Optimization Method the values of N are the same with either Model: Optimization Method 1 results in higher values of N than those obtained using Method 2, with the exception of cases when the same values of N arise. The differences in N arising from the two methods are due to the shape at the front of the response curve being affected more by the liquid mixing than is the tail (3). Method 1 gives the closer fit at the front of the curve. It is apparent that no correlation between the number

of tanks N and the liquid hold-up or flow-rate exists for results obtained with either the inclined plane or the Biopac rig. The lack of either of these correlations may possibly be due to the size of the experimental equipment. The liquid mixing on the inclined plane was found to vary from near plug flow (no mixing with $N = 10 \sim 11$) to almost perfect mixing ($N = 2 \sim 3$). This variation in liquid mixing on the inclined plane restricts its usefulness as an analytical tool and justifies the use of microbial film thickness/growth measurements, as opposed to concentration measurements, to evaluate the kinetic parameters (see sections 4.5 and 6.2). The liquid mixing in the Biopac rig was also found to vary, but to a lesser extent than in the inclined plane experiments; generally there was a tendency towards a higher level of mixing. The effect of bed depth has not been investigated by the author: however, it is obvious that plug-flow will be approached as bed depth is increased.

8.9 Experience with the Hydraulic Models.

Although the tracer technique and hydraulic analyses in this thesis were developed for the particular application of high rate biological filters, other applications may be found. Before any experimental studies are undertaken which may use either of the two Hydraulic Models, the potential limitations discussed here should be considered. Particular reference is made to the sizing of a pilot plant rig for the confirmation of the irrigation rate/specific wetted surface area plot for a high-rate filter. However, the points raised will also apply to other systems.

As suggested above, the hydraulic models may be overestimating the liquid thicknesses δ. The values

of δ are obtained from the estimates of the volume of the "active" stirred tanks arising from the hydraulic models. The hydraulic models will tend to overestimate the volume of the "active" stirred tanks to compensate for the assumption of a single "dead-space". This, in turn, will lead to low estimates of the wetted surface area; since some of the tracer that actually passes into the microbial film is seen by the model to be retained in an oversized "active" stirred tank series. This phenomenon is unlikely to have had a significant effect on the values of the wetted surface area presented in Figures (8.4) and (8.5) since the wetted surface area is taken as being proportional to the dilution rate of the dead-space (see equations (8.3) and (8.6)). With the relatively thick microbial films encountered in these tracer studies the dead-space forms the major part of the total liquid hold-up in spite of the tendency for the models to overestimate the volume of the "active" stirred tanks.

With relatively thin microbial films the over-sizing of the "active" stirred tanks could have a serious effect on the wetted surface area calculations as the size of the dead-space will be proportionally more seriously affected. As demonstrated in Appendix 3 the models will also fail if the dilution rates of the dead-space and "active" stirred tanks are similar. In biological filters this may arise with low flow-rates or thin microbial films. However, in the case of a biological filter with a thin microbial film, zero-order kinetics may well apply, in which case it is a relatively simple task to evaluate the wetted surface area from kinetic data.

The assumption of a single dead-space will tend to give rise to larger errors as the bed depth is increased,

due to the increased potential for repeated absorption of tracer. It is most unlikely that the errors will be restricted to the wetted surface area estimations; the degree of liquid mixing will also be in error. Hence, an upper limit to the experimental bed depth is envisaged. On the other hand, the bed depth and cross-sectional area used in this work were probably too small. A practical upper limit to the experimental bed's cross-sectional area is also envisaged, since the essential good liquid distribution (for experimental purposes) at the inlet becomes increasingly difficult to achieve as the cross-sectional area is increased.

The limitations of the hydraulic models are summarised below:

1) The liquid film thickness, δ, may be overestimated within an order of magnitude.
2) The wetted surface area may be underestimated, particularly on deep beds.
3) The degree of liquid mixing may not be correctly quantified on shallow or deep beds.
4) The models may fail if the flow-rate is low or the flowing liquid forms the major part of the liquid hold-up.

Figure(8.6) Inclined Plane Tracer Response

$V_T = 75cm^3$

Actual Response

Predicted Response

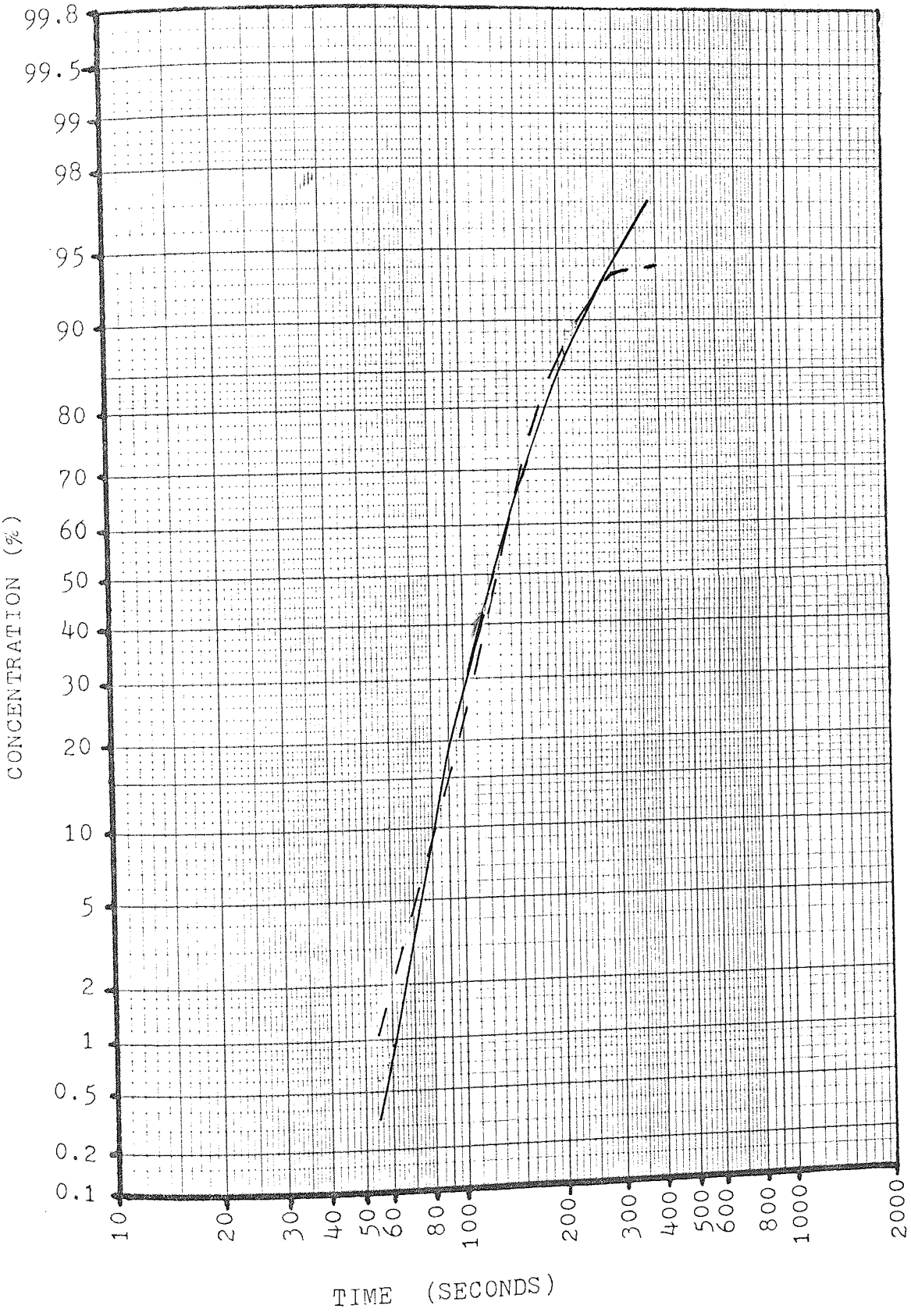

Figure(8.7) Inclined Plane Tracer Response

V_T =175cm^3

——— Actual Response

— — — — Predicted Response

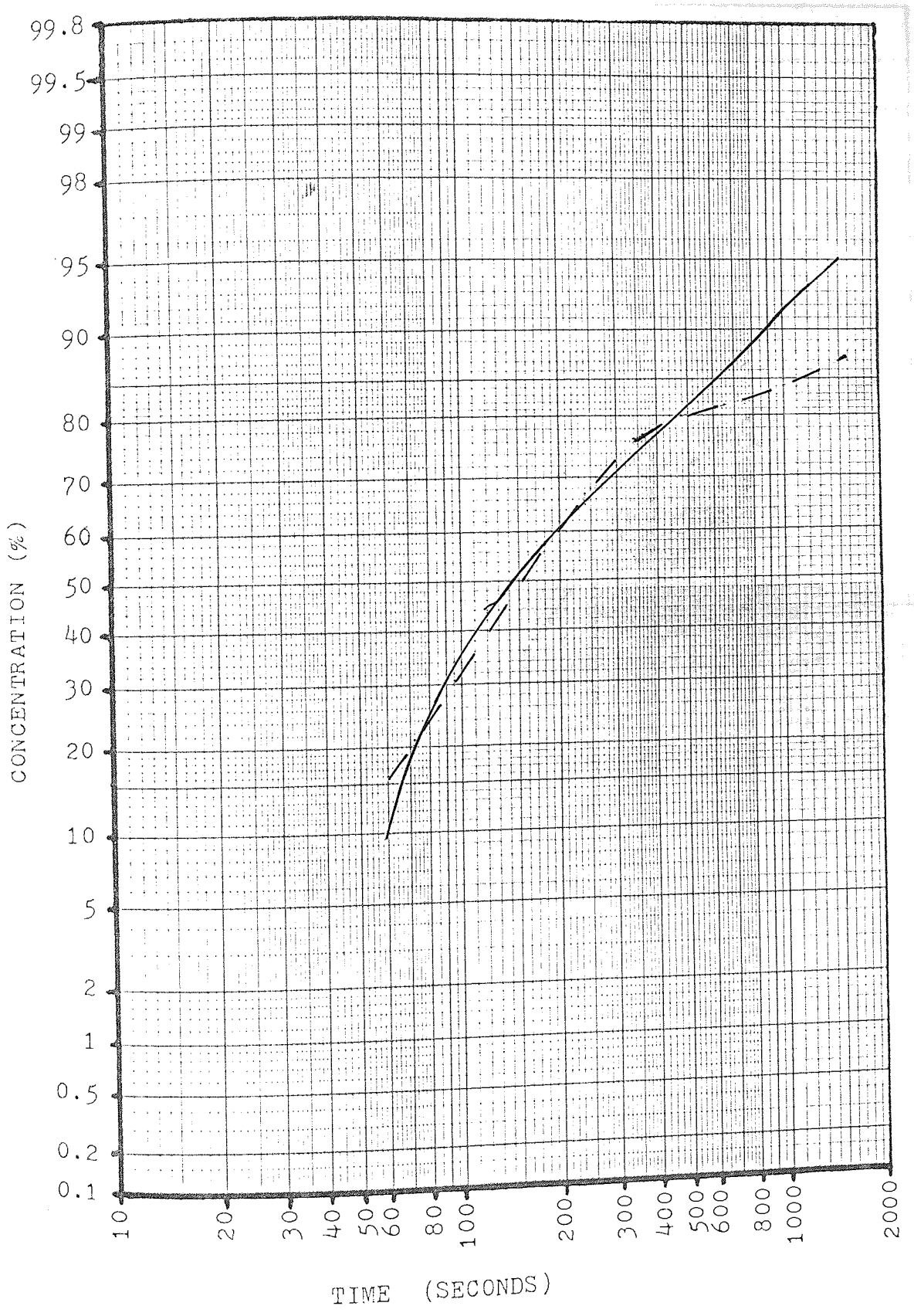

Figure(8.8) Inclined Plane Tracer Response

$V_T = 251 cm^3$

——— Actual Response

— — — Predicted Response

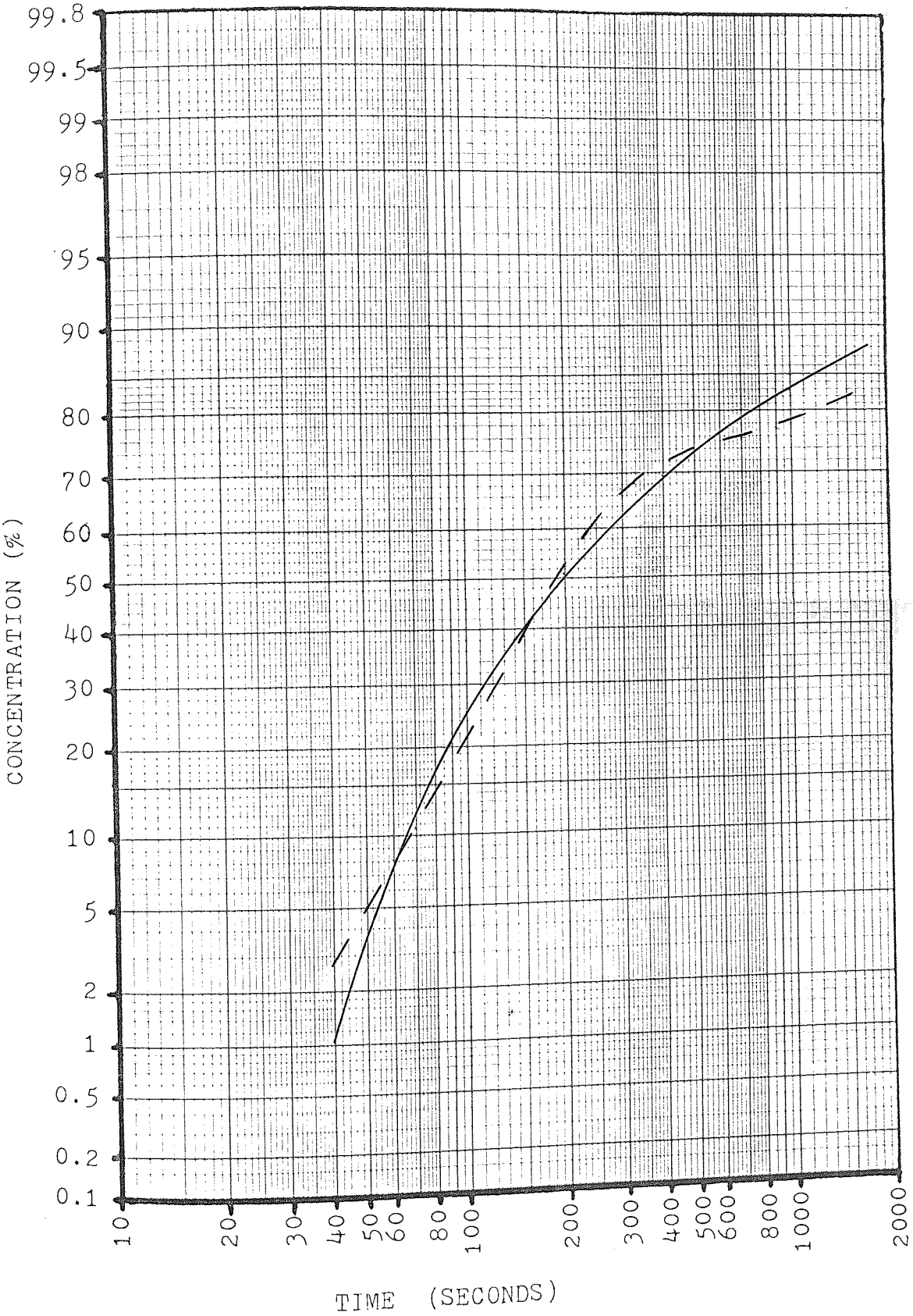

Figure(8.9) Inclined Plane Tracer Response

V_T = 350cm^3

——— Actual Response

– — — Predicted Response

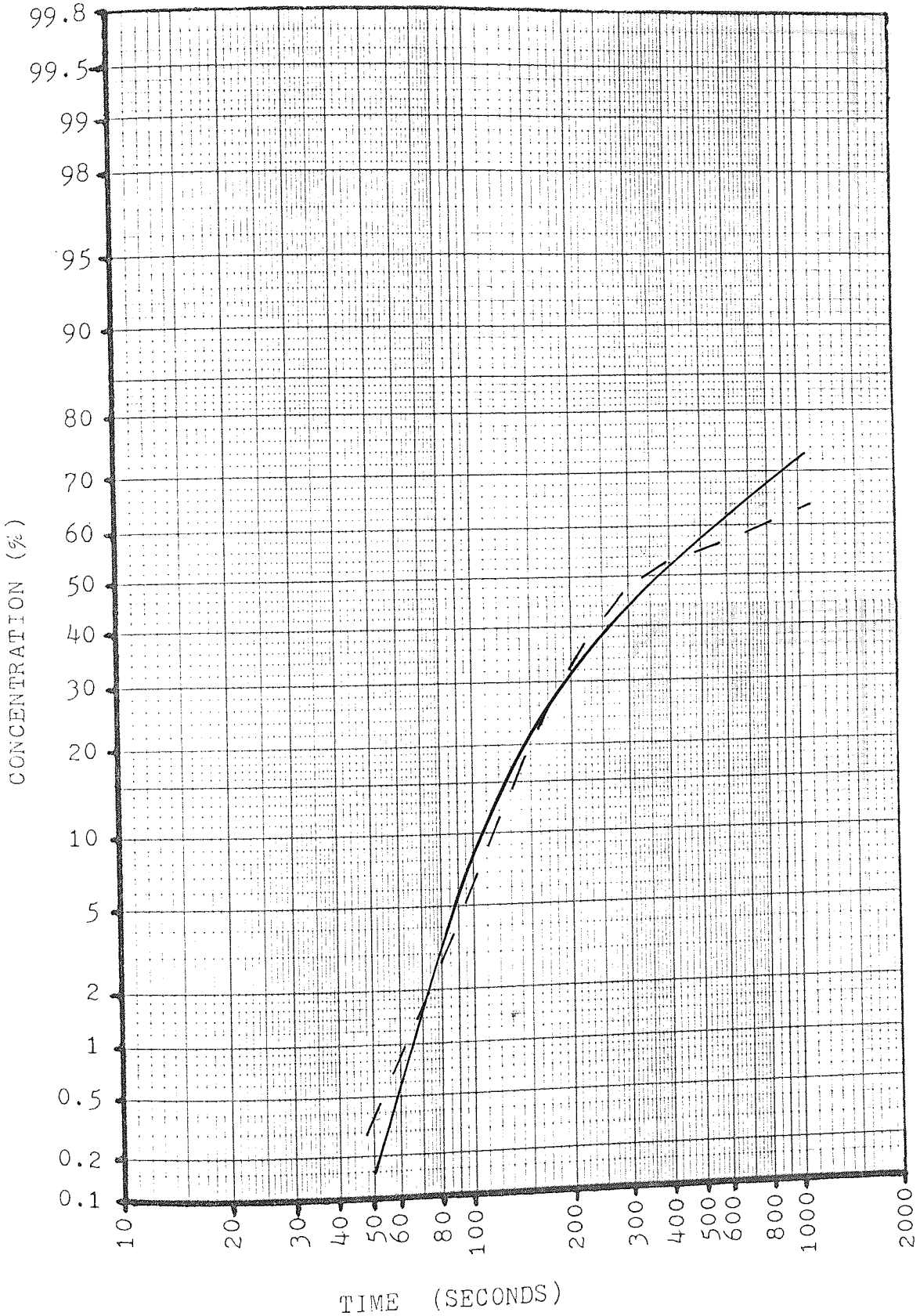

Figure(8.10) Biopac 50 Tracer Response

$u = 0.75 cm^3 s^{-1}$

——— Actual Response

— — — Predicted Response

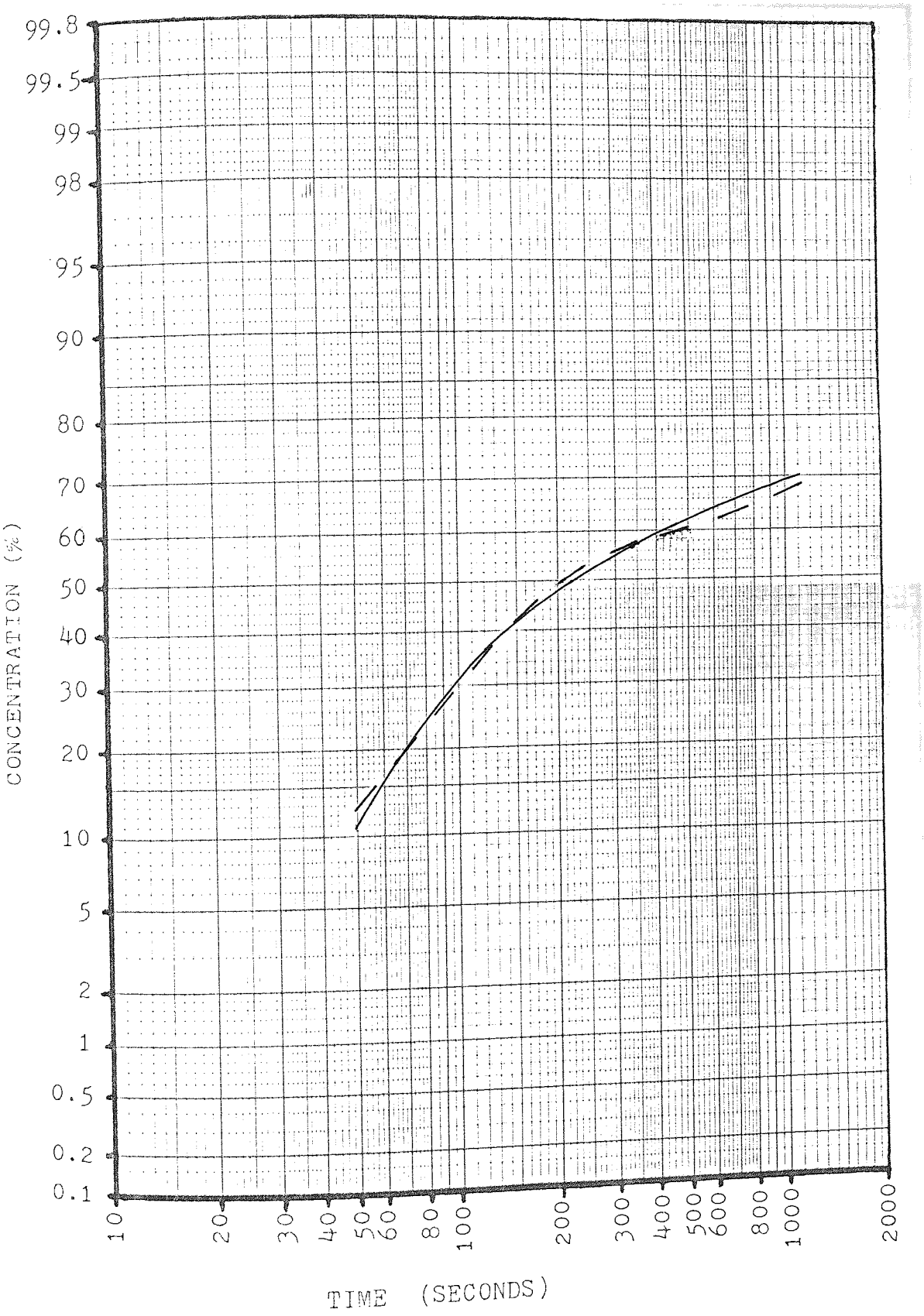

Figure(8.11) Biopac 50 Tracer Response

$u = 1.95 cm^3 s^{-1}$

———— Actual Response

— — — Predicted Response

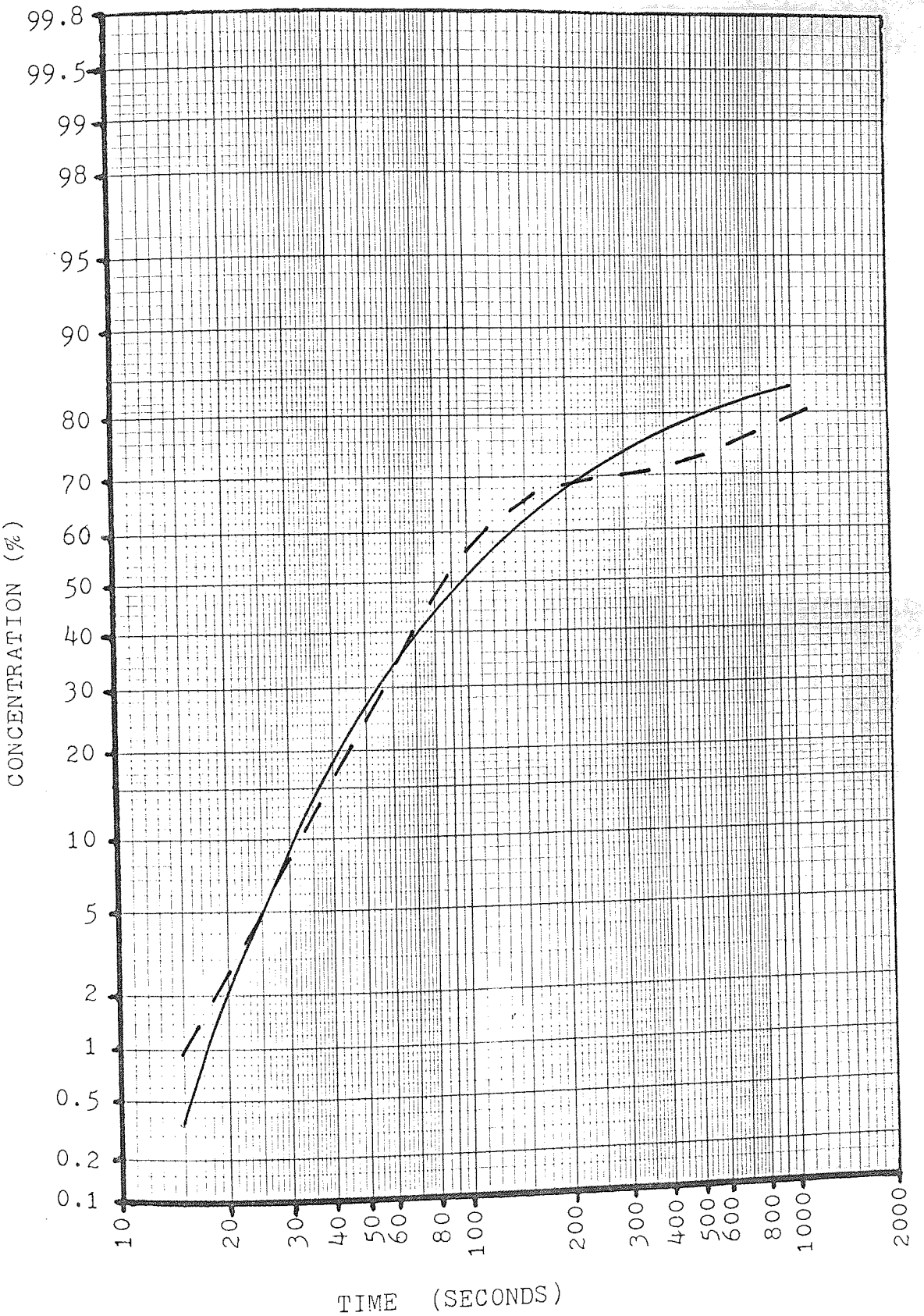

Figure (8.12) Biopac 50 Tracer Response

$u = 2.60 cm^3 s^{-1}$

——— Actual Response

— — — — Predicted Response

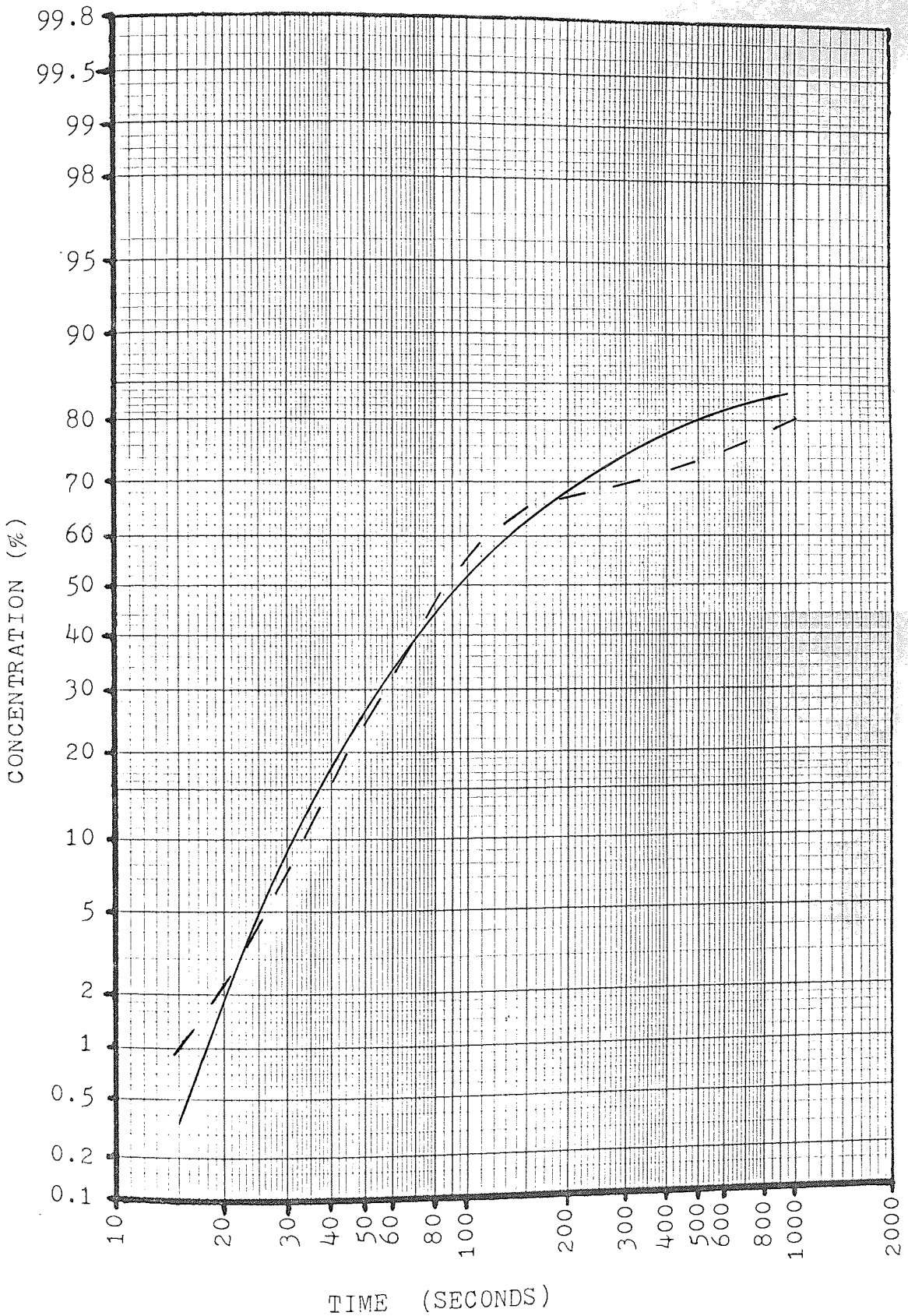

Figure (8.13) Biopac 50 Tracer Response

$u = 3.9 cm^3 s^{-1}$

——— Actual Response

— — — - Predicted Response

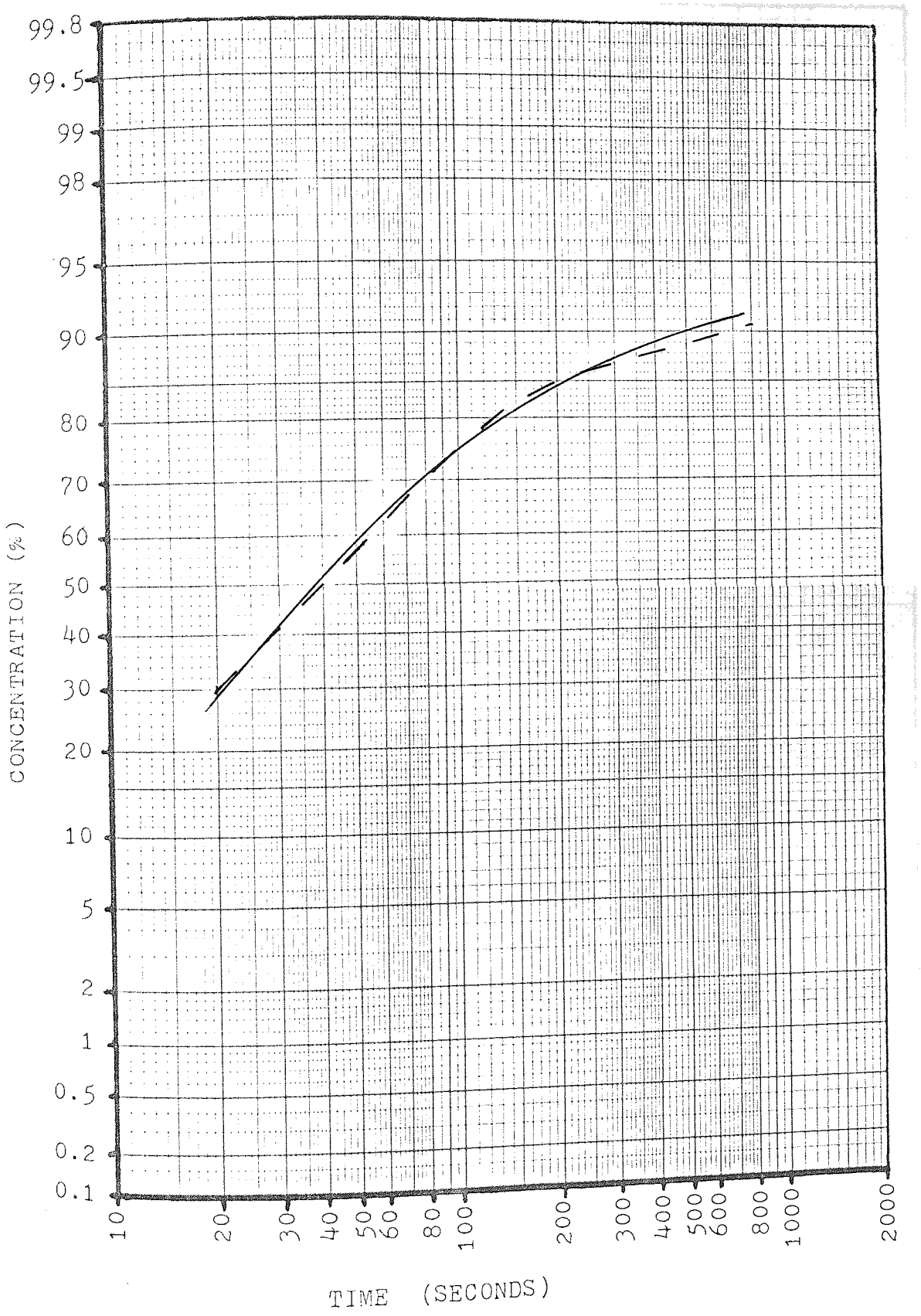

Figure (8.14) Biopac 50 Tracer Response

$u = 5.15 cm^3 s^{-1}$

——— Actual Response

— — — — Predicted Response

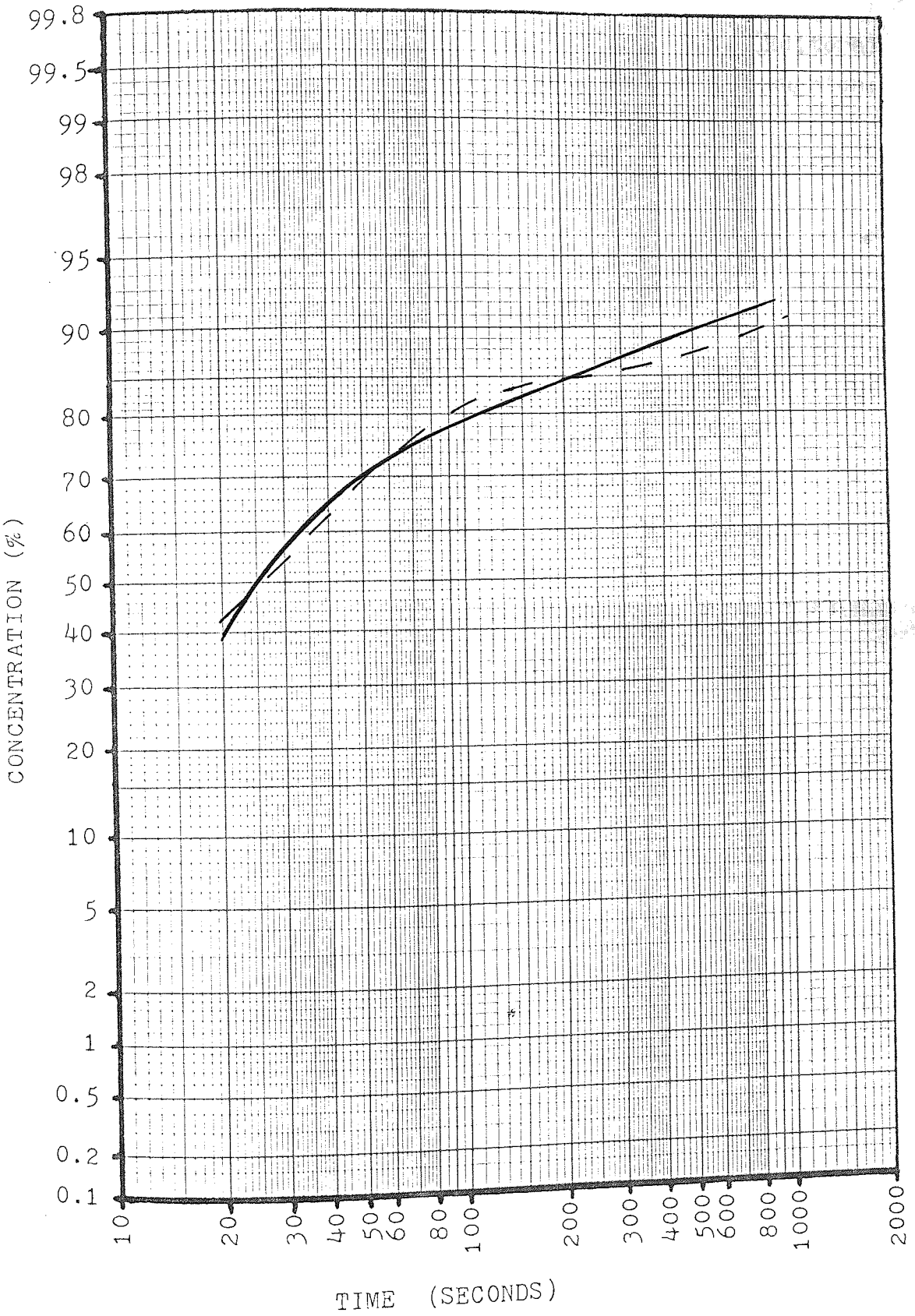

8.10 References.

1) Buffam, B.A. & Rathner, M.N. The influence of viscosity on axial mixing in trickle flow in packed beds. Trans. Tnst. Chem. Engrs. 58, (1978).

2) Calley, A.G., Forster, C.F. & Stafford, D.A. (Editors) Treatment of Industrial Effluents. Hodder & Stoughton; London, Sydney, Auckland, Toronto (1977).

CHAPTER 9

GENERAL SUMMARY AND DISCUSSION

By re-examining the three subject areas - kinetics, hydraulics and ecology - it has been possible to integrate them further and thus develop a clearer understanding of filter performance and behaviour.

9.1 Kinetic Models: Single and Multiple Substrates.

A kinetic model based on intrinsic zero-order kinetics coupled with a potential diffusion limitation is presented and developed in Chapter 2: this can be used in cases where either one or more substrates may be rate-limiting. The bulk kinetics that arise from the model are expressed in terms of the rate of substrate removal per unit wetted surface area of microbial film. In the case of a single limiting substrate, the bulk kinetics are either zero- or half-order with respect to the substrate concentration. In the zero-order regime, the rate of substrate removal is governed by the intrinsic rate constant and the microbial film thickness. In the half-order regime, the rate of substrate removal is governed by the same intrinsic rate constant, the substrate diffusivity through the film and the substrate concentration at the surface of the microbial film.

The multisubstrate model is based on the assumption that there is a sequential utilization of rate-limiting substrates, the more readily assimilated compounds being used prior to the use of the less readily assimilated compounds. However, the kinetic model demonstrates that simultaneous utilization of the rate-limiting substrates may occur. This arises when the less readily assimilated compounds are utilized in the deeper parts of the microbial film where the concentration of the more readily assimilated compounds is low. In these circumstances, the overall

removal of substrates may appear to follow first order kinetics. However, the apparently simple first order kinetics may give misleading results, particularly if a recycle is employed. The multi-substrate model should overcome this problem and, in addition, it should be possible to model the rate of removal of a chosen compound from within a multi-substrate mixture.

9.2 Determination of Kinetic Parameters.

The zero-order rate constants arising from a single rate-limiting substrate have been quantified by two independent methods. The first method was based on simple material balances and substrate concentration measurements within the zero-order regime. The second method was based on the use of film thickness measurements to locate the transition between the two regimes. Since consistent values for the intrinsic zero-order rate constants were obtained using the two independent methods, the modelling approach appears to be of value. In addition, the diffusivities of the rate-limiting substrates were quantified by this analysis prior to the identification of the rate-limiting substrate.

The major part of the kinetic study was carried out using an inclined plane to simplify hydraulic conditions and enable accurate microbial film thickness measurements to be made using a modified micrometer. A series of both qualitative and quantitative tracer experiments were carried out using dyes and bromide salts to establish the degree of liquid mixing and the extent of wetting of the inclined plane. The experiments confirmed the validity of the plug flow assumption used in the inclined plane material balances whilst the microbial film was relatively new and

enabled the author to judge when to cease collecting further data.

9.3 Determination of the Hydraulic Parameters.

Quantitative tracer studies were carried out on a commercial random packing (Biopac 50) to quantify the extent of surface wetting and the degree of liquid mixing as functions of liquid loading. A mathematical model was developed and used for analysing the tracer response data. By comparing the values of the mathematical model parameters obtained when using the Biopac 50 and tracer response data from the inclined plane, graphical plots of specific wetted surface area against liquid loading were obtained for the random packing (see Figures 8.4 and 8.5).

Due to the small scale of the experimental biological filter used in the tracer studies, no functional relationship between liquid mixing and liquid loading was obtained. However, the hydraulic parameters obtained were successfully used to demonstrate the independence of the kinetic parameters on the liquid loading (see Appendix 5), thus substantiating both the kinetic and hydraulic models.

9.4 Changes in Microbial Film Characteristics.

During the course of the kinetic experiments on the inclined plane, it was noted that the microbial film composition and characteristics were dependent on the concentrations of the nitrogen salts and the carbon source. These observations suggested that:

1) the growth of fungi was inhibited at relatively high nitrogen salt concentrations,
2) the production of extracellular slime by bacteria was

reduced at relatively low concentrations of the carbon source

3) the growth of bacteria was inhibited by fungi when both the nitrogen salts and carbon source concentrations were relatively low.

The bacterially produced extracellular slime was seen to provide the adhesive and cohesive properties of the microbial film. Hence films that were lacking the extracellular slime gave rise to turbid effluents. Fungi were found to strengthen the microbial film only when an extracellular slime was also present. The combined strength of the fungal hyphae and the extracellular slime allied with the slow degradation rate of the fungi have been identified as causes of ponding (a situation which is made worse at low ambient temperatures). Methods of mitigating ponding are suggested in Chapter 5 and are based on either inhibiting the growth of fungi or reducing the production of the extracellular slime.

9.5 Effect of Microbial Film Characteristics on Kinetic Parameters.

The parameters of the kinetic model were found to be affected by the microbial film composition and characteristics. The intrinsic zero-order rate constant of the rate-limiting substrate increased both as the proportion of bacteria and the concentration of organisms increased in the microbial film. However, at low ambient temperatures, fungi are expected to give the higher zero-order rate constant and hence become more dominant.

The diffusivity of substrates through the microbial film was found to be greatly in excess of that in water; this has been attributed to the presence of the bacterially-produced extracellular slime and not to "hyphal

streaming" in the fungi. The composition of the carbon source is thought to play an important role in affecting the diffusion properties of the extracellular slime. A domestic sewage effluent that contains little sugar is believed to yield a bacterial slime that does not enhance the substrate diffusivity. On the other hand, a sugary effluent, similar to the model effluent used in this study, may be expected to yield a bacterial slime that promotes substrate diffusion. The enhanced diffusivities will result in higher bulk rates of substrate removal and lead to thicker microbial films that may cause ponding if fungi are also present.

9.6 Filter Behaviour and Long-Term Performance.

As a result of work on the inclined plane, the author has found it useful to describe the behaviour of microbial films under three headings: shedding, long sloughing cycle and short sloughing cycle. The terms are described and discussed below in relation to the long-term filter performance when treating an effluent with a single rate-limiting substrate.

Shedding.

Shedding is the continuous loss of microbial film that matches the rate of growth. It arises when there is poor cohesion of the microbial film due to a lack of bacterial slime, and may occur with either predominantly bacterial or fungal films. As a consequence of the equilibrium between microbial film loss and growth, filter performance will not change with time.

It may be seen by comparing the film thickness data presented in Figures 5.8 and 6.5, that, in the case of a predominantly fungal film, the local average film thickness

may be maintained above the critical film thickness. In this case, the kinetics will always follow the half order regime once the microbial film is established. In the case of a predominantly bacterial film, shedding may occur with the kinetics following either or both regimes, the transition between the two regimes being at a fixed depth in the filter.

Long Sloughing Cycle.

A long sloughing cycle occurs when both fungi and bacterial silme are present together in the microbial film. The fungal hyphae strengthen the gelatinous bacterial slime in the same way that glass fibres strengthen plastic resins. This composite strength prevents the microbial film breaking away from the packing surface in small pieces, even after the adhesive strength is impaired by the reabsorption of the bacterial slime. The final break-away of the microbial film occurs simultaneously over large sections of the packing due to the cohesive strength of the film that remains even after the loss of adhesion. Some loss of cohesive strength is necessary before the film can break up and this occurs when the bacteria have partially degraded the fungi after reabsorbing the extracellular slime. The weight of the microbial filn breaking free from the top sections of the filter is likely to be sufficient to break off the loose film in the lower sections as it falls through the filter. In this way, the filter is likely to slough in phase.

The cycle of regular growth and loss of microbial film will give a cyclic pattern to the performance of the filter. Initially, the kinetics will be zero-order throughout the filter and the performance will be relatively poor due to a lack of microbial film. The performance will rapidly improve as the microbial film grows exponentially. A period

Figure 9.1 Long-Term Filter Performance with a Long Sloughing Cycle.

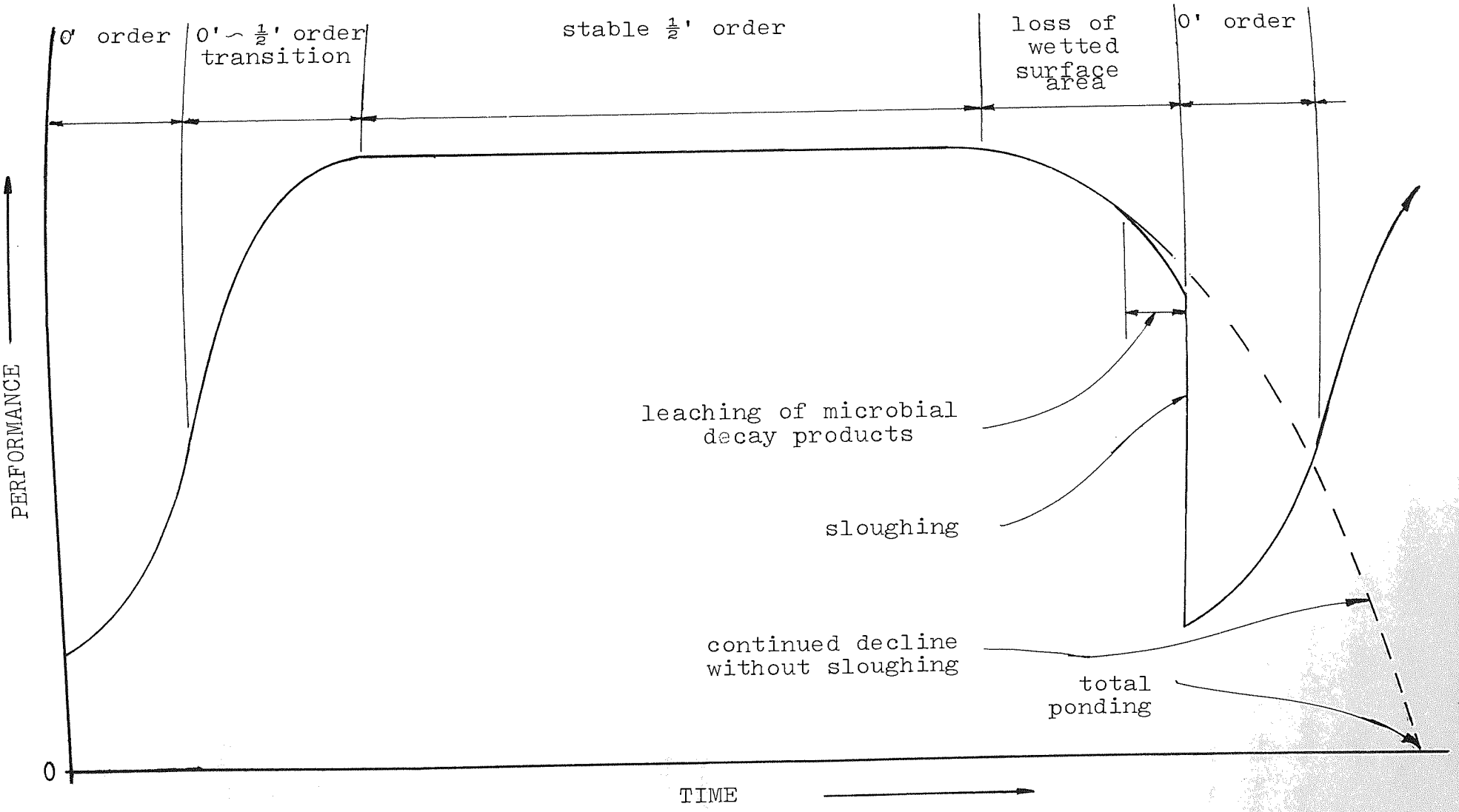

of transition between zero-order and half-order kinetics will then follow; this will be characterised by a slowing down in the improvement in performance. Once half-order kinetics have become established throughout the filter, the performance will be stable until the microbial film thickness becomes excessive or immediately prior to sloughing. At this latter point, a small but sharp drop in filter performance may be apparent; this is due to the release of decayed organisms from within the microbial film as it starts to break up. After sloughing, the performance will drop to the initial condition and the cycle repeated.

If, however, the microbial film thickness becomes excessive prior to sloughing, filter performance will be impaired due to a reduction in the wetted surface area. At this point there is a danger of partial blockages and, ultimately, ponding, in which case the filter will cease to function. The cyclic performance of a filter with a long sloughing cycle is summarised in Figure 9.1; the effect of an excessive development of microbial film is also shown.

Short Sloughing Cycle.

A short sloughing cycle will only occur with predominantly bacterial films that are held together by extracellular slime. As with a long sloughing cycle, the kinetics will initially be zero-order, becoming half-order. However, the stable period of half-order kinetics will be much shorter, due to the rapid break-up of the film in the absence of strengthening fungi. As a consequence of the relative ease with which the film will break up, there is little possibility of the film thickness becoming excessive and it is likely that the sloughing cycle in various sections of the filter will not be in phase. If the sloughing cycles

get out of phase, filter performace will cease to follow a regular pattern and will appear to be random. However, short-term temperature changes due to climate are likely to encourage regular sloughing and major changes in temperature due to seasonal variations may help to put sloughing cycles back in phase.

CHAPTER 10

RECOMMENDATIONS FOR FURTHER WORK

10.1 Hydraulic Studies.

Some recommendations for further work on hydraulic studies have been made in Chapter 8. These include using the hydraulic model and tracer technique in studying the behaviour of a larger pilot-plant biological filter: in this way it should be possible to obtain a functional relationship between liquid mixing and hydraulic loading and to reassess the values of the other hydraulic parameters obtained on Biopac 50. The size of such a pilot-plant is also discussed in Chapter 8.

Hydraulic studies should also be extended to cover a wide range of available packings, each operating under a variety of conditions. This work would further aid the process engineer in selecting the most appropriate type of packing for a given duty. For example, one type of packing may be less susceptible to giving a reduction in wetted surface area as the microbial film becomes excessive, but may be incapable of retaining a loose, poorly coherent film.

If different types of microbial film were to be investigated, it would be necessary to obtain tracer absorption data using a device like the inclined plane. A new experimenter would find it beneficial at the onset of such experiments to obtain experience using dyes as tracers.

10.2 Kinetics:Multisubstrates.

The application of the multisubstrate model should be investigated experimentally. Initially, this could be most conveniently carried out using selected pairs of organic compounds, progressing towards more complex multi-substrate mixtures. It may not be possible to use the

inclined plane and microbial film thickness measurements to obtain multisubstrate kinetic data: however, concentration measurements on a pilot-plant filter, operated under various recycle conditions, could provide the necessary information.

The pilot-plant filter for this purpose could be used to simultaneously obtain the hydraulic parameters. Indeed, the kinetic data could be more reliably assessed if the concentration measurements were taken immediately prior to a tracer experiment (as was the case with the data shown in Appendix 5).

10.3 Microbial Film Characteristics : Substrate Diffusivity.

The major influence on filter performance, aside from the microbial film composition, is the ability of certain compounds to yield extracellular slimes that enhance the diffusivity of the substrate and other compounds. Suggestions for further investigations into this subject are listed below:

1) identify groups or types of compounds that give rise to enhanced diffusivities,
2) identify any compounds that exhibit an enhanced diffusivity that is induced by the presence of other compounds,
3) identity compounds that may inhibit the emergence of enhanced diffusivities.

Many of these studies could be conveniently carried out using an inclined plane and/or a pilot-plant biological filter.

APPENDICES

APPENDIX (1)

Mathematical Development of the $0/\frac{1}{2}$ order Kinetic Model.

A1.1. A Single Limiting Substrate.

In Chapter 2 the intrinsic kinetics are described as zero order, i.e.

$$(-r_v) = k_o \qquad (2.2)$$

where $(-r_v)$ ——— rate of utilisation of limiting substrate per unit volume of microbial film $(M/L^3/\theta)$

k_o ——— intrinsic zero order rate constant $(M/L^3/\theta)$.

The microbial film is only contacted with liquid at the surface and the substrates are taken into the microbial film by diffusion. The bulk kinetics that arise from coupling of the intrinsic kinetics and the diffusion process are expressed by the rate of substrate removal per unit wetted surface area of microbial film. This rate of removal will clearly equal the flux of substrate into the microbial film and is expressed by the term $(-r_a)$. Figure A1.1 shows a diagrammatic section through the microbial film through which a single limiting substrate is diffusing and being utilised.

Figure A1.1. Diagrammatic Section Through Microbial Film.

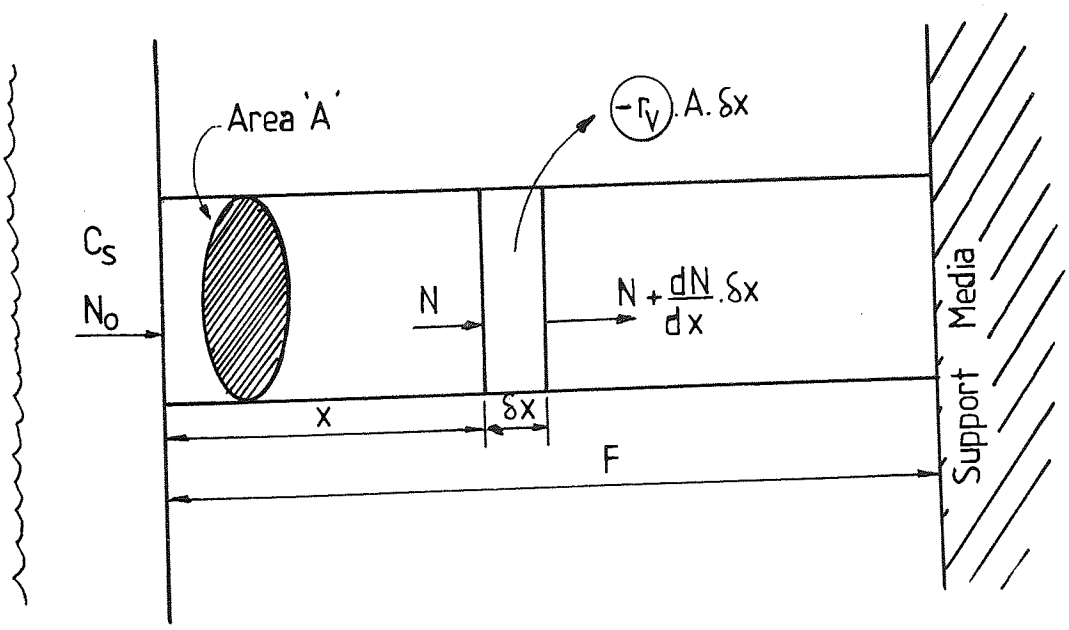

where C_s ——— concentration of substrate at the microbial film surface (M/L^3)

F ——— thickness of microbial film (L)

N ——— mass flow of substrate through area 'A' (M/θ).

Material Balance over Element δx

$$N = N + \frac{dN}{dx}.\delta x + (-r_v).A.\delta x$$

$$\therefore \frac{dN}{dx} = -(-r_v)A = -k_o.A$$

Alternatively, $$\frac{d\left(\frac{N}{A}\right)}{dx} = -k_o$$

and $$\frac{N}{A} = J$$

where J ——— flux of substrate through microbial film ($M/L^2/\theta$).

$$\therefore (-r_a) = \frac{N_o}{A} = J_{@x=0}$$

Fick's law.

$$J = -D.\frac{dC}{dx} \qquad \text{(A1.1)}$$

$$\therefore \frac{dJ}{dx} = \frac{d}{dx}\left(-D\frac{dC}{dx}\right)$$

where D ——— diffusivity of substrate through microbial film (L^2/θ).

For a uniform diffusivity:-

$$\frac{dJ}{dx} = -D\frac{d^2C}{dx^2}$$

$$\therefore -D\frac{d^2C}{dx^2} = -k_o$$

Putting into a dimensionless form,

where $c = \frac{C}{C_s}$ and $f = \frac{x}{F}$

$$\frac{d^2c}{df^2} = \frac{k_o F^2}{C_s D}$$

Integrating:-

$$\frac{dc}{df} = \frac{k_o F^2}{C_s D} \int df = \frac{k_o F^2 f}{C_s D} + K_1 \quad \text{——————} \quad (A1.2)$$

where K_1 —————— arbitrary constant of integration.

Integrating:-

$$c = \frac{k_o F^2 f^2}{2 C_s D} + fK_1 + K_2 \quad \text{——————} \quad (A1.3)$$

where K_2 —————— arbitrary constant of integration.

If the microbial film is fully penetrated, the boundary conditions are:-

@ $f = 0, \quad c = 1$

@ $f = 1, \quad \frac{dc}{df} = 0$

$$\therefore \quad K_2 = 1, \quad K_1 = -\frac{k_o F^2}{C_s D}$$

$$c = \frac{k_o F^2 f^2}{2 C_s D} - \frac{k_o F^2 f}{C_s D} + 1 \quad \text{——————} \quad (A1.4)$$

From equation (A1.1),

$$J = -D \frac{dC}{dx} = -D \frac{dc}{df} \left(\frac{C_s}{F} \right)$$

$$\textcircled{-r_a} = -\frac{D C_s}{F} \frac{dc}{df}, \quad @ \quad f = 0 \quad \text{——————} \quad (A1.5)$$

Hence from equation (A1.2) with

$$(-r_a) = -\frac{DC_s}{F}\left(\frac{k_o F^2 \beta}{C_s D} - \frac{k_o F^2}{C_s D}\right)$$

Therefore when the microbial film is fully penetrated,

$$(-r_a) = k_o F \qquad \text{——————————} \quad (2.4)$$

If full penetration is not achieved because the limiting substrate is exhausted at β

where $$\beta = \frac{F_{penetration}}{F}$$

the boundary conditions become:-

@ $f = 0, \quad c = 1$

@ $f = \beta, \quad c = 0, \quad \frac{dc}{df} = 0$

$$K_2 = 1, \qquad K_1 = -\frac{k_o F^2 \beta}{C_s D}$$

$$\& \quad \beta = \sqrt{\frac{2 C_s D}{k_o F^2}} \qquad \text{——————————} \quad (A1.6)$$

$$\therefore \quad F_{penetration} = \sqrt{\frac{2 C_s D}{k_o}} \qquad \text{——————} \quad (A1.7)$$

From equations (A1.5) and (A1.2) with $K_1 = \frac{k_o F^2 \beta}{C_s D}$

$$(-r_a) = \frac{C_s D}{F}\left(\frac{k_o F^2}{C_s D}\sqrt{\frac{2 C_s D}{k_o F^2}}\right)$$

Therefore if full penetration of film is not achieved,

$$(-r_a) = \sqrt{2k_oDC_s} \qquad (2.5)$$

Setting the two rate equations equal at the critical film thickness, F_{crit},

$$\sqrt{2k_oDC_s} = k_oF_{crit}$$

$$\therefore F_{crit} = \sqrt{\frac{2DC_s}{k_o}} = F_{penetration} \qquad (2.7)$$

Hence the critical film thickness, F_{crit}, also describes the depth of substrate penetration if full penetration is not achieved.

Multisubstrate Kinetics: Two Sequential Rate-Limiting Substrates

In the following example it will be assumed that there are two rate-limiting substrates or substrate groups; refered to as A and B . It is further assumed that substrate(s) A are utilised prior to substrate(s) B . By combining the rates or removal of the two substrates, the total rate of substrate removal is obtained i.e.

$$(-r_a)_T = (-r_a)_A + (-r_a)_B \qquad (A1.8)$$

where

$(-r_a)_T$ ——— total rate of substrate removal ($ML^{-2}\theta^{-1}$)

$(-r_a)_A$ ——— rate of removal of substrate A ($ML^{-2}\theta^{-1}$)

$(-r_a)_B$ ——— rate of removal of substrate B ($ML^{-2}\theta^{-1}$)

Essentially three expressions for $(-r_a)_T$ arise depending on the substrate concentrations and the microbial film thickness.

Case 1, 0' order in A .

When the microbial film is thin and/or the concentration of A is relatively high, the film may be fully penetrated by A . In this instance the rate of removal of will be zero order and B will not be removed. This is illustrated by the concentration profiles shown in Figure (A1.2).

Figure (A1.2) Concentration Profiles for Single Substrate Utilisation in a Two Substrate Mixture.

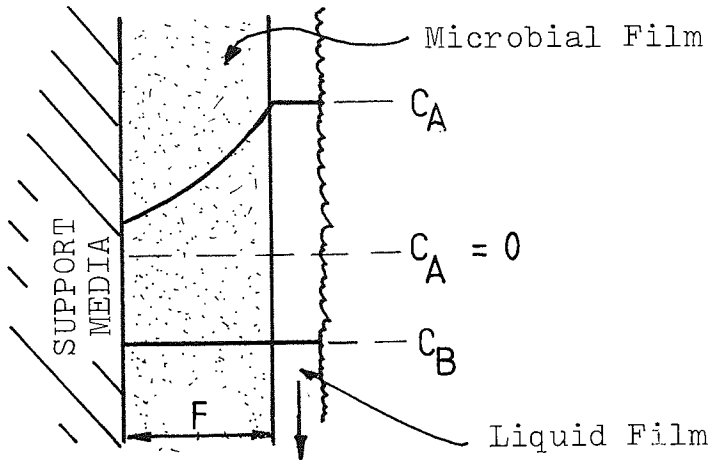

Hence from Figure (A1.2)

$$(-r_a)_A = k_{oA} F$$

$$(-r_a)_B = 0$$

$$(-r_a)_T = k_{oA} F \qquad \text{(A1.9)}$$

Case 2, $\frac{1}{2}$' order in A , 0' order in B .

In this instance, the microbial film thickness is sufficiently high and/or the concentration of A is sufficiently low to prevent full penetration of A . However, the conditions are such that a full penetration of B is possible. Hence the rate of removal of B is dependent on the

thickness of microbial film that A has not penetrated. This is illustrated by the concentration profiles in Figure (A1.3).

Figure (A1.3) Concentration Profiles for Simultaneous Utilization of Two Substrates With Differing Kinetic Regimes.

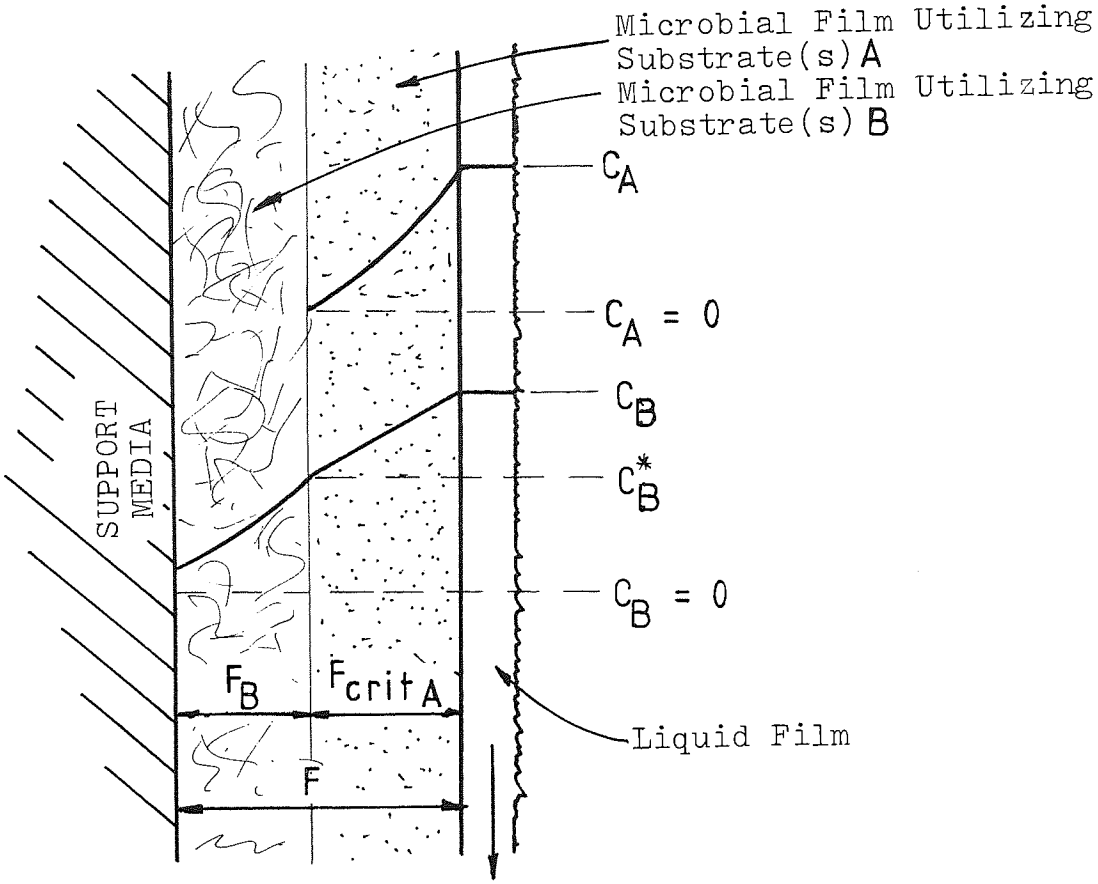

Hence from Figure (A1.3)

$$\left(-r_a\right)_A = \sqrt{2\, k_{oA} D_A C_A}$$

$$\left(-r_a\right)_B = k_{oB} F_B$$

where

$$F_B = F - F_{crit_A}$$

$$= F - \sqrt{\frac{2\, D_A C_A}{k_{oA}}}$$

$$\left(-r_a\right)_T = \sqrt{2 k_{oA} D_A C_A} + k_{oB} \left[F - \sqrt{\frac{2 D_A C_A}{k_{oB}}} \right] \quad \text{(A1.10)}$$

Case 3 $\frac{1}{2}$' order in both A and B.

In this instance, the conditions are such that neither A nor B can fully penetrate the microbial film. The

rate of removal of B is therefore $\frac{1}{2}$' order with respect to its concentration at the point where it begins to be utilized. This is illustrated by the concentration profiles shown in Figure (A1.4).

Figure (A1.4) Concentration Profiles for Simultaneously Utilized Substrates With Like Kinetic Regimes.

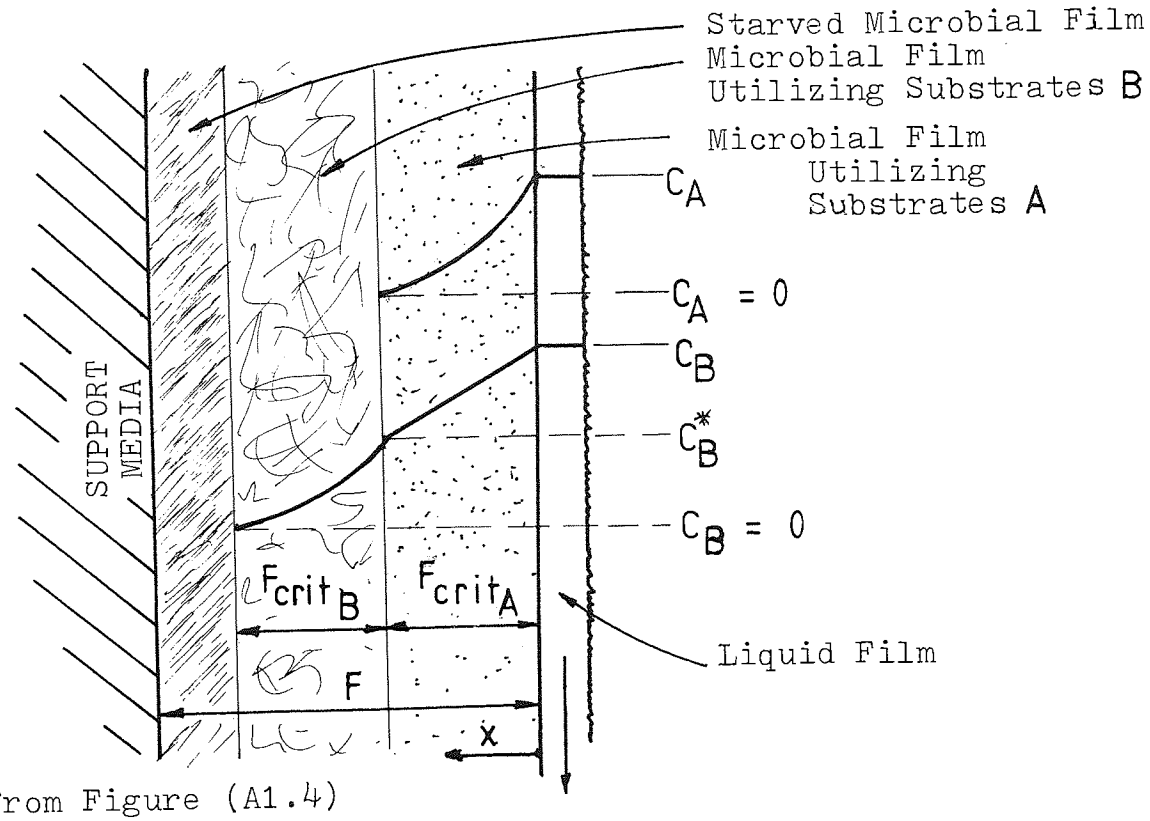

Hence from Figure (A1.4)

$$(-r_a)_A = \sqrt{2k_{oA}D_A C_A}$$

$$(-r_a)_B = \sqrt{2k_{oB}D_B C_B^*}$$

$$(-r_a)_T = \sqrt{2k_{oA}D_A C_A} + \sqrt{2k_{oB}D_B C_B^*}$$

Defining C_B^*

At steady state, the flux of B into the microbial film is equal to the rate of removal of B i.e.

$$(-r_a)_B = J_{B,x=0} = -D_B \frac{dC_B}{dx}$$

$$\sqrt{2k_{oB}D_B C_B} = \frac{D_B(C_B - C_B^*)}{F_{crit_A}} \qquad \text{(A1.11)}$$

squaring both sides of equation (A1.11) and rearranging:

$$\frac{2 k_{oB} C_B^*}{D_B} = \frac{\left(C_B^2 + C_B^{*2} - 2 C_B C_B^*\right)}{\left(F_{crit_A}\right)^2}$$

$$\left(F_{crit_A}\right)^2 = \frac{2 D_A C_A}{k_{oA}}$$

$$\frac{4 k_{oB} D_A C_A C_B^*}{D_B k_{oA}} = C_B^2 + C_B^{*2} - 2 C_B C_B^*$$

setting $$\sigma = \left(\frac{k_{oB} D_A}{D_B k_{oA}}\right) \qquad \text{(A1.12)}$$

$$\frac{C_B^{*2}}{2} - C_B^*(C_B + 2\sigma C_A) + \frac{C_B^2}{2} = 0$$

$$C_B^* = (C_B + 2\sigma C_A) \pm \sqrt{(C_B + 2\sigma C_A)^2 - C_B^2}$$

Since $C_B^* < C_B$ the -ve case must apply.

$$C_B^* = C_B + 2\sigma C_A - \sqrt{4\sigma C_A C_B + 4(\sigma C_A)^2} \qquad \text{(A1.13)}$$

The rate expression which applies for a given film thickness can be identified by considering the depth of penetration of each substrate. The maximum penetration depth of **A** is given by F_{crit_A} and the maximum penetration depth of **B** is given by:

$$\text{maximum penetration depth of } B = F_{crit_A} + F_{crit_B} = \sqrt{\frac{2 D_A C_A}{k_{oA}}} + \sqrt{\frac{2 D_B C_B^*}{k_{oB}}}$$

The film thickness conditions that give rise to each of the three cases are summarised in Table (A1.1) overleaf. A full summary of the kinetic and the film thickness criteria is presented in Table (2.1).

Table (A1.1) Summary of Microbial Film Thickness Criteria for a Two Substrate Mixture.

Microbial Film Thickness Criteria	Description of Kinetic Regime
$F < \sqrt{\frac{2 D_A C_A}{k_{oA}}}$	0' order in A B not removed
$\sqrt{\frac{2 D_A C_A}{k_{oA}}} < F < \sqrt{\frac{2 D_A C_A}{k_{oA}}} + \sqrt{\frac{2 D_B C_B^*}{k_{oB}}}$	$\frac{1}{2}$' order in A 0' order in B
$F > \sqrt{\frac{2 D_A C_A}{k_{oA}}} + \sqrt{\frac{2 D_B C_B^*}{k_{oB}}}$	$\frac{1}{2}$' order in both A and B.

APPENDIX (2.1)

Evaluation of the Exponential Growth Rate Phase and the F_{crit} Profile of the Microbial Film on the Inclined Plane.

The method of analysis introduced in Chapter 6 involves choosing the combination of parameters which give rise to minimum error in constructing the plot in Figure (A2.1). The parameters considered are:

1) the liquid film thickness, δ, term DELTA in the computer program;
2) the exponential growth rate, termed SLOPE in the computer program;
3) the eight values of F_{crit} termed FCRIT in the computer program, one value is determined for each of the eight sections designated by the value of J in computer program.

In evaluating the errors associated with fitting the two regions - the exponential and linear growth phases - to a set of film thickness measurements, it is first necessary to consider the two regions separately and then combine the resulting errors. In fact, it is more convenient to evaluate the errors in the growth rates $(+r_g)$ for the two regions, as this makes it simpler to combine the errors.

Evaluation of the Error Associated with Exponential Growth.

Exponential growth is given by equation (A2.1)

$$(+r_g) = \frac{dF}{dt} = (F_m - \delta)S \qquad \text{A2.1}$$

where
- F_m ——— measured film thickness (L)
- δ ——— liquid film thickness (L)
- S ——— exponential growth rate constant (θ^{-1})
- t ——— time (θ).

For a set value of δ, the exponential growth rate constants

Figure(A2.1) Graphical Representation of the Algorythm for the Evaluation of the F_{crit} Profile

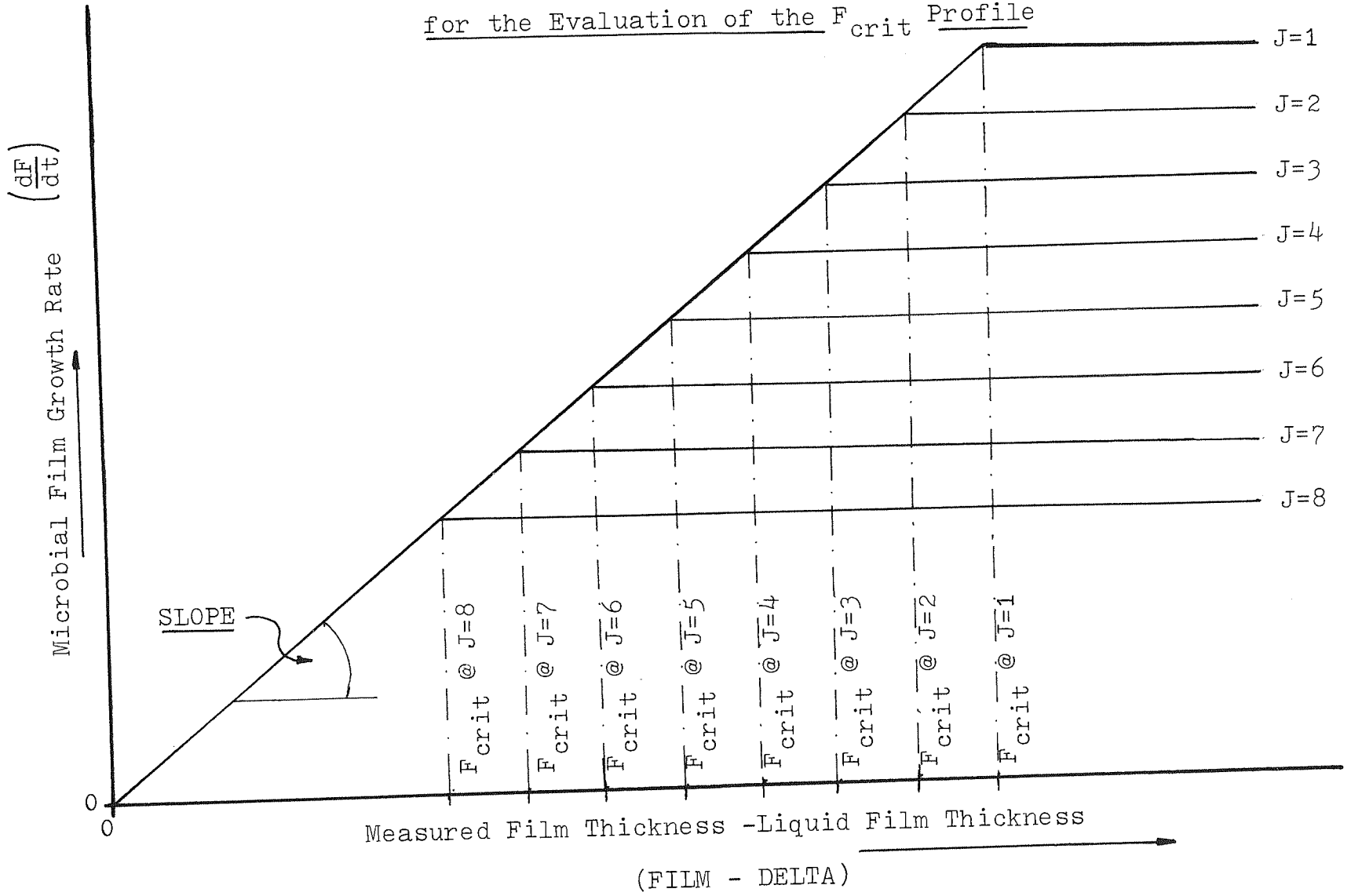

may be evaluated from two consecutive film measurements, as follows:

$$\int_{F_1}^{F_2} \frac{dF}{(F-\delta)} = S_m \int_{t_1}^{t_2} dt$$

$$S_m = \left[\ln\left(\frac{F_2-\delta}{F_1-\delta}\right)\right] \Big/ (t_2 - t_1) \qquad \text{A2.3}$$

where S_m ——— measured exponential growth rate constant (θ^{-1}).

For a set of n_e film measurements, where $(F_1 - \delta) < F_{crit}$ the errors in the growth rate with a data set (S, F_{crit} and δ) are given by:

$$E_e = \sqrt{\sum_{i=1}^{n_e} \frac{\left[(S_{m_i} - S).F_{i_i}\right]^2}{(n_e - 1)}} \qquad \text{A2.4}$$

The following special conditions can arise:

Condition	Comment
$F_2 = F_1 = \delta$ ———	Theoretically, this will occur when δ is exact. This is given due consideration by setting $S_{m_i} = S$ for that point, i.e. a zero error.
$F_1 \geqslant F_2$ ———	Shedding is assumed to be responsible for this condition and this point is ignored.
$\delta \geqslant F_1$ or F_2 ———	This condition is theoretically impossible for the correct value of δ, and this point is ignored.

Because the error calculation is based on a "Standard Error" method, the optimisation procedure will include as many data points as possible and so the latter condition will rarely be encountered.

Evaluation of the Errors Associated with Linear Growth.

For linear growth the growth rate is given by equation

$$(+r_g) = \frac{dF}{dt} = S \times F_{crit} \qquad \text{A2.5}$$

The growth rate constant, $S \times F_{crit}$, may be evaluated from two consecutive film measurements, as follows:

$$\int_{F_1}^{F_2} dF = (S \times F_{crit})_m \int_{t_1}^{t_2} dt$$

$$(S \times F_{crit})_m = (F_2 - F_1)/(t_2 - t_1) \qquad \text{A2.6}$$

where $(S \times F_{crit})_m$ ——— measured linear growth-rate constant ($L\theta^{-1}$).

For a set of n_l film measurements, where $(F_i - \delta) > F_{crit}$, the errors in the growth rate for a data set (S, F_{crit} and δ) are given by:

$$E_l = \sqrt{\sum_{i=1}^{i=n_l} \frac{\left[(S \times F_{crit})_{m_i} - (S \times F_{crit})\right]^2}{(n_l - 1)}} \qquad \text{A2.7}$$

The only special condition that may arise is $F_1 \geq F_2$, in which case the point is ignored.

Combining the Errors.

The errors associated with the two growth regimes are combined into a single term, E_c, by equation A2.8. It is the value of E_c that is minimized by the appropriate selection of the model parameters.

$$E_c = \sqrt{\frac{E_e^2 (n_e - 1) + E_l^2 (n_l - 1)}{(n_e + n_l - 1)}} \qquad \text{A2.8}$$

APPENDIX (2.2)

Computer Flow Diagram for the Evaluation of the Kinetic Parameters of Microbial Film Growth

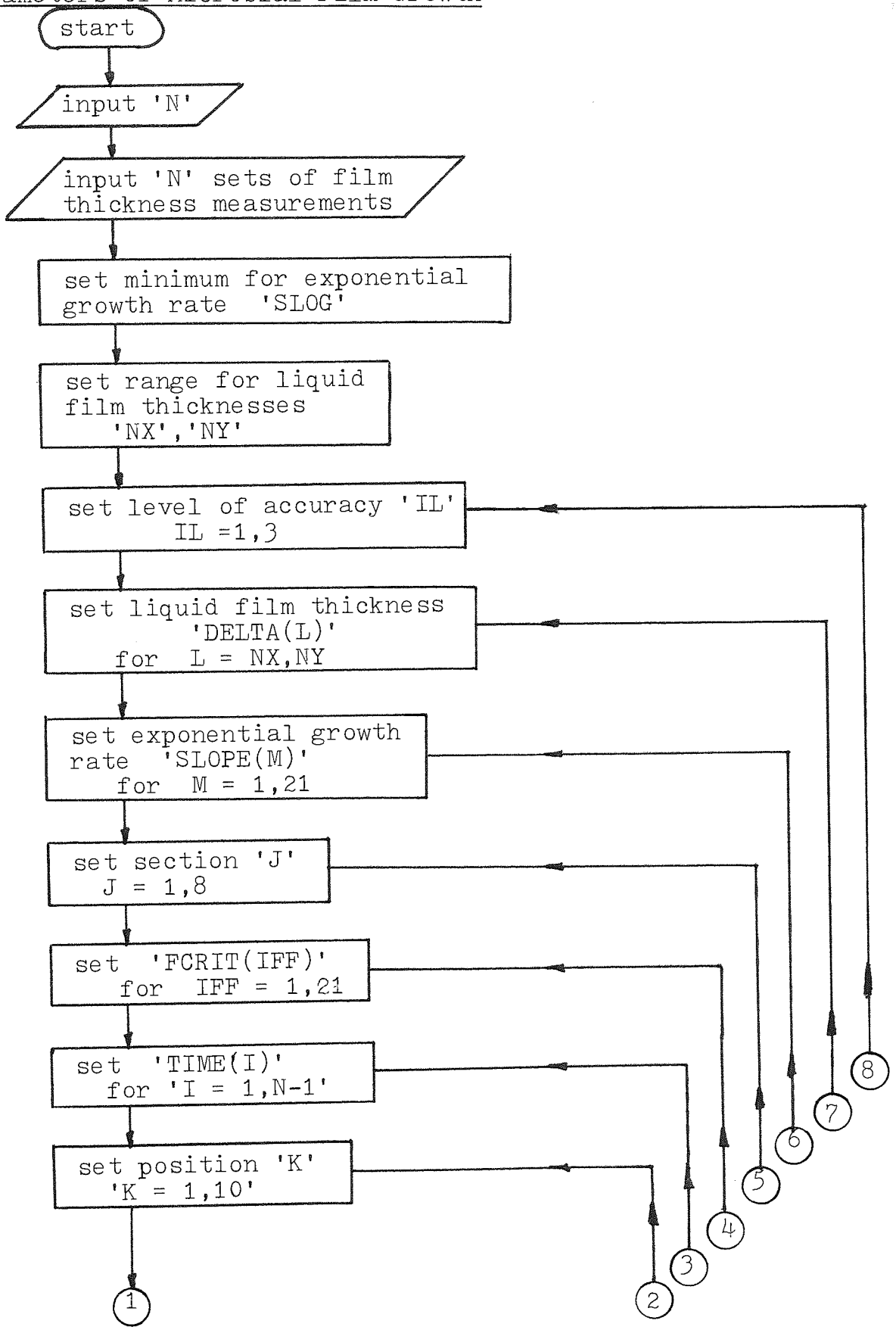

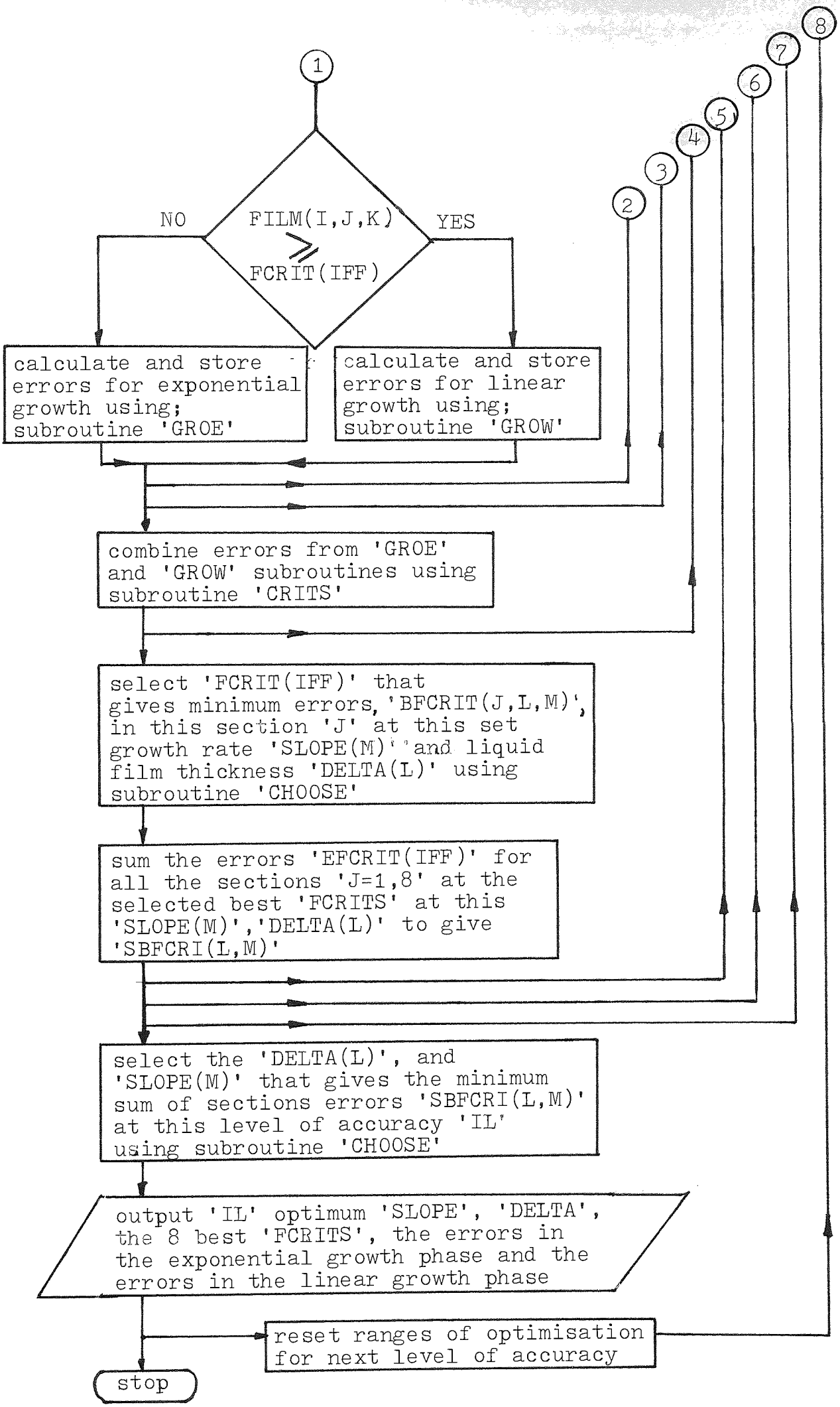
1
2
3
4
5
6
7
8
FILM(I,J,K)
≥
FCRIT(IFF)
NO
YES
calculate and store errors for exponential growth using; subroutine 'GROE'
calculate and store errors for linear growth using; subroutine 'GROW'
combine errors from 'GROE' and 'GROW' subroutines using subroutine 'CRITS'
select 'FCRIT(IFF)' that gives minimum errors, 'BFCRIT(J,L,M)', in this section 'J' at this set growth rate 'SLOPE(M)' and liquid film thickness 'DELTA(L)' using subroutine 'CHOOSE'
sum the errors 'EFCRIT(IFF)' for all the sections 'J=1,8' at the selected best 'FCRITS' at this 'SLOPE(M)','DELTA(L)' to give 'SBFCRI(L,M)'
select the 'DELTA(L)', and 'SLOPE(M)' that gives the minimum sum of sections errors 'SBFCRI(L,M)' at this level of accuracy 'IL' using subroutine 'CHOOSE'
output 'IL' optimum 'SLOPE', 'DELTA', the 8 best 'FCRITS', the errors in the exponential growth phase and the errors in the linear growth phase
reset ranges of optimisation for next level of accuracy
stop

APPENDIX(2.3)

Computer Program Listing for the Evaluation of the Kinetic Parameters of Microbial Film Growth

```
      PROGRAM GROWTH(INPUT,OUTPUT,TAPE1=INPUT,TAPE2=OUTPUT)
      DIMENSION BFCRIT(8,21,21),DELTA(11),FCRIT(21),SLOPE(21),
     1EFCRIT(21),TIME(30),FILM(30,8,10),ERK1(21),ERK2(21),
     2BFCRI(8,21,21),BERK2(8,21,21),SBFCRI(21,21),BEFCRI(8,21,21)
      COMMON/GRE/NU1/GRW/NU2
      READ(1,101)N
      DO 10 I=1,N
      READ(1,102)TIME(I)
      READ(1,103)((FILM(I,J,K),K=1,10),J=1,8)
C
   10 CONTINUE
C
      SLOG=0.00
      IA=22
      IB=22
      NX=1
      NY=11
C
      DO 11 J=1,8
   11 BFCRIT(J,IA,IB)=0.
      DO 400 IL=1,3
      DO 300 L=NX,NY
C
C     DELTA IS LIQUID FILM THICKNESS
C
      DELTA(L)=FLOAT(L)/100.-0.01
C
      DO 310 M=1,21
C
C     SLOPE IS EXPONETIAL GROWTH RATE,THE SAME FOR ALL SECTIONS
C
      SLOPE(M)=SLOG+(FLOAT(M)-1.)/10.**(IL+2)
      IF(SLOPE(M).LE.0.)SLOPE(M)=0.0001
C
C     SBFRCRI IS THE SUM OF THE ERRORS IN THE BEST CRITICAL
C     FILM THICKNESSES (BFCRIT) FOR A GIVEN SECTION,SLOPE AND
C     DELTA
C
      SBFCRI(L,M)=0.
      DO 320 J=1,8
      DO 200 IFF=1,21
C
C     FCRIT IS THE GIVEN CRITICAL FILM THICKNESS OF A SECTION
C
      FCRIT(IFF)=BFCRIT(J,IA,IB)+(FLOAT(IFF)-1.)/10.**IL
      IF(FCRIT(IFF).LE.0.)FCRIT(IFF) =0.001
C
C     BFCRIT IS CHOSEN BEST FCRIT FOR A GIVEN SLOPE,DELTA
C     AND SECTION
C
      ERK1(IFF)=0.
      ERK2(IFF)=0.
      NU1=0
      NU2=0
C
C     ERK1 IS THE ERROR IN'SLOPE'FOR GIVEN DELTA,SECTION AND
C     FCRIT
```

```
C       ERK2 IS THE ERROR IN LINEAR GROWTH RATE FOR A GIVEN
C       DELTA,SLOPE,FCRIT AND SECTION
C       NU1 IS THE NUMBER OF DATA POINTS LESS THAN FCRIT
C       NU2 IS THE NUMBER OF DATA POINTS GREATER THAN FCRIT
        NA=N-1
C
        DO 110 I=1,NA
        DO 100 K=1,10
        IF(FILM(I,J,K).GE.FCRIT(IFF))GO TO 50
        NU1=NU1+1
        CALL GROE(FILM(I+1,J,K),FILM(I,J,K),TIME(I+1),TIME(I),
       1DELTA(L),SLOPE(M),ERK1(IFF))
        GO TO  100
   50   NU2=NU2+1
C
        CALL GROW(FILM(I+1,J,K),FILM(I,J,K),TIME(I+1),TIME(I),
       1SLOPE(M),FCRIT(IFF),ERK2(IFF),DELTA(L))
  100   CONTINUE
  110   CONTINUE
        CALL CRITS(ERK1(IFF),ERK2(IFF),NU1,NU2,
       1EFCRIT(IFF))
  200   CONTINUE
        CALL CHOOSE(EFCRIT,BEFCRI(J,L,M),21,1,1,21,LFF,MFF)
        BERK2(J,L,M)=ERK2(LFF)
        BFCRIT(J,L,M)=FCRIT(LFF)
        SBFCRI(L,M)=SBFCRI(L,M)+BEFCRI(J,L,M)
  320   CONTINUE
  310   CONTINUE
        WRITE(2,217)(SBFCRI(L,M),M=1,21)
  217   FORMAT(7F10.4)
  300   CONTINUE
        CALL CHOOSE(SBFCRI,SMALL,21,21,NX,NY,LO,MO)
        IA=LO-1
        IB=MO-1
        SLOG=SLOPE(MO-1)
C
        WRITE(2,202)IL,SLOPE(MO),DELTA(LO)
        WRITE(2,203)(J,J=1,8)
        WRITE(2,204)(BFCRIT(J,LO,MO),J=1,8)
        WRITE(2,205)(BEFCRI(J,LO,MO),J=1,8)
        WRITE(2,206)(BERK2(J,LO,MO),J=1,8)
  400   CONTINUE
C
  101   FORMAT(1I7)
  102   FORMAT(1F8.3)
  103   FORMAT(10F5.2)
  202   FORMAT(' NUMBER OF SIGNIFICANT FIGURES=',I3,/' EXPONETIAL
       1 GROWTH=',F10.5,/' LIQUID FILM THICKNESS=',F6.2)
  203   FORMAT(' SECTION',I2,I4,6I8,/)
  204   FORMAT(' BEST CRITICAL FILM THICKNESSES'/,8F8.4)
  205   FORMAT(/' ERRORS IN CRITICAL FILM THICKNESSES'/,8F8.4)
  206   FORMAT(/' ERRORS IN LINEAR GROWTH'/,8F8.4,///)
C
        STOP
        END
```

SUBROUTINE GROE

```
C
      SUBROUTINE GROE(F2,F1,T2,T1,D,S,E)
C     SUBROUTINE TO CALCULATE ERRORS INVOLVED EXPONENTIAL
CC    REGIME,WHERE DATA IS LESS THAN CRITICAL FILM THICKNESS
C
      COMMON/GRE/N
      IF(F1.EQ.F2.AND.F2.EQ.D)GO TO 16
      IF(F1.GE.F2)GO TO 5
      IF(F2.LE.D)GO TO 5
      IF(F1.LE.D)GO TO5
      AK=(ALOG((F2-D)/(F1-D))/(T2-T1))
      GO TO 17
   16 AK=S
   17 IF(N.EQ.1)GO TO 6
      IF(N.EQ.2)GO TO 7
      E=SQRT(((FLOAT(N)-2.)*E**2+((AK-S)*(F1-D))**2)/(FLOAT(N)-1.))
      GO TO 8
    6 E=ABS((AK-S)*(F1-D))
      GO TO 8
    7 E=SQRT(E**2+((AK-S)*(F1-D))**2)
      GO TO 8
    5 N=N-1
    8 RETURN
      END
```

SUBROUTINE GROW

```
      SUBROUTINE GROW(F2,F1,T2,T1,S,FC,E,D)
C
C     SUBROUTINE TO CALCULATE ERRORS IN LINEAR GROWTH REGIME
      COMMON/GRW/N
      IF(F1.GE.F2)GO TO 9
      AK=(F2-F1)/(T2-T1)
      IF(N.EQ.1)GO TO 2
      IF(N.EQ.2)GO TO 3
      E=SQRT(((FLOAT(N)-2.)*E**2+((AK-S*(FC-D)))**2)/(FLOAT(N)-1.))
      GO TO 4
    2 E=ABS((AK-(FC-D)*S))
      GO TO 4
    3 E=SQRT(E**2+((AK-(FC-D)*S))**2)
      GO TO 4
    9 N=N-1
    4 RETURN
      END
```

SUBROUTINE CRITS

```
      SUBROUTINE CRITS(E1,E2,NU1,NU2,EF)
C     SUBROUTINE TO CALCULATE ERROR IN CRITICAL FILM THICKNESS
C
      IF(NU1.EQ.1)GOTO21
      IF(NU2.EQ.1)GOTO22
      EF=SQRT((E1**2*FLOAT(NU1-1)+E2**2*FLOAT(NU2-1))/FLOAT(NU1+NU2-1))
      GOTO23
   21 EF=SQRT((E1**2+E2**2*FLOAT(NU2-1))/FLOAT(NU2))
      GOTO23
   22 EF=SQRT((E1**2*FLOAT(NU1-1)+E2**2)/FLOAT(NU1))
   23 RETURN
      END
```

SUBROUTINE CHOOSE

```
      SUBROUTINE CHOOSE(ARRAY,SMALL,L,M,LS,IHS,LO,MO)
      REAL ARRAY(L,M)
      SMALL=ARRAY(LS,1)
      LO=LS
      MO=1
      DO 15 IM=1,M
      DO 19 IL=LS,IHS
      IF(ARRAY(IL,IM).GE.SMALL)GO TO 18
      SMALL=ARRAY(IL,IM)
      LO=IL
      MO=IM
   18 CONTINUE
   19 CONTINUE
   15 CONTINUE
      RETURN
      END
```

APPENDIX (3)

Mathematical Development of the Hydraulic Model.

A3.1. Liquid Hold-up and Mean Residence Time.

The biological filter, for the purpose of tracer analysis, may be regarded as a vessel with one inlet stream, one outlet stream and with no loss of tracer, as shown in figure (A3.1).

Figure A3.1. Representation of the Tracer System.

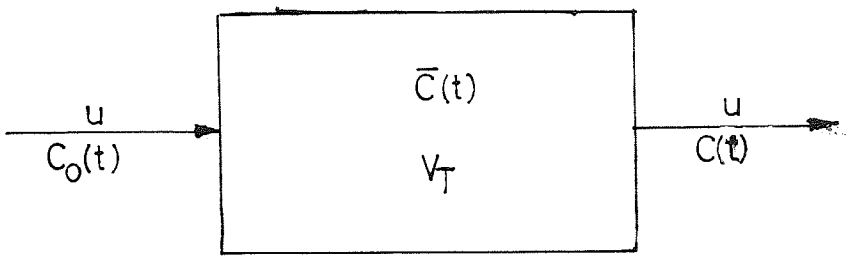

where $C_o(t)$ —— the inlet tracer concentration at time 't', for a step change = 0 @ $t<0$, = 1 @ $t>0$. (M/L^3).

$C(t)$ —— the outlet tracer concentration at time 't'. (M/L^3).

$\bar{C}(t)$ —— the mean tracer concentration within the system at time 't'. (M/L^3).

V_T —— system volume (L^3).

u —— flow-rate through the system (L^3/θ).

The mass of tracer held within the system may be found from an analysis of the step-change response, which is assumed to be equivalent to an integration of the pulse response.

Figure A3.2. Representation of a Step-Change Response.

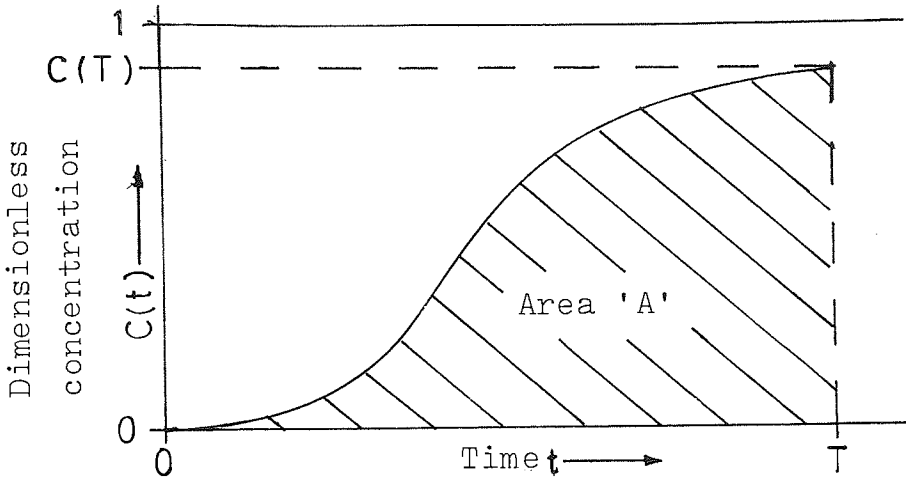

Overall tracer mass balance.

Mass of tracer retained in time T = Mass of tracer entered in time T − Mass of tracer passed in time T. ——— (A3.1)

$$\text{Mass of tracer entered in time T} = u\int_0^T C_0(t).dt = u.T.1 \qquad \text{(A3.2)}$$

$$\text{Mass of tracer passed in time T} = u\int_0^T C(t).dt = u.\text{Area 'A'} \qquad \text{(A3.3)}$$

$$\therefore \text{Mass of tracer retained in time T} = u(T - \text{Area 'A'}) \qquad \text{(A3.4)}$$

Given that at time 'T', C(T) is close to unity (>0.95), the mean concentration within the system may be reasonably approximated by:-

$$\bar{C}(T) = (C(T) + C_0(t))/2 \qquad \text{(A3.5)}$$

Also

$$\bar{C}(T) = \frac{\text{Mass of tracer retained}}{\text{Liquid Hold-up}}$$

$\therefore$ Liquid Hold-up 'V_T' $= \dfrac{2u(T - \text{Area } 'A')}{(C(T) + 1)}$ ——————— A3.6

and

Mean Residence Time $= \dfrac{V_T}{u} = \dfrac{2(T - \text{Area } 'A')}{(C(T) + 1)}$ ——————— A3.7

The Area 'A' may be evaluated by graphical or numerical integration such as Trapezium rule or Simpson's rule.

A3.2. Response to a step-change through a simple series of uniform stirred tanks.

Mass balance over a single tank; general case from figure A3.3.

Figure A3.3. Single Stirred Tank; General Case.

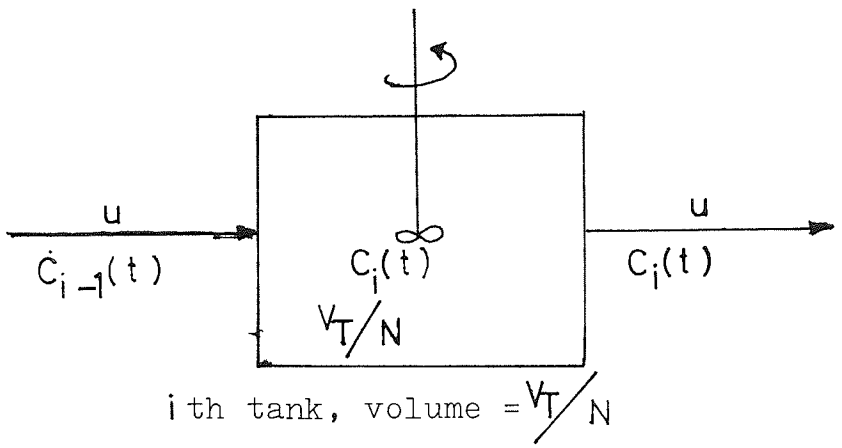

where $C_{i-1}(t)$ —— tracer concentration flowing into ith tank at time 't' (M/L^3).

$C_i(t)$ —— tracer concentration flowing out of and within ith tank at time 't'. (M/L^3).

N —— number of tanks in series.

V_T —— total volume of series (L^3).

Steady State Mass Balance

$$uC_{i-1} = uC_i \quad \text{——————} \quad \text{A3.8}$$

Dynamic Mass Balance

$$uC_{i-1}(t) = uC_i(t) + \frac{V_T}{N}\cdot\frac{dC_i(t)}{dt} \qquad \text{A3.9}$$

Since all initial concentrations are zero, the dynamic mass balance taking perturbation variables will be equivalent to taking actual concentrations; hence the perturbation notation will not be required.

Rearranging equation A3.9

$$C_{i-1}(t) = C_i(t) + \frac{V_T}{uN}\cdot\frac{dC_i(t)}{dt} \qquad \text{A3.10}$$

Taking Laplace Transforms

$$C_{i-1}(s) = C_i(s) + \frac{V_T}{uN}(sC_i(s) + 0) \qquad \text{A3.11}$$

$$\therefore C_i(s) = \frac{\frac{uN}{V_T}}{\left(\frac{uN}{V_T} + s\right)}\cdot C_{i-1}(s) \qquad \text{A3.12}$$

Let $a = \frac{uN}{V_T}$ and consider $i = 1$.

$$\therefore C_1(s) = \left(\frac{a}{a+s}\right)\cdot C_0(s) \qquad \text{A3.13}$$

$C_0(s) = \frac{1}{s}$ for a step-change of 1, then for the general case of N stirred tanks:

$$C_N(s) = \left(\frac{a}{a+s}\right)^N\cdot\frac{1}{s} \qquad \text{A3.14}$$